

METAL COMPLEX CATALYSED REACTIONS OF ANILS

By

ALAN RICHARD BOATE, B.A. (Mod.)

A Thesis

Submitted to the Faculty of Graduate Studies

in Partial Fulfilment of the Requirements

for the Degree

Doctor of Philosophy

McMaster University

September 1975

©

ALAN RICHARD BOATE

1976

METAL COMPLEX CATALYSED REACTIONS OF ANILS

But as for certain truth, no man has known it,  
Nor will he know it, neither of the gods,  
Nor yet of all the things of which I speak.  
And even if by chance he were to utter  
The final truth, he would himself not know it;  
For all is but a woven web of guesses.

Xenophanes

I have measured out my life with coffee spoons.

T. S. Elliot

DOCTOR OF PHILOSOPHY  
(Chemistry)

McMASTER UNIVERSITY  
Hamilton, Ontario

TITLE: Metal Complex Catalysed Reactions of Anils

AUTHOR: Alan Richard Boate B.A. (Mod.) (University of Dublin)

SUPERVISOR: Dr. D. R. Eaton

NUMBER OF PAGES: xi, 216

## ABSTRACT

It has been found that a series of thiourea metal complexes are very efficient catalysts for a number of reactions involving anils. These reactions, the formation and hydrolysis of the anil and a transimination reaction, were studied using acetone and various substituted anilines as substrates. The catalysts were Co(II) and Zn(II) complexes of thiourea and substituted thioureas and were found to have a wide range of effectiveness as catalysts.

Kinetic studies have been carried out using a number of NMR techniques, including measurement of initial rates by integration, line broadening studies and spin saturation transfer (SST) experiments. Equilibrium constants for association of various substrates with the catalysts have also been determined, taking advantage of the paramagnetism of the Co(II) complexes.

The results indicate that the rate determining step for the formation of the anil involves nucleophilic attack of aniline on coordinated acetone. The aniline in this case is in the second coordination sphere of the metal complex and the acetone is in the first analogous mechanisms. The utility of SST experiments is demonstrated by the identification of the transimination reaction and the measurement of two exchange processes in this reaction.

## ACKNOWLEDGEMENTS

The author would like to express his deep appreciation to his supervisor, Dr. D. R. Eaton, for his assistance and encouragement and not least for his apparently limitless patience. Thanks are also due to the staff of the NMR laboratory, to Mrs. H. Kennelly for her rapid typing and to McMaster University and the National Research Council of Canada for financial support. Finally I would like to thank all those people at McMaster who helped (in either a positive or negative way) towards the completion of this thesis.

## TABLE OF CONTENTS

		<u>Page</u>
CHAPTER ONE	CATALYSIS BY METAL IONS	
	(A) INTRODUCTION	1
	(B) ESTER HYDROLYSIS	3
	(C) REACTIONS OF IMINES	6
CHAPTER TWO	BASIC MAGNETIC RESONANCE THEORY	
	(A) INTRODUCTION	14
	(B) NMR IN PARAMAGNETIC SYSTEMS	15
	(C) EFFECTS OF CHEMICAL EXCHANGE	
	(i) General Considerations	18
	(ii) Slow Passage Experiments	21
	(iii) Spin Saturation Transfer	23
	(D) SURVEY OF SST LITERATURE	27
CHAPTER THREE	EXPERIMENTAL	
	(A) SOURCES OF CHEMICALS	29
	(B) SAMPLE PREPARATION	30
	(C) NMR SPECTROMETERS	30
	(D) SPIN SATURATION TRANSFER WITH cw SPECTROMETERS	33
	(E) SPIN SATURATION TRANSFER WITH FT SPECTROMETERS	
	(i) General Aspects	41
	(ii) Practical Considerations	44
CHAPTER FOUR	THE OVERALL REACTION	
	(A) INTRODUCTION	48
	(B) REACTION OF ACETONE WITH ANILINES	50
	(C) PREPARATION OF ANILS	
	(i) Synthesis	53
	(ii) Comparison with observed spectra	59
	(D) ROLE OF THE METAL COMPLEX	60
	(E) COMPARISON OF CATALYTIC EFFICIEN- CIES	62
	(F) ACID CATALYSED REACTION	64
	(G) EQUILIBRIUM CONSTANT	67
	(H) SUMMARY	69

TABLE OF CONTENTS (continued)

	<u>Page</u>
CHAPTER FIVE	INITIAL RATE MEASUREMENTS
(A)	INTRODUCTION 71
(B)	THE FORWARD REACTION 72
(i)	Dependence of rate on concentration of catalyst
(ii)	Dependence of rate on concentration of aniline 78
(iii)	Overall concentration dependence 85
(iv)	Dependence of rate on thiourea concentration 89
(C)	THE BACK REACTION
(i)	Dependence on anil concentration 92
(ii)	Dependence on water concentration 95
(iii)	Dependence of initial rate on overall concentration 95
(D)	THE KINETIC ISOTOPE EFFECT 98
(E)	SUMMARY 107
CHAPTER SIX	LIGAND EXCHANGE
(A)	INTRODUCTION 108
(B)	THIOUREA AS A LIGAND IN ACETONE SOLUTION 109
(C)	THIOUREA AS A LIGAND IN ACETONITRILE SOLUTION 112
(D)	WATER AS A LIGAND
(i)	Water concentration 116
(ii)	Equilibrium constant for water as a ligand 120
(E)	ANILINES AND ANILS AS LIGANDS
(i)	NMR spectra 125
(ii)	Determination of equilibrium constants 132
(iii)	Kinetics 135
(iv)	General considerations 138
(F)	ACETONE IN MIXED LIGAND SOLUTIONS 139
(G)	ANILINES IN ACETONITRILE 143
(H)	EXCHANGE REACTIONS 145
(I)	SUMMARY 150



TABLE OF CONTENTS (continued)

	<u>Page</u>
CHAPTER SEVEN. SPIN SATURATION TRANSFER EXPERIMENTS	
(A) INTRODUCTION	152
(B) EXPERIMENTS USING $^{19}\text{F}$ NMR	152
(C) EXPERIMENTS USING $^1\text{H}$ NMR	157
(D) COMPARISON OF $^1\text{H}$ AND $^{19}\text{F}$ LIFETIMES	163
(E) FT SST MEASUREMENTS	168
(F) DISCUSSION	172
CHAPTER EIGHT DISCUSSION AND CONCLUSIONS	
(A) INTRODUCTION	176
(B) NATURE OF THE CATALYTIC SPECIES	176
(C) NATURE OF THE RATE-DETERMINING STEP	191
(D) TRANSIMINATION	193
(E) NATURE OF THE SECOND SPHERE SITE	195
(F) SUGGESTIONS FOR FURTHER WORK	197
(G) CATALYTIC EFFICIENCY	197
(H) CONCLUSIONS	199
APPENDIX A	201
APPENDIX B	210
BIBLIOGRAPHY	211

## LIST OF FIGURES

<u>Figure</u>		<u>Page</u>
2.1	NMR lineshapes as a function of exchange rate	22'
3.1	An initial rate experiment	32
3.2	A schematic of the SST equipment	36
3.3	Output from a SST experiment	38
3.4	Effect of decoupler output power on intensity	46
4.1	The 100 MHz $^1\text{H}$ NMR spectrum of p-f aniline/ anil in $\text{CD}_3\text{CN}$	55
4.2	Methyl region of the $^1\text{H}$ NMR spectrum (100 MHz) of p-toluidine anil in $\text{CDCl}_3$	58
4.3	The acid catalysed reaction	65
5.1	Graphical determination of the initial rate	73
5.2	Dependence of initial rate on catalyst concen- tration	76
5.3	(a) Dependence of initial rate on p- toluidine concentration	81
	(b) Double reciprocal plot	
5.4	Double reciprocal plot for initial rate of formation of anil from p-toluidine (d-2) with $\text{ZnTu}_2\text{Cl}_2$ as catalyst	84
5.5	(a) Dependence of initial rate on added Tu	
	(b) Dependence of initial rate on $(\text{added Tu})^{-1}$	91
5.6	(a) Dependence of initial rate of formation of p-toluidine on anil concentration	
	(b) Double reciprocal plot	94
5.7	(a) Dependence of initial rate of formation of p-toluidine on water concentration	
	(b) Double reciprocal plot	97
5.8	Dependence of initial rate of formation of p-toluidine on dilution with $\text{CCl}_4$	100

LIST OF FIGURES (continued)

<u>Figure</u>		<u>Page</u>
5.9	The kinetic isotope effect . $\frac{\text{Rate H}}{\text{Rate D}}$ against [p-toluidine]	103
5.10	The kinetic isotope effect. $\sigma$ against $X_{\infty}$	106
6.1	A dilution plot for $\text{CoTu}_2\text{Cl}_2$ in $\text{CH}_3\text{CN}$	114
6.2	Dilution plot for $\text{CoTu}_2\text{Cl}_2$ in $\text{CH}_3\text{CN}$ (non linear portion)	115
6.3	Susceptibility of $\text{CoTu}_2\text{Cl}_2$ in $\text{CH}_3\text{CN}$	117
6.4	Dependence of $K_2$ (association constant for water with $\text{CoTu}_2\text{Cl}_2$ ) on water concentration	124
6.5	100 MHz $^1\text{H}$ NMR spectra with p-toluidine	126
6.6	56.4 MHz $^{19}\text{F}$ NMR spectra with p-F aniline	129
6.7	Plot of $\Delta\nu_c$ against $\frac{1}{T}$ for complexed anil (meta resonance)	134
6.8	Plot of $\ln[M_0 - M(t)]$ against t for determining $T_1$	142
6.9	Plot of log K against Hammett $\sigma$ for a series of para substituted anilines	147
6.10	(a) $^1\text{H}$ spectrum of p-toluidine in acetone d-6 (b) As (a) after addition of $\text{ZnTu}_4(\text{ClO}_4)_2$	148
7.1	$^1\text{H}$ NMR SST experiment	161
7.2	Intensity of acetone peak as a function of time after addition of water	167
8.1	The calculated term $([\text{MTuAcCl}_2] + [\text{MANAcCl}_2]) \cdot [\text{An}]$ plotted against the experimental initial rate from table 5.3.	187
8.2	(a) A plot of the calculated term $\frac{1}{X}$ (where $X = ([\text{MTuAcCl}_2] + [\text{MANAcCl}_2]) \cdot [\text{An}]$ ) against $(\sqrt{[\text{ptol}]})^{-1}$ . (b) Initial rate $^{-1}$ plotted against $(\sqrt{[\text{ptol}]})^{-1}$ for data from table 5.3.	188
8.3	Initial rate $^{-1}$ plotted against the added Tu concentration for the data of table 5.5	190

LIST OF TABLES

<u>Table</u>		<u>Page</u>
4.1	Comparison of the efficiency of various catalysts in the reaction of p-F aniline with acetone	63
4.2	Composition and equilibrium constant for p-F aniline in acetone	68
5.1	Results of experiment on the dependence of the initial rate on the catalyst concentration	75
5.2	Results for the dependence of initial rate on p-toluidine (d-2) concentration with $ZnTu_4(ClO_4)_2$ as catalyst	80
5.3	Results for dependence of initial rate on p-toluidine (d-2) concentration with $ZnTu_2Cl_2$ as catalyst	83
5.4	Results for dependence of initial rate of formation of anil on dilution with $CCl_4$	86
5.5	Results for dependence of initial rate of formation of anil on added Tu concentration	90
5.6	Results for dependence of initial rate of formation of p-toluidine on the concentration of the p-toluidine-anil	93
5.7	Dependence of initial rate of formation of p-toluidine on water concentration	96
5.8	Dependence of initial rate of formation of p-toluidine on degree of dilution with $CCl_4$	99
5.9	Determination of the kinetic isotope effect for the forward reaction	102
5.10	Determination of best value for $X_\infty$ by linear regression	105
6.1	Shift of Tu peak of $CoTu_2Cl_2$ as a function of water concentration	121
6.2	Determination of equilibrium constants for ligand exchange of p-toluidine and its anil with $CoTu_2Cl_2$	136

LIST OF TABLES (continued)

<u>Table</u>		<u>Page</u>
6.3	Determination of the equilibrium constants for various anilines with $\text{CoTu}_2\text{Cl}_2$ in $\text{CH}_3\text{CN}$	146
7.1	$^{19}\text{F}$ SST results	156
7.2	Time dependence of $M_{\text{O}}^{\text{A}}/M_{\infty}^{\text{A}}$	158
7.3	Comparison of $^1\text{H}$ and $^{19}\text{F}$ SST lifetimes	165
7.4	Results of FT SST experiments	170
8.1	Calculated Concentrations	181

## CHAPTER 1

### CATALYSIS BY METAL IONS

#### (A) INTRODUCTION

Metal ions have long been known to be capable of modifying the properties of chemical species coordinated to them. This modification may be manifested in various ways; e.g. in spectral properties or in changes in reaction rates or mechanisms. The changes induced by coordination to a metal ion are of great importance in the study of homogeneous catalysis of chemical reactions by metal complexes or ions in solution.

In recent years homogeneous catalysis by metal ions, metal complexes and metalloenzymes has been much studied. These reactions are necessarily multistep processes involving at least three steps, ie; (a) coordination of the substrate molecule or molecules, (b) reaction of the coordinated substrate(s) and (c) dissociation of products, leaving the metal ready to undergo another catalytic cycle. An added requirement for the use of the term catalysis is, of course, that the process must be faster than that occurring in the absence of the metal ion or metal complex. If step (c) is missing, the reaction

will not be catalytic and the metal ion will be consumed stoichiometrically; in this case the term "metal ion promotion" should be used, a fact sometimes ignored in the literature on the subject.

Most of the work done on homogeneous catalysis involving metal ions or complexes in solution may be divided into two main areas. The first of these involves the reactions of small molecules, generally capable of  $\pi$ -bonding, with transition metal complexes in non-aqueous solution. The individual reaction steps, where known, can usually be interpreted in terms of ligand substitution, oxidative addition, reductive elimination and insertion or ligand migration, with each step obeying the 16/18 electron rule<sup>(1)</sup>. Typical examples are: hydrogenation using Wilkinson's compound  $(\text{Ph}_3\text{P})_3\text{RhCl}$ <sup>(2)</sup> polymerization of olefins<sup>(3)</sup>, and oxidation of olefins to aldehydes in the Wacker process<sup>(4)</sup>. The second main area of research in homogeneous catalysis has been in the study of the effect of metal ions in aqueous solution on such reactions as ester hydrolysis, Schiff base formation and hydrolysis, transaminations, etc. This area has been periodically reviewed<sup>(5-13)</sup>. The subject of this thesis, i.e. the formation and hydrolysis of Schiff bases as catalysed by metal complexes, properly falls into the latter area although the study was carried out in non-aqueous solutions.

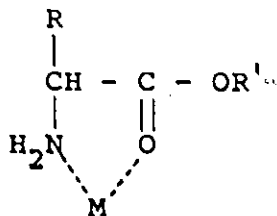
The first observations of changes in chemical properties brought about by coordination were made in 1857 by Gibbs and

Geneth<sup>(14)</sup>, who noted that oxalate coordinated to cobalt (III) was much less susceptible to oxidation than free oxalate.

Another early example was the relative non-toxicity of cyanide complexes of Fe(II), Au(I), G(III), and Co(III) compared to any source of free cyanide ion<sup>(10)</sup>. Over the past twenty five years most of the work on metal ion catalysis or metal ion promoted reactions has been in the areas of ester hydrolysis and of reactions of Schiff bases, including formation, hydrolysis and transamination.

#### (B) ESTER HYDROLYSIS

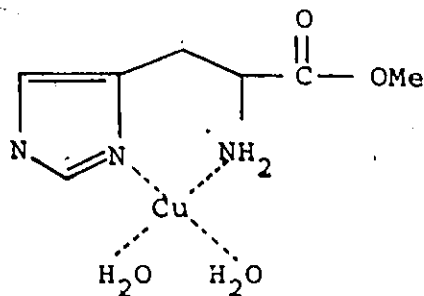
Metal ions will effectively catalyse the hydrolysis of esters if they have a secondary functional group that will coordinate to the metal ion. The hydrolysis of  $\alpha$ -amino acid esters was studied by Kroll<sup>(15)</sup>, who determined that a 1:1 complex between the metal ion and the ester was the most active species. He also compared the effectiveness of various divalent metal ions in promoting hydrolysis, and found that the rate increased with the increasing tendency of the metal to coordinate with amines. He postulated that the ester acted as a chelating agent, coordinating to the metal ion via the  $\alpha$ -amino group and the carbonyl oxygen, i.e.





The role of the metal in this and similar cases has been likened to that of a "superacid", that is, the increase in the rate of hydrolysis is far greater than one would be led to expect on the basis of electrostatic considerations alone.

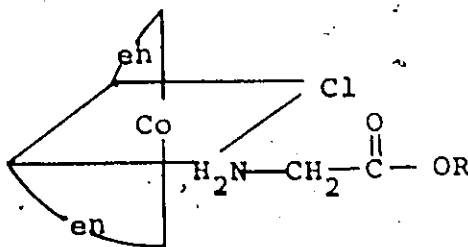
Conley and Martin<sup>(16)</sup> measured the second order rate constants for hydroxide attack on glycine ethyl ester, protonated glycine ethyl ester and the Cu(II) complex of glycine ethyl ester. The effect of Cu(II) compared to that of a proton is much larger than expected on a simple electrostatic basis. In this case, coordination to the metal ion by the carbonyl group is postulated to occur. This is also the conclusion drawn from a study by Bender<sup>(17)</sup> using kinetic measurements and O<sup>18</sup> tracer methods; i.e., the ester is chelated to the metal ion via the amino and carbonyl groups. With histidine methyl ester however, the metal ion can chelate at two sites other than the carbonyl group, i.e.



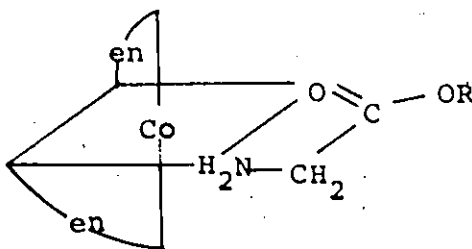
In this case, where the carbonyl group is not coordinated, the observed effect of the metal ions on the rate of hydrolysis was roughly the same per unit charge as the effect of protonation of the ester<sup>(18)</sup>. The "superacid" catalysis is usually explained in terms of the polarisation of the carbonyl group by the metal

ion which facilitates nucleophilic attack on the now relatively more positively charged carbon atom.

However, intramolecular attack by a coordinated nucleophile is also possible, and is difficult to distinguish kinetically from external nucleophilic attack. In a number of cases, it has been possible to distinguish and demonstrate each mechanism. The effect of the polarisation of the carbonyl group by coordination to a metal ion was demonstrated in the case of the hydrolysis of an  $\alpha$ -amino ester coordinated to a Co(III) complex containing two kinetically inert ethylenediamine (en) ligands<sup>(19)</sup>. The starting complex was

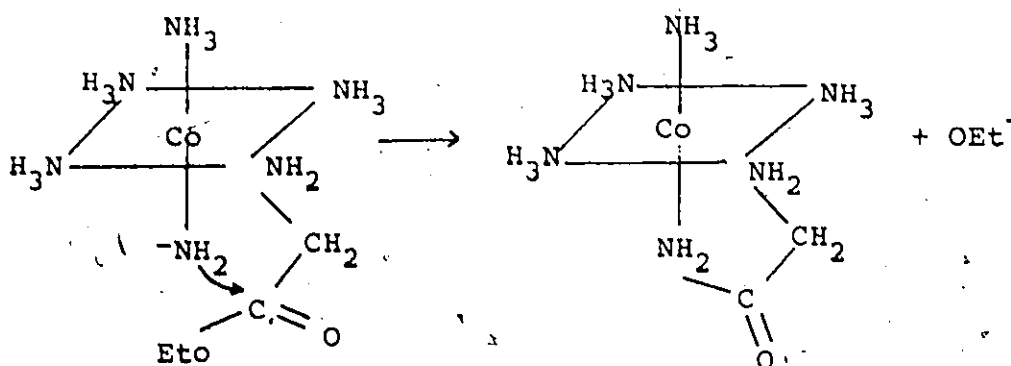


which was stable to hydrolysis. The  $\text{Cl}^-$  was removed by addition of mercurous ion giving as an intermediate,



which was detected by infrared spectroscopy and which underwent hydrolysis via the attack of an external hydroxide ion.

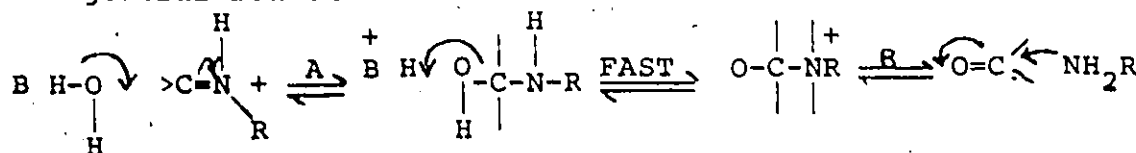
An example of intramolecular nucleophilic attack on a coordinated ligand is the amidolysis of glycine ethyl ester complexed to pentamincobalt (III) (20). Loss of a proton from one of the coordinated  $\text{NH}_3$  groups gives an  $-\text{NH}_2$  ligand which attacks the carbon atom of the carbonyl group, displaces  $\text{OEt}^-$  to yield the glycine imide complex, i.e.



### (C) REACTION OF IMINES

Compounds containing the carbon nitrogen double bond, i.e.  $\begin{matrix} R_1 \\ \diagdown \\ C = N - R_3 \\ \diagup \\ R_2 \end{matrix}$ , are variously known as Schiff bases, azomethines, imines, ketimines, aldimines (if  $R_1 = \text{H}$ ) and anils (if  $R_3$  is aromatic). The non-metal catalysed formation and hydrolysis of these compounds has been widely studied in aqueous solution, and the mechanisms involved are well understood (21).

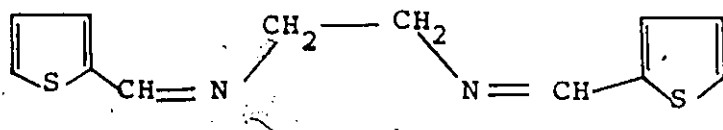
The general reaction is:



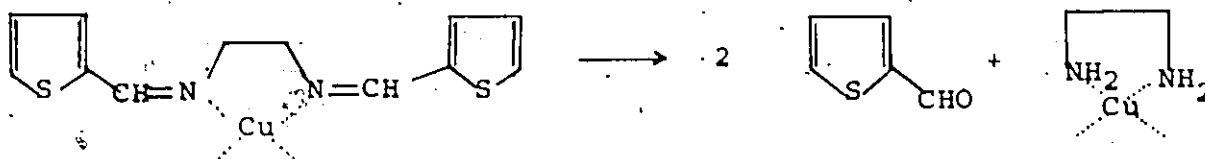
There is a change in the rate determining step which occurs between pH2 and pH5. Below this pH, the attack or loss of

water, (step A) is fast and the attack or loss of amine (step B), is rate determining. Above this pH, the situation is reversed with step B being fast and attack or loss of water or hydroxide ion being rate determining.

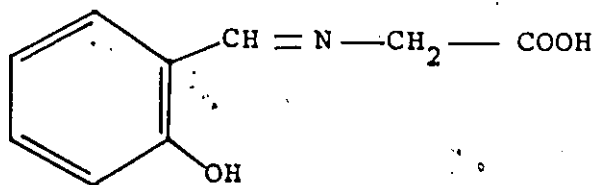
The influence of metal ions on the formation of Schiff bases has long been recognized, but serious study of the metal ion catalysis, or promotion, of the reactions of imines was started by Eichhorn et al (22,23). They observed that in the case of the Schiff base formed from ethylenediamine and 2-thiophenylaldehyde, i.e.



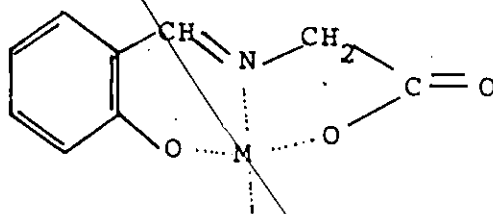
the hydrolysis is catalysed by divalent metal ions. Spectrophotometric evidence suggested the fast formation of a metal complex, e.g. with Cu(II), which then underwent hydrolysis:



The carbon-nitrogen double bonds are polarised by the metal ion and, furthermore, the reaction does not disrupt the chelate ring. In the case of the Schiff base formed from salicylaldehyde and glycine, i.e.



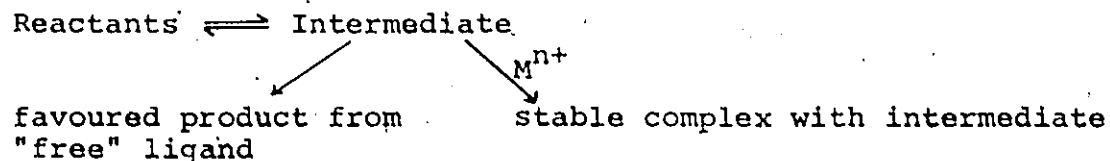
coordination with Cu(II) results in a stabilisation of the C=N bond under conditions where the free base undergoes hydrolysis<sup>(24)</sup>. This retardation of hydrolysis is ascribed to the stabilising influence of the two chelate rings in the Schiff base complex, i.e.



which would be reduced to one if the salicylaldehyde were removed. In a study<sup>(25)</sup> of the effects of Cu(II) and Ni(II) on the formation of the Schiff base referred to above, the reaction was shown to proceed much slower when one of the reactants, i.e. either salicylaldehyde or glycine, was mixed with the metal ion prior to the addition of the other reagent than when both reagents were mixed together before addition of the metal ion.

In connection with the synthesis of macrocyclic ligands, particularly those formed by Schiff base formation, Thompson and Busch defined what they called the "template" effect<sup>(26)</sup>. In its loosest form, this effect has been said to be operating if the presence of a metal ion promotes the formation of a Schiff base as its metal complex in solution<sup>(13)</sup>. This template effect may be further divided into a kinetic template effect and an equilibrium template effect. As originally

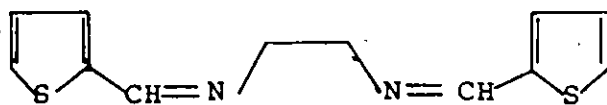
defined<sup>(26)</sup>, a kinetic template reaction is one in which "a metal ion may hold reactive groups within a substitution-inert complex in a proper array to facilitate a stereochemically selective multistep reaction". An equilibrium template reaction involves stabilisation of an intermediate in a purely thermodynamic effect, i.e.



Obviously, a simple equilibrium template effect, unless it was followed by a kinetic template reaction, would have no place in a true metal ion catalysed reaction as opposed to a metal promoted one.

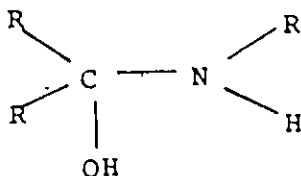
Much of the more recent literature reporting the metal ion catalysed formation or hydrolysis of imines is concerned with whether or not there is a template effect operating. In some cases, this effect is defined, or interpreted, as meaning whether or not both reagents must be bound to the metal ion prior to reaction. Some of the results in this area will be discussed in the next few pages.

In the light of the above statements, the further investigation<sup>(27)</sup> of the hydrolysis of



coordinated to a series of different metal ions is of some interest. This work led to the suggestion that coordinated water is responsible for the hydrolysis of the coordinated Schiff base and, in complexes where the maximum coordination number of the metal is satisfied by the ligand, hydrolysis will be resisted.

One case where the metal does not kinetically catalyze the formation of the Schiff base is in the reaction between pyridoxal phosphate and glutamate ions in the presence of Cu(II) ions<sup>(28)</sup>. Here the metal ion acts only as a trap for both the Schiff base and an amino-alcohol intermediate. A similar conclusion, i.e. the absence of a kinetic template mechanism, resulted from a study of Cu(II) ion promoted formation and hydrolysis of the Schiff bases formed from salicylaldehydes and aliphatic amines<sup>(29)</sup>. The mechanisms were shown to be similar to those obtaining in the absence of metal ions, and the role of the metal ion was to trap the carbinolamine intermediate:



Leussing, one of the major contributors in this field, investigated the kinetics of formation of the zinc (II) complex of the Schiff base formed from glycine and pyruvate<sup>(30)</sup>. Again, Zn (II) was found not to be acting as a kinetic template, but rather stabilizing the intermediate carbinolamine and imine product through coordination, while the effective catalyst in both the

addition and dehydration steps is a proton. The initial step, addition of glycine to pyruvate, was observed to be independent of Zinc (II).

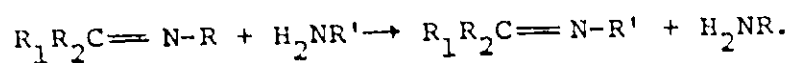
The first quantitative evidence in favour of a kinetic template mechanism was also reported by Leussing<sup>(31)</sup>. Studying the kinetics of formation of the Schiff base complexes from salicylaldehyde, glycine and Ni(II), Cu(II) and Zn(II) ions he found that, in the cases of Ni(II) and Cu(II), the rates were independent of the metal ion. For the case of Zn(II) there was a metal independent path, as in the other two cases, but there also was a metal dependent one. The metal independent path in all three cases indicated rate-determining formation of the free Schiff base followed by rapid reaction of this with the metal ion. For the metal dependent path in the Zn(II) case there is a fast equilibrium forming a ternary complex, in which the ligands are independently bound, i.e.  $Zn(Sal)(Gly)$ , which then undergoes a first order, rate-determining reaction to give  $Zn(Salgly) + H_2O$ , i.e. the complexed Schiff base. In an extension<sup>(32)</sup> of this study to a wider range of divalent metal ions, it was found that the order of catalytic activity for the metals tested was  $Pb \gg Cd > Mn \sim Mg > Zn \gg Co, Ni, Cu$ . It was also suggested that the term "promnastic" (from the Greek, matchmaker) be applied to describe a catalyst which forms a labile ternary complex with two substrates, but which imposes a minimum steric requirement on them. The term template is considered to imply



a fixed spatial orientation of the substrates, which, it is suggested, would in fact cause inactivity of the metal ion as a catalyst.

The kinetics of formation of the Zn(II) complex of the Schiff base of pyruvate and glycine have been shown to exhibit similar features<sup>(33)</sup>, as have the Zn(II) complexes of Schiff bases derived from salicylaldehyde and various amines<sup>(34)</sup>.

A reaction which is closely related to the formation and hydrolysis of imines is amine-exchange or transimination, i.e.



The metal ion catalysis of these reactions has apparently been little studied. In one report<sup>(29)</sup> the effect of Cu(II) ions on Schiff base formation between 5-sulfosalicylaldehyde and both ethylamine and glycinate was observed. The ethylamine Schiff base formed first, with a slow transformation to that of the glycinate. This is a metal ion promoted reaction, and the tridentate chelate of the glycinate Schiff base will be more stable. The results are interpreted to indicate that the transimination reaction, like the Schiff base formation in this system, does not go via a kinetic template mechanism, but it does, of course, show a thermodynamic "template" effect.

The second report<sup>(34)</sup>, on transimination in the presence of metal ions, was concerned with Schiff bases formed from salicylaldehyde with various amines and using Zn(II) as the metal ion.

The conclusion was that the transamination reactions were much faster, both for the metal dependent "promnastic" mechanism and the metal independent mechanism, than the corresponding reactions of the amines with salicylaldehyde.

One of the strongest stimuli for much of the work on metal ion catalysed reactions of Schiff bases or imines has been the very important role that these compounds play in enzyme catalysis. Schiff bases are believed to be intermediates in such reactions of amino acids as racemization, decarboxylation, transamination, transamination,  $\beta$ -substitution, elimination and condensation<sup>(9)</sup>. In many cases, the enzymes involved contain metal ions, e.g. both carboxypeptidase and carbonic anhydrase contain Zn(II).

## CHAPTER 2

### BASIC MAGNETIC RESONANCE THEORY

#### (A) INTRODUCTION

The use of nuclear magnetic resonance (NMR) is now very widespread in almost all areas of chemistry. The theory of NMR is well developed and understood. Many excellent reviews and books have been published dealing with both the theory and with applications to chemistry<sup>(35-37)</sup>.

The detection of nuclear magnetic resonance in bulk materials can be accomplished in several ways. The earlier commercial instruments, or spectrometers, used continuous wave (cw) techniques. In these instruments the radiofrequency (rf) is applied continuously during the time the spectrum is observed. The signal is detected by slowly varying the frequency of the rf signal applied to the sample in a fixed magnetic field or, alternatively, sweeping the field with the rf fixed in frequency. Such instruments constitute the vast majority of those in operation at present and most of the results in this thesis were collected using spectrometers of this kind.

Another method for obtaining NMR spectra involves the application of pulses of rf power at a particular frequency. The information is obtained by observing the decay of the rf signal

after the termination of the pulse. The Fourier transform of this decay gives the normal NMR spectrum. Such an instrument was acquired by the McMaster chemistry department in August 1974 and a number of experiments using this spectrometer are reported. Several books covering the area of FT NMR are now available (38,39).

#### (B) NMR IN PARAMAGNETIC SYSTEMS

Many of the NMR spectra reported in this thesis are of solutions containing paramagnetic metal complexes, and a short review of the pertinent theory is therefore appropriate. The application of NMR to the study of paramagnetic systems commenced about 1960 and since then has expanded rapidly. Several reviews (40-43) and a recent book (44) have been written on the subject.

Whether or not the NMR spectrum of a paramagnetic molecule can be observed at all, depends primarily on the relaxation time of the electron or electrons responsible for the paramagnetism. If the electron spin relaxation time  $T_{1e}$  is much less than  $A^{-1}$  (where  $A$  is the hyperfine coupling constant, in Hz, between the electron and the nucleus in question) then a reasonably sharp NMR spectrum may be observed. The condition for observing a well resolved electron spin resonance (ESR) spectrum is just the opposite, i.e.  $T_{1e} \gg A^{-1}$ .

One of the great advantages of studying paramagnetic systems is that there are usually large shifts in the resonance frequencies of various nuclei from their normal diamagnetic positions. These shifts originate from two types of interactions,

designated as contact and dipolar. The effect of the latter interaction is sometimes called a pseudocontact shift.

The contact shift is given by the expression (40):

$$\frac{\Delta\nu}{\nu_0} = \frac{\Delta H}{H_0} = -A \frac{g_e^2 \beta_e^2}{g_N \beta_N} \cdot \frac{S(S+1)}{3kT} \quad 2.1$$

where  $\frac{\Delta\nu}{\nu_0}$  or  $\frac{\Delta H}{H_0}$  is the fractional shift,  $g_e$  and  $g_N$  are the  $g$  factors of the electron and nucleus respectively,  $\beta_e$  and  $\beta_N$  are the Bohr magneton and nuclear magnetons,  $S$  is the spin quantum number of the electronic state and  $A$  is the hyperfine coupling constant.

The hyperfine coupling constant  $A$ , and thus the contact shift may be related to the unpaired electron spin density at the nucleus by the Fermi formula (40):

$$A = \frac{8\pi}{3h} g_e g_N \beta_e \beta_N [\psi(0)]^2 \quad 2.2$$

where  $\psi(0)$  is the wave function describing the electron evaluated at the nucleus.

The dipolar or pseudocontact shift arises from the direct interaction of the nuclear and electron dipoles and, for the case of a metal complex with axial symmetry, is given by the equation (44):

$$\frac{\Delta\nu}{\nu_0} = -\frac{\beta^2(S+1)}{27kT} (g_{||} + 2g_{\perp})(g_{||} - g_{\perp}) \frac{(3\cos^2\theta - 1)}{r^3} \quad 2.3$$

where  $\theta$  is the angle between the principal magnetic axis and the line connecting the central metal atom with the nucleus under consideration and  $r$  is the distance between the metal atom and

this nucleus. The components of the  $g$  tensor which are parallel and perpendicular to the principal axis of the complex are  $g_{||}$  and  $g_{\perp}$ , respectively. The above expression holds for a rapidly tumbling complex in solution and the dipolar shift will be zero if  $g_{||}^2 = g_{\perp}^2$ . For organic radicals  $g_{||} - g_{\perp}$  is rather small but this is not the case for metal complexes.

The contact and dipolar terms together give rise to the "isotropic" shifts observed in paramagnetic transition metal complexes. Attempts to separate these effects have aroused much interest, and provided employment for many chemists over the past ten years. The above equations for the contact and dipolar shifts will, in general, be correct for complexes with A or E electronic ground states. Molecules having triply degenerate T ground states usually require the more detailed theory of Kurland and McGarvey<sup>(45)</sup>.

The two expressions 2.1 and 2.3 predict a simple dependence of the isotropic shift on temperature. The Curie law should be obeyed, i.e. a linear dependence on  $T^{-1}$  with a zero intercept is anticipated. Experimentally many complexes do show a linear dependence on  $T^{-1}$  but, in most cases, the plot does not pass through the origin and the intercepts vary widely. The factors which can give rise to curvature of such plots are: (a) a degenerate ground state leading to a sizable orbital contribution to the magnetic moment<sup>(46)</sup>, (b) a rapid structural isomerisation involving a diamagnetic and a paramagnetic structure or a "spin equilibrium" i.e. a complex with two thermally accessible spin states in equilibrium<sup>(44)</sup>, or (c) ion pairing<sup>(44)</sup>. The origin of the non-zero intercepts is not well understood but has been discussed by

various authors (46,47).

The other major effect of paramagnetism is on the relaxation times of nuclei in the complex or in the surrounding solution. Depending on the electron spin relaxation time and the rate of tumbling of the complex in solution, broadening of the NMR spectral lines may occur. This leads to loss of resolution and, in extreme cases, to a complete inability to locate the resonance. Cobalt(II) complexes usually have a very short electron spin relaxation time, leading to only modest broadening of their NMR spectra. They are, therefore, particularly well suited to the type of studies described in the present thesis.

### (C) EFFECTS OF CHEMICAL EXCHANGE

#### (i) General Considerations

Processes which cause interchange of nuclei from one environment in a solution to another may have marked effects on the observed NMR spectra. In cases where the time scale of these processes or motions is of the same order of magnitude as the reciprocal of the frequency separations of the lines in the NMR spectrum, information about the rates of the processes in question may be obtained from a study of the spectrum. Typically, NMR chemical shifts differences range from a few Hz to a thousand Hz, which corresponds to lifetimes for the rate processes of  $10^0$  to  $10^{-3}$  seconds. The significance of this approach is that it can provide information about fast and very fast reactions from measurements on systems that are chemically at equilibrium. This area has been extensively reviewed (36,37,44,48).

The first quantitative theory of chemical exchange in NMR was given by Gutowsky, McCall and Slichter<sup>(49)</sup>. Later McConnell<sup>(50)</sup> gave a simpler derivation of the same result. Both descriptions start with the phenomenological Bloch equations<sup>(37)</sup>. The Bloch equations, as modified by McConnell<sup>(50)</sup>, are given below for the case where a nucleus X is reversibly transferred between two molecular environments A and B.

$$\frac{du_A}{dt} + \Delta\omega_A v_A = -\frac{u_A}{\tau_A} + \frac{u_B}{\tau_B} \quad 2.4$$

$$\frac{du_B}{dt} + \Delta\omega_B v_B = -\frac{u_B}{\tau_B} + \frac{u_A}{\tau_A} \quad 2.5$$

$$\frac{dv_A}{dt} - \Delta\omega_A u_A = -\frac{v_A}{\tau_A} + \frac{v_B}{\tau_B} - \omega_1 M_z^A \quad 2.6$$

$$\frac{dv_B}{dt} - \Delta\omega_B u_B = -\frac{v_B}{\tau_B} + \frac{v_A}{\tau_A} - \omega_1 M_z^B \quad 2.7$$

$$\frac{dM_z^A}{dt} - \omega_1 v_A = \frac{M_z^A}{T_{1A}} - \frac{M_z^A}{\tau_{1A}} + \frac{M_z^B}{\tau_B} \quad 2.8$$

$$\frac{dM_z^B}{dt} - \omega_1 v_B = \frac{M_z^B}{T_{1B}} - \frac{M_z^B}{\tau_{1B}} + \frac{M_z^A}{\tau_A} \quad 2.9$$

Here  $u$ ,  $v$  and  $M_z$  are the components of the X magnetisation which are in phase with the rotating component of the applied rf field, out of phase with this rf field, and along the large static magnetic field  $H_0$ , respectively. These magnetisations can be written as the sum of the contributions from nuclei in the A and B



environments.

$$u = u_A + u_B$$

$$v = v_A + v_B$$

$$M_z = M_z^A + M_z^B$$

$M_O^A$  and  $M_O^B$  are the equilibrium z magnetisations, where the z direction is defined by the static field  $H_O$ .  $\omega_1 = \gamma H_1$  where  $H_1$  is the applied rf field. The lifetimes  $\tau_{1A}$  and  $\tau_{2A}$  are defined by

$$\frac{1}{\tau_{1A}} = \frac{1}{T_{1A}} + \frac{1}{\tau_A} \quad 2.10$$

$$\frac{1}{\tau_{2A}} = \frac{1}{T_{2A}} + \frac{1}{\tau_A} \quad 2.11$$

where  $T_{1A}$  and  $T_{2A}$  are the longitudinal (spin-lattice) and transverse relaxation times of X in site A, and  $\tau_A$  is the lifetime of X in site A. Analogous expressions define  $\tau_{1B}$  and  $\tau_{2B}$ . The equations 2.4 to 2.9 are obtained from the Bloch equations by adding terms to allow for the effects of chemical exchange. For example, in equation 2.4 the term  $-u_A/\tau_A$  is added to allow for the rate at which  $u_A$  decreases due to loss of magnetisation to site B, and  $u_B/\tau_B$  is added to allow for the rate at which  $u_A$  increases due to the chemical transfer of magnetisation into site A from site B. The unmodified Bloch equation is

$$\frac{du_A}{dt} - \Delta\omega_A v_A = -\frac{u_A}{T_{2A}}$$

which, with the addition of the terms  $-u_A/\tau_A + u_B/\tau_B$ , yields equation 2.4.

The modified Bloch equations may be used to describe both the line broadening effects, as observed by the slow passage technique, and the transient effects in rapid passage or multiple resonance experiments. Both applications will be encountered in the present thesis.

#### (ii) Slow Passage Experiments

In a slow passage experiment, the observing rf field of low power (to avoid saturation) is swept slowly through the resonance maintaining equilibrium of the spin system. Under these conditions the rate of change of magnetisation is zero and therefore

$$\frac{du_A}{dt} = \frac{du_B}{dt} = \frac{dv_A}{dt} = \frac{dv_B}{dt} = \frac{dM_z^A}{dt} = \frac{dM_z^B}{dt} = 0$$

The resulting simultaneous linear equations (from equations 2.4 to 2.9) can be solved explicitly in many special cases and can always be evaluated numerically.

For the case of two diamagnetic molecular environments, A and B, with equal populations, i.e.  $\tau_A = \tau_B = \tau$ , and where  $T_{1A} = T_{1B} = T_1$  and  $T_{2A} = T_{2B} = T_2$ , some of the limiting spectra are shown in figure 2.1(a) (44).

Spectrum (i) is for the case of very slow exchange where  $\frac{1}{\tau} \ll \Delta\omega$  and  $\frac{1}{T_2}$ , with  $\Delta\omega$  being the frequency separation of the two lines. If the exchange rate is increased slightly ( $\frac{1}{\tau} \sim \frac{1}{T_2} \ll \Delta\omega$ ) the lines are still separate but the linewidth

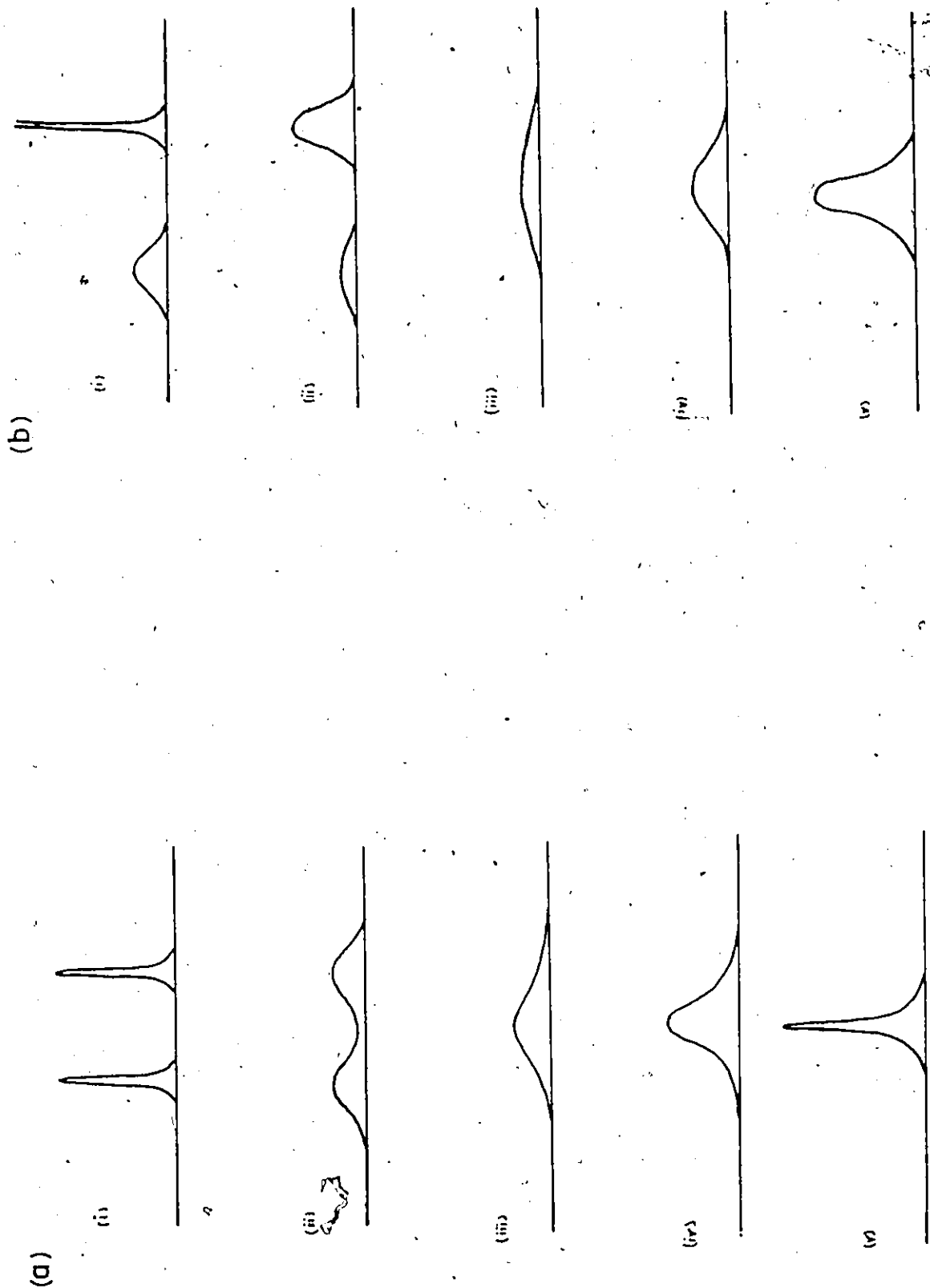


Fig. 2.1 NMR lineshapes as a function of exchange rate: (a) two diamagnetic sites; (b) one paramagnetic and one diamagnetic site. From reference 44

has been increased by the chemical exchange. This is shown in fig. 2.1(a) (ii) and is known as the slow exchange region. Spectrum (iii) shows an intermediate region where the lineshape is described by a complicated expression. In the region of spectrum (iv) the halfwidth of the single line is given by

$$\frac{1}{T_e} = \frac{1}{T_2} + \frac{1}{8} \Delta\omega^2 \tau. \quad 2.12$$

Finally, in the fast exchange limit the spectrum is a single line located halfway between the two original peaks with a linewidth  $\frac{1}{T_2}$ , as shown in spectrum (v). If  $T_1$  and  $T_2$  are not strongly influenced by temperature, then the exchange lifetimes  $\tau$ , and thus the exchange or reaction rates, may be determined by the study of the line shape at various temperatures using the approximations in their appropriate region, or using a full computer-fitted line shape analysis.

In the case where one of the environments is paramagnetic, the largest difference is that the separation of the two lines is now of the order of thousands of Hz due to the isotropic shift. In figure 2.1(b) are shown the spectra corresponding to those in figure 2.1(a), but with site A now being a paramagnetic environment. Similar equations apply to the various regions as in the previous case of two diamagnetic sites.

### (iii) Spin Saturation Transfer

The second area in which information about rates of reaction or exchange can be extracted from NMR spectra involves perturbing the spin magnetisation equilibrium. This may be done

using rapid passage, multiple resonance or pulse techniques. McConnell and Thompson<sup>(51,52)</sup> used the rapid passage method to study the proton transfers in the  $\text{NH}_4^+$  ion in acid solution. However, experimental factors make a multiple resonance experiment superior to rapid passage in most cases<sup>(48)</sup>.

The transfer of non-equilibrium magnetisation from one site to another can occur if one site in a two site exchange is irradiated with an rf field sufficiently strong to cause saturation. In a system where X exchanges between site A and site B, and where the resonance at B is completely saturated, then a decrease in intensity will be observed in the A resonance if  $\tau_A \sim T_{1A}$ . Here,  $\tau_A$  is the average lifetime that X spends in site A and  $T_{1A}$  is the spin lattice relaxation time of X in site A. Such a decrease in intensity is due to spin saturation transfer and measurements of the effect can yield information about rates of exchange or of reaction.

The equations which describe the time dependent behaviour of the spin system in a multiple resonance experiment (one saturating rf field and one weak observing field) may be simply derived from McConnell's equations, i.e. equations 2.4 to 2.11. For a two site system where  $\tau_A$  and  $\tau_B$  are sufficiently long to give well resolved resonances for nucleus X in sites A and B (i.e. between spectrum (i) and spectrum (ii) in figure 2.1(a)), the time dependence of the z magnetization of X in site A ( $M_z^A$ ) is given by equation 2.8<sup>(53)</sup>.

$$\frac{dM_z^A}{dt} - \omega_1 v_A = \frac{M_0^A}{T_{1A}} - \frac{M_z^A}{T_{1A}} + \frac{M_z^A}{T_B}$$

If we now assume that resonance B is completely saturated by a strong rf field centred on B, then  $M_z^B$  will be zero. Also, if A is observed with a very weak rf field so as to cause negligible perturbation of the spin equilibrium, then the term  $-\omega_1 v_A$  can be dropped giving:

$$\frac{dM_z^A}{dt} = \frac{M_0^A}{T_{1A}} - \frac{M_z^A}{T_{1A}} \quad 2.13$$

Under the conditions of slow passage, the intensity of the observed signal due to X in site A will be proportional to the value of  $M_z^A$ . If site B is instantaneously saturated at time  $t=0$  when  $M_z^A = M_0^A$ , then the decay of the magnetisation  $M_z^A$  is given by:

$$M_z^A(t) = M_0^A \left[ \frac{T_{1A}}{\tau_A} e^{-\frac{t}{T_{1A}}} + \frac{\tau_A}{T_{1A}} \right], \quad 2.14$$

and the new equilibrium value of  $M_z^A (=M_\infty^A)$  is given by :

$$M_\infty^A = M_0^A \left( \frac{\tau_A}{T_{1A}} \right) \quad 2.15$$

Thus, measuring the intensity at A with and without the saturating field at B will give the ratio  $\frac{\tau_A}{T_{1A}}$ . The spin-lattice relaxation time at A,  $T_{1A}$ , may either be measured independently, or a plot of  $\ln[M_z^A(t) - M_\infty^A]$  against  $t$  for the decay will yield a value of  $\tau_{1A}$  from the slope. The value of  $\tau_A$  may be determined by either method. Similar considerations apply to the reverse experiment of observing B while saturating A which should yield  $\tau_B$ . A check

is provided by the fact that  $\frac{M_O^A}{M_B^A}$  should equal  $\frac{\tau_A}{\tau_B}$ .

Another case of interest involves the recovery of signal A after the saturating rf field at B is removed. The recovery of  $M_Z^A$  is given by

$$M_Z^A(t) = M_O^A + c_1 e^{-\lambda_1 t} + c_2 e^{-\lambda_2 t} \quad 2.16$$

where

$$c_1 = M_O^A \frac{\lambda_2 (T_{1A} - \tau_{1A})}{(\lambda_1 - \lambda_2) T_{1A}}$$

$$c_2 = M_O^A \frac{\lambda_1 (T_{1A} - \tau_{1A})}{(\lambda_2 - \lambda_1) T_{1A}}$$

and

$$\frac{c_1}{c_2} = - \frac{\lambda_2}{\lambda_1}.$$

In general, the recovery of  $M_Z^A$  will not be a simple exponential function, but, if  $\lambda_1/\lambda_2$  is much greater or less than unity, there will only be one dominant term in equation 2.16, and the recovery of  $M_Z^A$  will be a simple exponential function. In the case of two equally populated sites where  $\tau_{1A} = \tau_{1B}$  the recovery will be of the form (54)

$$M_Z^A(t) - M_O^A = c_2 e^{-\frac{t}{T_{1A}}} \quad 2.18$$

where  $\frac{\lambda_1}{\lambda_2} \gg 1$  and  $\lambda_2 = \frac{1}{T_{1A}}$ .

In this case,  $T_{1A}$  may be determined from the slope of the plot of  $\log[M_Z^A(t) - M_O^A]$  against time. Anet and Brown (54) suggest that  $\frac{\lambda_1}{\lambda_2} > 2$  is a sufficient condition to allow determination of  $T_{1A}$  from the recovery curve.

#### (D) SURVEY OF SST LITERATURE

In the previous section the simple theory which will be used to interpret the spin saturation transfer experiments in this work has been described. The method has been variously described as double resonance, transfer of spin saturation (TOSS)<sup>(55)</sup>, or spin saturation labeling<sup>(2)</sup>. A review entitled "Spin saturation labeling", written by Faller, has been published<sup>(56)</sup> which gives a selective coverage of the literature prior to 1970. This review also discusses the theory in the manner of Forsen and Hoffman<sup>(53,57)</sup> and includes a section on experimental methods. The earlier work is also discussed in more detail in a chapter in "The Nuclear Overhauser Effect"<sup>(58)</sup>, and in a review by von Philipsborn<sup>(59)</sup>.

The majority of applications of SST techniques have been non-quantitative, that is, they have been concerned with determining whether two sites are or are not in exchange on the NMR time scale. This has proved very useful in elucidating the mechanism of many varied exchanges and reactions. This aspect has been covered by Faller<sup>(56)</sup>.

Recent papers have discussed the theory of SST. Fung<sup>(60)</sup> has used density matrix methods to describe the transfer of magnetisation via spin-spin coupling which leads to indirect spin saturation. Yang<sup>(61)</sup> has given a full density matrix treatment of double resonance in chemically exchanging systems. Gore and Gutowsky<sup>(62)</sup> have discussed the effects of intramolecular



chemical exchange on NMR spectra and give some conditions to be observed in SST experiments.

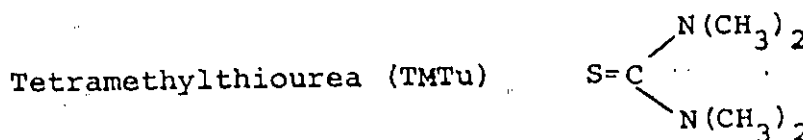
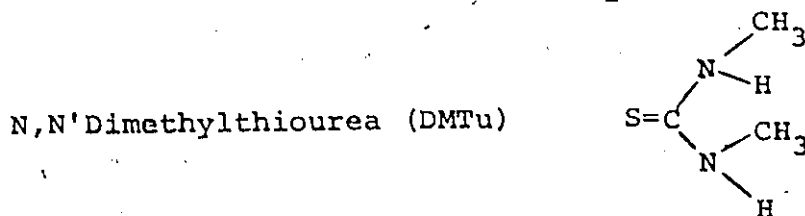
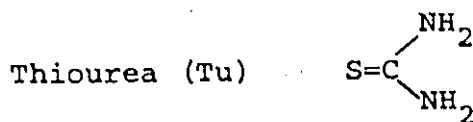
Practical quantitative studies have been rare. In their original work Forsen and Hoffman<sup>(53,57)</sup> measured exchange rates with acetylacetone in solution. Sherrod et al<sup>(63)</sup> used SST to determine a kinetic isotope effect in [2,2] metaparacyclophanes. Kabakoff and Namanworth<sup>(64)</sup> have measured a rotation barrier in the dimethylcyclopropylcarbinyll cation, information not available from methods other than SST because of decomposition at temperatures where line broadening occurs. Van Leewveen and Praat<sup>(65)</sup> measured exchange rates in  $\pi$ -allyl Pd complexes and discuss the theory, experimental conditions, and problems of the technique. In an interesting study, Creelmore and Reilly<sup>(66)</sup> used the Forsen and Hoffman method to determine exchange rates for water with an ion exchange resin and the relaxation times of free and bound water. Finally, Redfield et al<sup>(67,68)</sup> have used an FT SST technique to study the rate of electron transfer between the two oxidation states of cytochrome C and also the rate of exchange by ligands with ferricytochrome C.

## CHAPTER THREE

### EXPERIMENTAL

#### (A) SOURCES OF CHEMICALS

The following are the structures of the thiourea ligands used in this study, together with their usual abbreviations:



A variety of zinc, cobalt and nickel complexes of these, and similar ligands, have been prepared in this laboratory<sup>(69)</sup> by Dr. K. Zaw and were available for the present study. Some further complexes, eg,  $\text{Co}(\text{TMTu})_2\text{Cl}_2$ ,  $\text{Zn}(\text{TMTu})_2\text{Br}_2$  and  $\text{Co}(\text{Tu})_4(\text{ClO}_4)_2$  were prepared using methods similar to those used previously<sup>(69)</sup>. In a typical preparation, stoichiometric quantities of the metal halide and ligand were each dissolved in a minimum quantity of hot alcohol, usually n-butanol. The solutions were mixed, cooled,

and the product collected. The compounds were recrystallised from the alcohol and pumped dry on a vacuum line.

The deuterated solvents used in this study (acetone d-6 and acetonitrile d-3) were obtained from Merck, Sharp and Dohme. The extent of deuteration was 99% or better. The anilines were obtained from various suppliers, and were either sublimed or distilled before use.

#### (B) SAMPLE PREPARATION

Since the reactions studied are effectively catalysed by traces of metal salts or complexes as well as by acids, it was necessary to maintain extremely clean working conditions and equipment. New NMR tubes were used whenever possible; and used tubes were cleaned in aqua regia, then with a commercial cleaning and decontaminating fluid, RBS 25 (Norell Chemical Company), followed by repeated washings in distilled water. Before use, tubes were rinsed with acetone and dried with a heat gun under a stream of dry nitrogen. Catalyst solutions were prepared by weighing a single crystal of catalyst on a balance capable of weighing to  $10^{-6}$  of a gram, and then adding solvent volumetrically. Samples were prepared by weighing the aniline or the anil into the NMR tube, adding solvent (0.50 ml) by syringe, and then adding the catalyst solution from a 30  $\mu$ l syringe.

#### (C) NMR SPECTROMETERS

Three NMR spectrometers were used during the course of this study. A Varian DP60 instrument was used to observe both  $^1\text{H}$  and  $^{19}\text{F}$  at 56.4 MHz (later modified to 58.3 MHz). Most of the

proton NMR was carried out on a Varian HA100 which could also observe  $^{19}\text{F}$  at 94.1 MHz. In the later stages of this work, a Bruker WH90 Fourier transform spectrometer became available and was used for spin saturation transfer experiments, and to run  $^{13}\text{C}$  NMR spectra. All three instruments were capable of variable temperature operation using liquid nitrogen as a cooling agent. A thermocouple in an NMR tube was used to measure the temperature before and after running a spectrum at low temperature. The normal operating temperatures in the probes were HA100 34.5° to 35.0°C, DP60 27°C and WH90 26.5°C.

The experiments involving the measurement of the initial rate of a reaction, which are discussed in Chapter 5, were carried out on the HA100 spectrometer. The reaction was followed by using a voltage controlled frequency generator (by Wavetek) to provide the sweep frequency so that the area of interest in the spectrum was repetitively scanned while the pen recorder was running. The sample containing the aniline or anil, and a little TMS (tetramethylsilane) (to provide a locking signal), was placed in the probe and allowed to come to thermal equilibrium. The sample was then rapidly removed, the catalyst solution injected, a stopwatch started, and the tube shaken and replaced in the probe. The lock signal was relocated and the recorder started. This whole operation could be carried out in about 25 seconds and the first spectra were obtained about 30 seconds after the reaction had commenced. A typical output of this kind of experiment is shown in figure 3.1. This shows

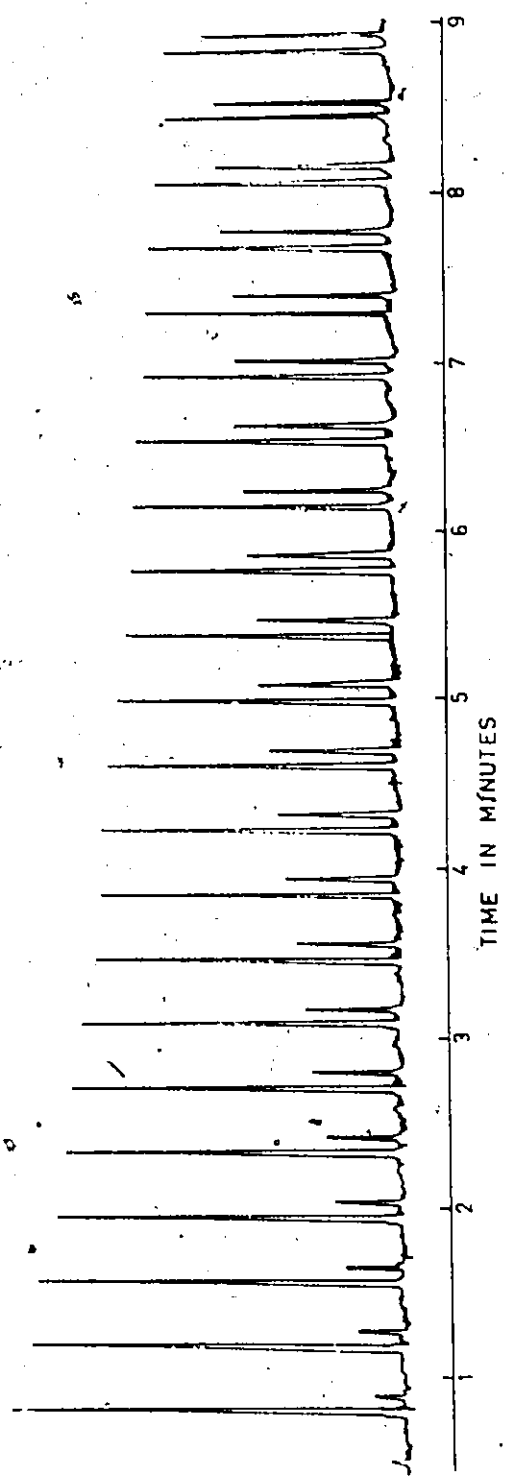


Fig. 3.1 An initial rate experiment. Repeated scanning of the methyl region monitors the reaction of p-toluidine to form its acetone anil

p-toluidine reacting with acetone to form the acetone anil. The large peak at the start is that of the para-methyl group of the p-toluidine which reacts to give the anil. The para-methyl group of the anil gives rise to the second, growing peak. The HA100 was locked to TMS and was swept from 190 Hz from TMS to 240 Hz from TMS every 23 seconds. The sweep is from high to low field and the resonance due to the residual  $^1\text{H}$  in the acetone d-6 is not shown.

When running the spectra of compounds such as  $\text{CoTu}_2\text{Cl}_2$  or  $\text{CoTu}_4(\text{ClO}_4)_2$ , where the proton signal due to the Tu is very broad ( $\sim 300$  Hz) and has a large isotropic shift caused by the paramagnetic cobalt atom, it was not possible to use the NMR spectrometer in a locked mode. In these cases it is possible to use non-deuterated solvents, and this affords an accurate method for determining the shift of the ligand protons. With two external oscillators set 1000 Hz apart, the ligand resonance can be straddled with two sharp sidebands of the solvent signal during an unlocked field sweep. The shift of the ligand signal relative to the solvent peak is then simply and accurately determined.

#### (D) SPIN SATURATION TRANSFER WITH CW SPECTROMETERS

The theory of the spin saturation transfer method for determining reaction lifetimes and rates has been discussed, in Chapter 2 Section C(iii). For a system consisting of two chemical environments, A and B, where a nucleus X is exchanging

between A and B, there are two possible experimental approaches to determining the rate. The first of these is to measure the ratio  $\frac{M_A^{\infty}}{M_A^0}$  which, from equation 2.15, gives  $\frac{\tau_{1A}}{T_{1A}}$ . If  $T_{1A}$  is known independently under these conditions then  $\tau_{1A}$  and thus  $\tau_A$  may readily be determined. For a first order reaction  $k_A = \frac{1}{\tau_A}$  where Rate =  $k_A[A]$ . The second method is to attempt to monitor the time dependence of the changes occurring at signal A as the saturating rf field is switched on and off at signal B. This latter method is considerably more difficult to carry out experimentally, and a set-up was evolved to automate such measurements on a Varian DP60 NMR spectrometer operating at 56.4 MHz, observing the  $^{19}\text{F}$  nucleus.  $^{19}\text{F}$  N.M.R. was used because of the large chemical shift ( $\sim 400$  Hz) between the fluorine resonances of para-F aniline and the acetone anil of p-F aniline, which were the two environments or sites. This meant that there was no fear of direct saturation at site A from the saturating field situated at site B, but rather that any effect at signal A must have been transferred by chemical exchange from site B to site A.

In order to simplify the spectrum, the spin-spin coupling between the fluorine atom and the ring protons was removed by irradiating the sample in the probe with a strong rf signal at 60.0 MHz. This was supplied from a crystal controlled frequency generator (General Radio Company) amplified with an operational amplifier (Model 805, RF Communications Inc.) and fed into two specially tuned coils fitted in the spectrometer probe. The exact frequency was selected by adjusting 1 Hz at a time until

the sharpest  $^{19}\text{F}$  signal in p-F aniline was obtained. This had a linewidth of less than 0.5 Hz. The spectrometer was operated in a locked frequency swept mode on the first upper sideband, and both the observing and saturating fields were generated by modulating with audio frequencies.

The method used was to position the observing frequency in the exact centre of one, say A, of the two peaks and then to observe the intensity at that frequency while the saturating field at peak B was switched on and off. Owing to the fact that the amplitude of the observing field had to be small so as to cause no saturation, the signal to noise ratio was low, and in order to improve this, the results of many cycles were added together in a CAT or computer of average transit (Varian Associates). An automatic device for switching the various fields and triggering the CAT was built and a schematic representation is shown in figure 2.2. The main component of this device was an accurate variable speed electric motor driving a plastic disc. Three microswitches pressing against the disc were opened and closed by cutouts in the disc. The first of these switches (1) activated a trigger pulse generating circuit built basically according to a published description <sup>(7.0)</sup>, and also opened a relay which caused a voltage to be applied to the input of a voltage controlled frequency generator (V.C.F.G.) (manufactured by Wavetek). This voltage was set by the potentiometer (4), and resulted in a jump in the frequency generated by the V.C.F.G. which was being used to saturate signal B. The reason for jumping the frequency to



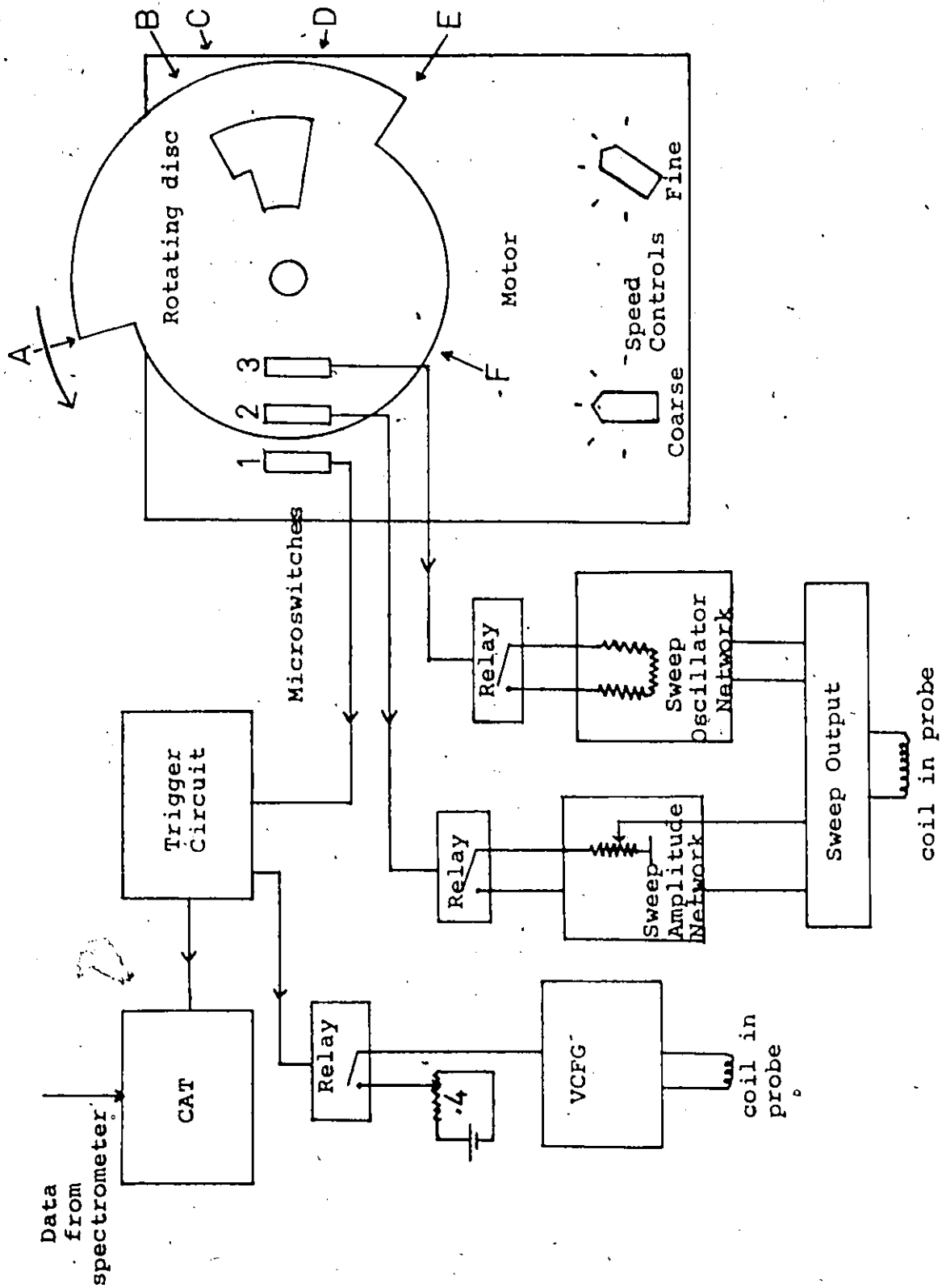


Fig. 3.2 A schematic of the equipment for spin saturation transfer experiments on a CW spectrometer.

an area of the spectrum removed from peaks A and B, rather than simply switching it off altogether, was that, by switching it off, the power in the other fields, also produced by modulating the basic rf frequency, would be changed thus disrupting the experiment.

Microswitch 2 controlled a relay which could switch off the observing field completely. This enabled the baseline to be determined so that the intensities could be measured. However, it was discovered that when the amplitude of the observing field was zero, there was a small residual peak at the frequency of the resonance which was about  $180^\circ$  out of phase with the normal absorption signal. This negative peak frequently had an intensity of about 10% of the intensity of the signals obtained with the amplitude of the observing field normally used in these experiments. In order to obtain a correct baseline, the observing frequency had to be shifted away from the resonance frequency of site A. This was accomplished by microswitch 3 which activated a relay changing a resistance in the sweep oscillator network. On the 50 Hz sweep width used in these experiments, the sweep frequency could be shifted 55 Hz downfield by opening microswitch 3.

In figure 3.3 is shown the result of a spin saturation transfer experiment. This was carried out with a mixture of p-F aniline and the acetone anil of p-F aniline in acetone,  $ZnTu_4(ClO_4)_2$  as a catalyst and Freon 112 as a lock. The y axis represents intensity at the centre of the decoupled anil resonance (site A), and the x axis represents time. The time elapsed

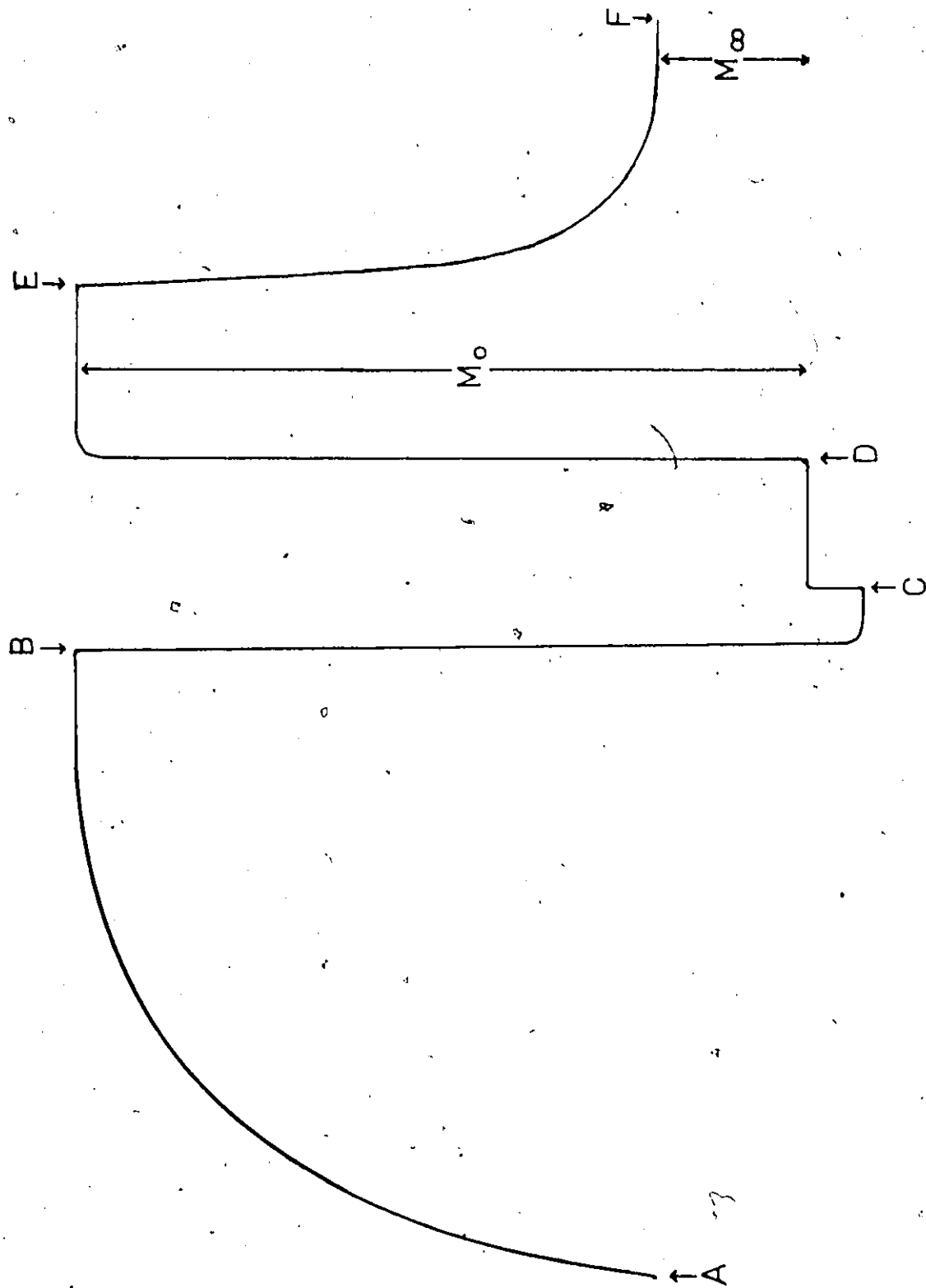


Fig. 3.3 Output from a spin saturation transfer experiment. Points labelled correspond to those in figure 3.2

from point A to point F was 100 sec. The points labelled A to F correspond to those in figure 3.2. At point A the CAT was triggered and simultaneously the saturating field at the aniline resonance (site B) was shifted to a point some 400 Hz away. Thus the anil resonance slowly recovered its intensity, eventually reaching the value  $M_0^A$ . At point B, the observing field was switched off, and the intensity of magnetisation rapidly decayed away. At C the observing frequency was jumped to a region away from any signals while it was still switched off. The difference in intensity noted between these last two settings represents the negative signal obtained at the frequency of the anil resonance, even when the observing field was switched off and was on open circuit. At D the observing field was returned to its original frequency and simultaneously switched on. At point E, the saturating field was returned to the frequency of the aniline (B) resonance and the anil (A) intensity decayed away exponentially, as predicted by equation 2.14. At the point F, the CAT finished its sweep and waited until the cycle was recommenced at point A. The time taken for one revolution of the disc was 180 sec, and data from as many cycles as desired could be accumulated in the CAT. The contents of the memory of the CAT were printed out using the spectrometer recorder. The decay of the magnetisation commencing at point E could be plotted in the form  $\ln[M_z^A(t) - M_\infty^A]$  against  $t$  in seconds, the slope of which gave  $\tau_{1A}$ . The ratio  $M_\infty^A/M_0^A$ , which equals  $\tau_{1A}/T_{1A}$ , enables  $T_{1A}$  to be determined and thus  $\tau_A$  from equation 2.11. The experiment can be repeated

observing site B and saturating site A yielding  $\tau_B$ . If the lifetimes are sufficiently short relative to the spin lattice relaxation times, then  $T_{1A}$  and/or  $T_{1B}$  can be determined from the recovery curves commencing at point A and using equation 2.17.

Practically, this experiment was complicated by the fact that all the frequency generators were required to be stable to at least  $\pm 0.1$  Hz; otherwise, the observing frequency would drift off the precise centre of the observed peak, causing a decrease in the observed intensity. Furthermore, the tuning of the decoupling frequency was very sensitive, and small drifts of the order of a few Hz in 60 MHz, caused broadening of the observed  $^{19}\text{F}$  signals. Since none of the frequency sources in the DP60 were tied to a common crystal source or clock, slight changes in room temperature caused them to drift relative to one another. For example, it was noted that a change in temperature of  $1^\circ\text{C}$  would cause a drift of about 12 Hz in the frequency generator producing the 60 MHz decoupling frequency. The conditions in the spectrometer room were not such as to prevent minor drifts in temperature from occurring. Unfortunately, the consequences of the resultant frequency drifts were not obvious until the method and equipment had been refined for some time by improving homogeneity and decoupling to sharpen the observed peaks. The actual experimental results will be presented in Chapter 7.

A simpler alternative method was to measure the intensity of peak A with the saturating field at peak B, and then again with the same field at a position remote from B. This was done

with the same equipment as before but with a different disc using only microswitch 1. The V.C.F.G. was used to sweep through signal A very slowly while the data was stored in the CAT. The saturating field at B was jumped away and after a delay the signal at A was scanned again. Both signals were recorded on a single sweep of the CAT and the cycle was repeated until the desired signal to noise ratio was achieved. The magnetization ratio  $\frac{M_{\infty}^A}{M_0^A}$  was measured by cutting out the peaks and weighing them. To determine  $T_1$  for p-F aniline the saturation recovery technique<sup>(71)</sup> was used with the same basic equipment. Now, however, the saturating frequency and the observing frequency was the same. At the same time as the CAT was triggered the saturating field was removed, and the recovery of the peak recorded. After as many cycles as desired were accumulated,  $T_1$  was determined by plotting  $\ln[M_0 - M_z(t)]$  against  $t$ , a graph which has a slope of  $T_1$ . Knowing  $T_{1A}$  and the ratio  $M_{\infty}^A/M_0^A$  means that  $\tau_A$  can be determined.

#### (E) SPIN SATURATION TRANSFER WITH FT SPECTROMETERS

##### 1. General Aspects

Fourier transform NMR spectroscopy is a difficult and involved field. The description which follows is brief and therefore somewhat simplified.

In FT NMR<sup>(38)</sup> a short pulse, a few microseconds long, of rf power is applied to the sample. This has the effect of causing the net magnetization ( $\vec{M}$ ) to precess about the axis along

which the pulse is applied. The length of the pulse determines what angle  $\vec{M}$  will be carried through; hence the terms  $90^\circ$  pulse or  $180^\circ$  pulse. After the pulse is turned off, the detector measures the  $M_{xy}$  component of the magnetisation, where the large static magnetic field ( $H_0$ ) lies along the z axis. The  $M_{xy}$  component decays with time due to transverse relaxation. This decay is called the free induction decay (FID); free since no rf is applied. The characteristic time for the FID is  $T_2^*$ , which is defined by the observed linewidth at half peak height of the signal, i.e.  $\nu_{1/2} = \frac{1}{\pi T_2^*}$ .  $T_2^*$  is frequently determined primarily by the magnetic field inhomogeneity. In FT NMR the detector is not continuously open during the decay, but rather samples the FID at various intervals. The time spent at each point of the FID is known as the dwell time and depends on the sweep width chosen. The Fourier transformation of the FID is carried out by the spectrometer's computer, and yields the normal NMR spectrum.

There are two methods for homonuclear decoupling available on the WH90 FT NMR spectrometer. One of these is pulsed homonuclear decoupling, where a single frequency is applied to the sample to saturate or decouple a single peak. The pulsed decoupler is only off during the actual sampling time which is very short, eg. 20 nanoseconds in a dwell time of 500 microseconds<sup>(72)</sup>. Thus, the pulsed decoupler is on virtually continuously. The second method is gated decoupling, and here the single frequency is applied for a suitable time before the rf pulse, and is switched off

as the pulse is beginning. The FID is collected and then the decoupler is switched on again for another cycle.

Measurements of  $T_1$ , the spin lattice or longitudinal relaxation time, are usually made on FT spectrometers using a  $180^\circ$ - $\tau$ - $90^\circ$  pulse sequence. Here a  $180^\circ$  pulse inverts the magnetisation  $\vec{M}$  from lying along the  $+z$  axis to lie along the  $-z$  axis. Longitudinal relaxation now occurs, and eventually the magnetisation will return to its original value ( $M_0$ ) along the  $+z$  axis with a characteristic time  $T_1$ . If, at any time after the  $180^\circ$  pulse, a  $90^\circ$  pulse is applied, the intensity of the signals observed will be a measure of the value of  $M_z$  when the pulse was applied. Thus, by varying the delay time  $\tau$  between the  $180^\circ$  and  $90^\circ$  pulses the recovery of  $M_z$  to its final value ( $M_0$ ) can be monitored. The expression for the recovery of  $M_z$  is

$$M_z = M_0 (1 - 2e^{-\frac{t}{T_1}}) \quad 3.10$$

Thus,  $T_1$  can be determined from the slope of a plot of  $\ln[M_0 - M_z]$  against  $\tau$ . The measurement of  $T_1$  by this method is fully automated on the WH90 spectrometer, and includes a routine to calculate  $T_1$  for each line in the spectrum.

There are three main advantages to using a FT spectrometer for spin saturation transfer experiments. One is that it is possible to measure  $T_1$  for each line in a sample, even when chemical exchange is taking place. This is because  $T_1$  is only affected by processes taking place with a frequency close to the



Larmor frequency, ie  $\sim 100$  MHz, whereas chemical exchange processes have frequencies close to the separation of the peaks involved, ie a few Hz to a few hundred Hz. Thus the problems of determining  $T_1$  from decays or recoveries, or else of transferring a value determined in the absence of exchange are removed. The second advantage is that the separation of the saturated and the observed peak can be quite small (less than 10 Hz) without causing direct saturation of the observed peak. The third advantage is that good signal to noise ratios may be quickly obtained by accumulating FIDs in the computer.

(ii) Practical Considerations

The spin saturation transfer experiments using the WH90 were carried out on solutions containing p-toluidine and its acetone anil. In the  $^1\text{H}$  NMR spectrum, the two para-methyl resonances in this system are 10 Hz apart at 90 MHz. The gated decoupler was found to be the most satisfactory, as the pulsed decoupler produced more distortion of the baseline and of other signals near to the decoupling frequency. The gated decoupling method ideally requires the observed peak to remain at constant intensity whilst the FID is acquired. However, if  $T_2^* \ll T_1$ , then the information will be acquired before changes in the intensity of the observed peak become important. In the system in question,  $T_1$  was about 3 seconds and  $T_2^*$  about 1 second. To make  $T_2^*$  even smaller, the homogeneity of the magnetic field could be deliberately reduced, or the same effect could be produced artificially in the computer by multiplying the FID by an exponential factor

before Fourier transformation. In a check experiment involving spin saturation transfer, the same FID was multiplied by various exponential factors, but no changes in intensity (measured relative to a reference peak) of the observed or site A peak were noted. Another way to minimise the effect of changing intensity in spin saturation transfer experiments would be to keep  $\tau_A > T_{1A}$  or  $M_{\infty}^A/M_0^A$  roughly greater than 0.5. These conditions were adhered to. Experimentally, the gated decoupler was switched on for 20 seconds, then a 4  $\mu$ sec pulse was applied, the FID collected within 5 seconds, and then the decoupler switched on again. The 20 second period was necessary to ensure that the observed peak had reached its  $M_{\infty}$  value before its intensity was measured.

Since the peaks were only 10 Hz apart, it was necessary to determine if there was any direct effect of the saturating field on the observed peak. This was accomplished by taking a solution of p-toluidine on its own and fixing the decoupler frequency where the anil peak would be. The power output of the decoupler was then varied and the intensity of the p-toluidine peak relative to a reference peak (TMS) was measured. The results are shown in figure 3.4. A power setting of -0.5 was selected for use in the spin saturation transfer experiments. This should eliminate any direct saturation effects. Finally, because of the distortion of the baseline in the vicinity of the saturating frequency, the internal routines for intensity and area calculations were unreliable, and so the intensities

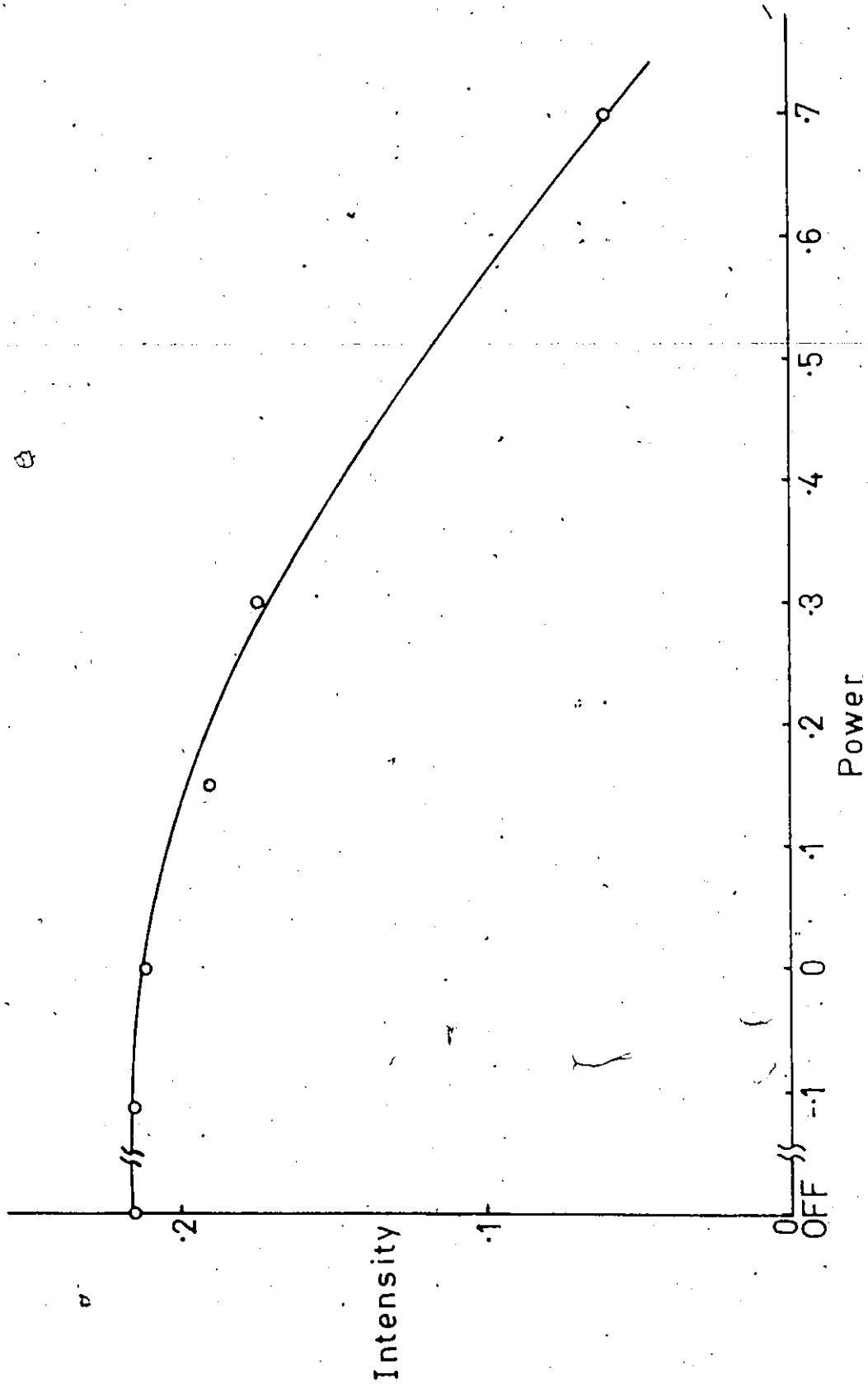


Fig. 3.4 Effect of decoupler output power on intensity. The intensity of the p-toluidine signal, measured as a fraction of a standard signal, is plotted against the power setting on the gated decoupler.

were measured directly from spectra. Intensities were always measured relative to a standard reference peak, usually TMS.

CHAPTER FOUR  
THE OVERALL REACTION

(A) Introduction

As outlined in Chapter 1 there has been a sizeable amount of work devoted to the study of metal catalysed or promoted reactions, particularly in the area of reactions of esters and imines. Most of this work has been carried out in water or in predominantly aqueous solvent mixtures. This leads to some major complications. One of the foremost of these is the problem of knowing exactly which species are present in a solution and more difficult still, which ones are reacting. This is due in part to the possibility of protonating a species A to yield  $AH^+$ ,  $AH_2^{2+}$  etc., or of the loss of a proton from AH to give  $A^-$ . A prerequisite of any kinetic work in aqueous solution is thus to determine what species will be present at various values of the pH. Frequently the pH will also change during a reaction which can complicate matters further. Changes in ionic strength must also be considered. When the metal ion is added to such a system then all the equilibrium constants for the complexing of the various reactant and product species, including the formation of mixed complexes, must be known or determined.

Another problem in aqueous solution is the possibility of many contributing terms to a particular observed rate. These may be terms involving the metal ion, involving two protons or one proton or independent of both metal ion and proton concentration. Most frequently spectrophotometric methods have been used to follow the reactions with occasional use being made of pH-Stat. measurements, i.e. keeping the pH constant as a reaction proceeds. Among the problems in using spectrophotometry are the assignments of peaks and the possibilities of overlap and coincidence. An excellent illustration of all of the above mentioned problems (and their resolution) can be found in the paper by Leach and Leussing<sup>(34)</sup> on the "Stabilities, rates of formation and rates of transimination in aqueous solutions of some Zn(II)-Schiff base complexes derived from salicylaldehyde".

Most of the metal ion "catalysed" reactions are really metal ion promoted, in that the metal ion is present in stoichiometric quantities and is frequently converted to an inactive form due to chelation by the product. In addition, little attention has been given to measuring the exchange rates of the various species with the catalyst, possibly because of the difficulty of applying spectrophotometric techniques to this kind of problem.

There are, therefore, advantages to a thorough study of a metal complex catalysed reaction, in non-aqueous solution and with non-chelating reactants and products. Such a reaction

5

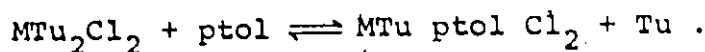
may be truly catalytic and amenable to study under equilibrium conditions. If this is the case NMR becomes a potentially valuable tool. This approach has been adopted in the present work.

(B) Reaction of acetone with anilines

A reaction of the type postulated in the previous paragraph was encountered somewhat serendipitously in solutions of anilines in acetone. While using NMR to study ligand replacement of thiourea in  $\text{CoTu}_2\text{Cl}_2$  by aniline with acetone d-6 as a solvent additional aromatic resonances were observed. A similar phenomenon was noted with  $\text{ZnTu}_2\text{Cl}_2$ . An extra aromatic peak was found downfield of the normal aniline resonances. It was a triplet in the case of aniline, for which the meta protons give a triplet, but a doublet in the case of p-toluidine, for which the meta protons give a doublet. The spectra obtained in the case of p-toluidine are reproduced in figure 6.5. In spectrum A, that of p-toluidine in acetone d-6, the peaks may be assigned as follows (using TMS = 0.0 ppm): acetone quintet at 2.1 ppm (due to  $\text{CD}_2\text{H}$  groups), methyl para to the amino group at 2.2 ppm,  $\text{H}_2\text{O}$  and  $\text{HDO}$  at 2.75 ppm, amino group at 4.2 ppm, ortho protons at 6.55 ppm and meta protons at 6.8 ppm. Comparing this spectrum with that obtained in the presence of  $\text{ZnTu}_2\text{Cl}_2$  (E), the new peaks are (a) a sharp peak at 2.45 ppm from TMS in the methyl region, (b) a doublet in the aromatic region at 7.0 ppm and (c) peaks overlapping with the ortho protons of the p-toluidine. The broad band at

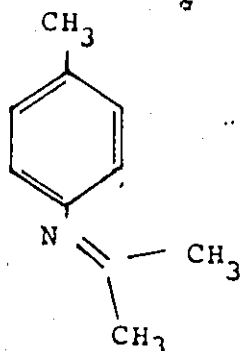
7.7 ppm is due to the protons in thiourea. The amino group protons and water protons are in fast exchange, giving a peak centered at 3.4 ppm.

When the paramagnetic complex  $\text{CoTu}_2\text{Cl}_2$  was used, the peaks were subject to isotropic shifts but when excess thiourea was added both the normal p-toluidine peaks and the additional ones returned to positions similar to those found with diamagnetic  $\text{ZnTu}_2\text{Cl}_2$ . This indicates that ligand exchange is occurring and that both species, the p-toluidine and whatever is giving rise to the extra resonances, are in fast exchange with the thiourea on the metal complex, i.e.



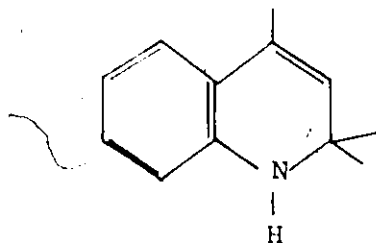
Various anilines were examined, e.g. p-anisidine, p-Cl-aniline, m-toluidine and p-F aniline (using  $^{19}\text{F}$  NMR) and similar results were obtained, i.e. extra resonances appeared which behaved in the manner described above. When N-methyl and N,N-dimethyl aniline were used no extra peaks were observed but the shifts obtained with  $\text{CoTu}_2\text{Cl}_2$  indicated that they did complex slightly. Using  $\text{CD}_3\text{CN}$  as a solvent no additional resonances were observed; however such peaks were found when either diethylketone or methylethylketone was used as a solvent. The conclusion from these results could only be that aniline was reacting with acetone (or any other ketone). The most likely product would be an imine or anil, i.e.





known as N-isopropylidene p-toluidine resulting from the condensation of one molecule of the aniline with one of acetone, and also producing one water molecule. This assignment was confirmed by direct synthesis of the anils (see below).

There do not seem to be any reports in the literature of the direct reaction of anilines with acetone to yield the acetone anils. In fact there is a flat statement: "Acetone anil cannot be obtained by direct reaction of the components" <sup>(73)</sup>. Acetone and aniline, when heated together, first yield mesityl oxide which reacts with the aniline to give 1,2 dihydro 2,2,4 trimethylquinoline <sup>(74)</sup>, i.e.



This compound was long called "acetone anil" until its identity was established <sup>(75)</sup>. Presumably in the reactions described above, the metal complex is catalysing the direct reaction of acetone and aniline to yield the anil under conditions very mild in comparison with those used to prepare the dihydroquinoline. Although the homogeneously catalysed formation of anils does not appear to have been extensively investigated, the synthesis of anils of aromatic ketones using anhydrous  $ZnCl_2$  as a

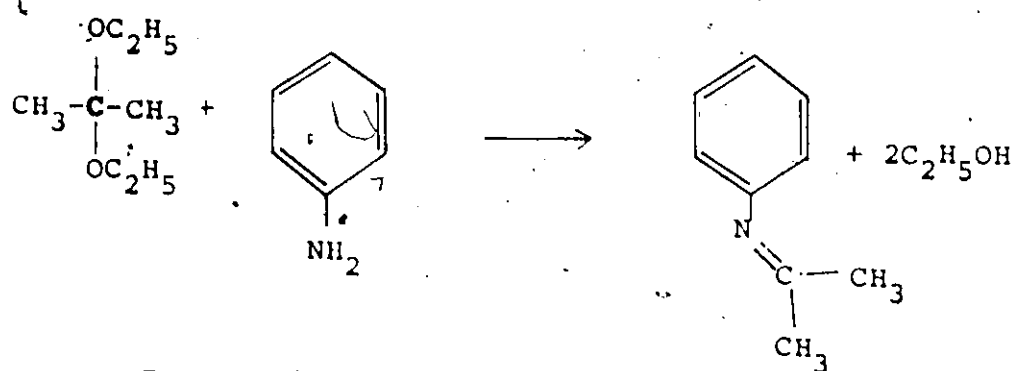
heterogeneous catalyst has been in common use for many years. The original discovery of this method is due to Reddelien<sup>(75a,b,c)</sup> The conditions for the reaction involve heating the reagents to 170°C which may be compared with the homogeneously catalysed reaction which proceeds at room temperature.

(C) Preparation of anils

(i) Synthesis

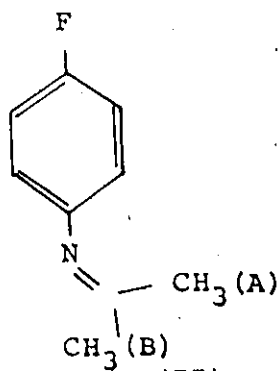
Although the acetone anils cannot be prepared directly there are a number of alternative routes available. Two of these routes were attempted.

The first method was the reaction of 2,2 diethoxypropane with the aniline at high temperature<sup>(76)</sup>.



In a typical experiment 3.3 g of p-F aniline and 5.0 g of 2,2 diethoxypropane were slowly heated on an oil bath to 185°C. An air condenser was used and a very gentle stream of N<sub>2</sub> removed the ethanol formed. After about ten minutes at the high temperature the flask was cooled under a stream of N<sub>2</sub> and the contents distilled under vacuum. The p-F aniline and its acetone anil must have very similar boiling points and fractiona-

tion was not possible. This method yielded a mixture of p-F aniline and its acetone anil, usually about equal quantities of each. The  $^1\text{H}$  NMR spectrum of the product run in  $\text{CD}_3\text{CN}$  is shown in figure 4.1. In the methyl region, the quintet is due to the residual  $^1\text{H}$  in the  $\text{CD}_3\text{CN}$  and the sharp peaks are assigned to the methyl groups A and B:



This assignment is due to Curtin<sup>(77)</sup> who determined it by substituting a tertiary butyl group for one of the methyl groups. The two methyl groups are different due to the fact that the ring-N-C angle is  $\sim 180^\circ$  and that there is restricted rotation about the carbon-nitrogen double bond.

Attempts to prepare the acetone anil of p-toluidine by the above method were never successful in producing more than 10% of the anil in a mixture with the unreacted p-toluidine. Another method, basically due to Kuhn<sup>(78)</sup>, was used in this case since the pure anil was required for kinetic measurements.

The first step involved preparation of the hydroiodide salt of the p-toluidine which was accomplished by dissolving the aniline in diethyl ether and adding 50% aqueous HI until precipitation ceased. The solid hydroiodide was filtered off

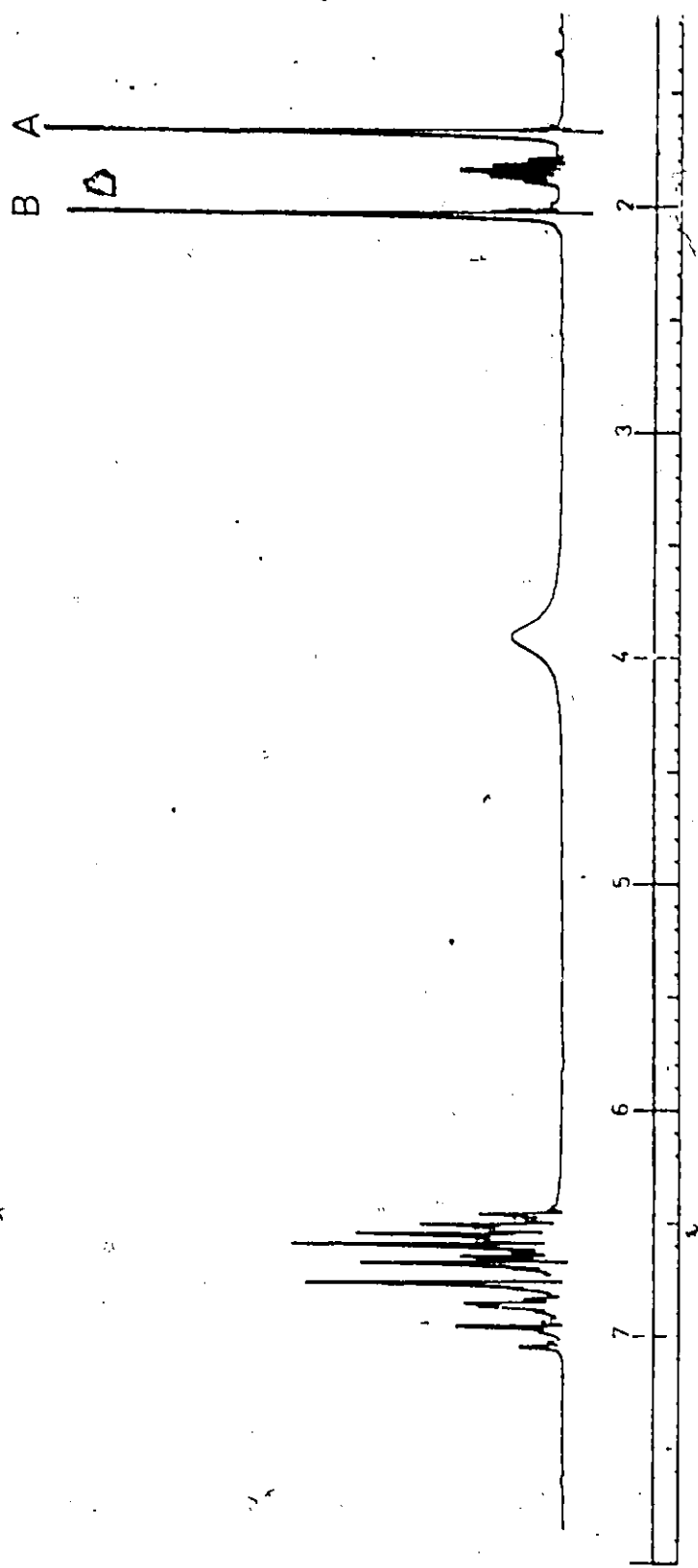
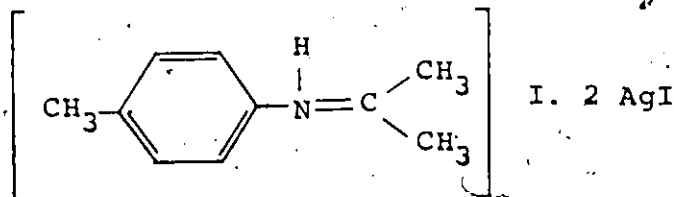


Fig. 4.1 The 100 MHz  $^1\text{H}$  NMR spectrum of p-F aniline/anil in  $\text{CD}_3\text{CN}$ . The markings are ppm from TMS

S

and dissolved in the absolute minimum quantity of methanol and then reprecipitated by addition of diethyl ether. The filtered material was washed with more ether and dried. Silver iodide was prepared by mixing aqueous solutions of KI and AgNO<sub>3</sub>, decanting the supernatant liquid, washing the solid with water, then methanol, and then drying it. It was found that the methanol washing seemed to prevent any photodecomposition of the AgI, which otherwise occurred.

The next step involved preparation of a complex of the aniline hydroiodide with silver iodide. Typically, 10 g of p-toluidine HI and 20 g of AgI were dissolved in the minimum quantity of hot dimethylformamide (~ 40 ml) and then a large volume (~ 4 l.) of acetone was added to the cooled solution. This was kept at about 35°C for a few days during which time a precipitate formed. This was filtered off and washed with acetone and then ether and air dried. Once dry the product was completely stable and the yield was about 15 g or about 50%. From the work of Kuhn this compound should be the silver iodide complex of N-isopropylidene p-toluidene hydroiodide,



Of the two methods recommended by Kuhn for conversion of the above complex to the free acetone anil, the one which was found to be most satisfactory involved refluxing with triethylamine. First a 10% Et<sub>3</sub>N in benzene solution was made up and

dried over calcium hydride. In a typical experiment 12 g of the AgI complex was refluxed with 80 ml. of  $\text{Et}_3\text{N}$ /benzene solution. The equipment had been carefully flushed out with  $\text{N}_2$  and a  $\text{P}_2\text{O}_5$  guard tube was placed on top of the condenser during refluxing. After 45 minutes of refluxing the solution was cooled, transferred to a glove bag filled with  $\text{N}_2$  and filtered. The solution was then transferred to a vacuum line where the benzene,  $\text{Et}_3\text{N}$  and any acetone were distilled off. This was checked by running an NMR spectrum. When no trace of  $\text{Et}_3\text{N}$  was left, the flask was filled with  $\text{N}_2$  and returned to the glove bag. The anil, which remained in the flask, was carefully transferred to one arm of an inverted Y-shaped apparatus which was then evacuated and sealed. The anil was then distilled into the other arm of the apparatus by immersing it in liquid  $\text{N}_2$ . Returning to the glove bag, the Y-shaped apparatus was broken open and the distilled anil removed and kept in a carefully stoppered vial in the refrigerator. All further handling of the material was done under  $\text{N}_2$ . The final distillation was found to be necessary to remove AgI which is apparently slightly soluble in the anil. The final product was a colourless heavy liquid and about 0.5 ml was obtained. The anil contained ~ 5% p-toluidine and virtually nothing else. The methyl region of the NMR spectrum of a sample of p-toluidine anil in  $\text{CDCl}_3$  is shown in figure 4.2. The peaks are assigned as shown below.

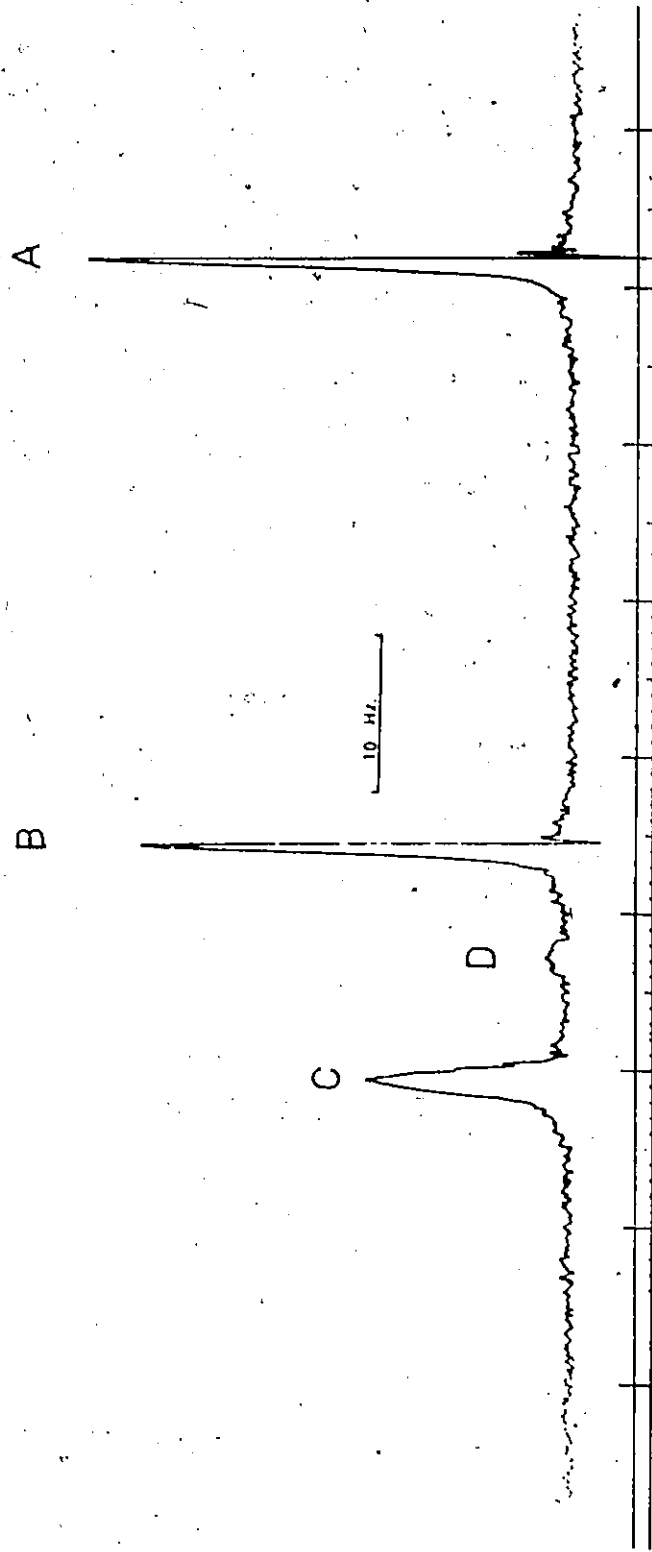
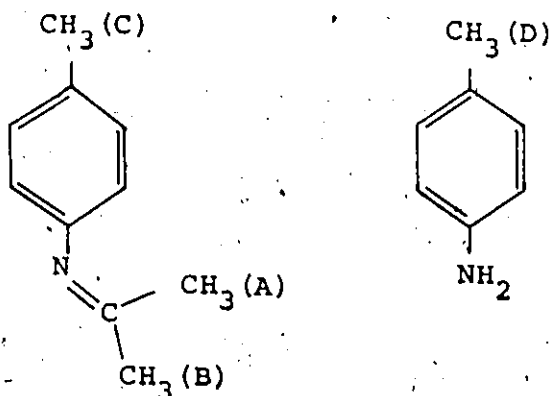


Fig. 4.2 Methyl region of the  $^1\text{H}$  NMR spectrum (100 MHz) of p-toluidine in  $\text{CDCl}_3$



This NMR spectrum is in excellent agreement with those reported for anils in the literature (77,79).

(ii) Comparison with observed spectra

The <sup>19</sup>F NMR spectrum of the p-F anil/aniline mixture was identical in chemical shifts with that produced from p-F aniline in acetone with a little ZnTu<sub>2</sub>Cl<sub>2</sub> added. The meta resonance in the spectrum of N-isopropylidene p-toluidine (hereafter referred to as p-toluidine anil) coincides with the extra aromatic doublet observed on addition of ZnTu<sub>2</sub>Cl<sub>2</sub> to p-toluidine in acetone d-6 and the para methyl peak coincides with the extra one observed in that region. The methyl peaks of the isopropyl portion of the anil are not observed when ZnTu<sub>2</sub>Cl<sub>2</sub> is added to p-toluidine, or any other aniline in acetone d-6, since they would be deuterated, being derived from the solvent. Using acetone d-6 the solvent peak is so intense that the methyl peaks are completely obscured. The independent preparation of the anils definitely establishes the reaction observed with anilines in acetone as being the formation of anils in the presence of metal thiourea complexes at room temperature.



## (D) Role of the metal complex

In order to obtain some idea of the effectiveness of metal complexes in promoting the reaction of anilines with acetone, the rate of the uncatalysed reaction was measured. A series of three samples was prepared using acetone d-6 as solvent, each sample being 0.2 M in p-toluidine which had been recently sublimed. The first tube had been used previously but had been cleaned with aqua regia, a commercial decontaminating fluid and then washed many times with distilled water. The other two tubes were new. The samples were kept in the dark at room temperature and periodically the NMR spectrum was run to check progress of the reaction. After 200 hours some  $\text{ZnTu}_4(\text{ClO}_4)_2$  was added which very quickly brought the reaction to its equilibrium position. There was no significant difference in the equilibrium concentrations in the three samples. From the early measurements of the reaction position the initial rate of formation of anil may be determined. The following values were obtained for the initial rate:

Sample 1	$1.33 \times 10^{-7}$ moles/l. sec
Sample 2	$6.4 \times 10^{-8}$ moles/l. sec
Sample 3	$8.3 \times 10^{-8}$ moles/l. sec

The variation is quite likely due to contamination by minute traces of metal or metal complexes in the tubes or reagents. The uncatalysed rate is certainly not faster than  $\sim 6 \times 10^{-8}$  moles/l. sec and may in fact be much slower.

Experiments with thiourea added to solutions of aniline in acetone showed that thiourea alone was not effective in

promoting anil formation.

In order to determine if the metal complex was a true catalyst and not promoting the reaction by complexing strongly with the product anil, the quantity of complex was reduced until the reaction could be followed conveniently by NMR, i.e. when the time to produce on half of the equilibrium concentration of anil ( $t_{1/2}$ ) was a few minutes. The rate thus depended roughly on the metal catalyst concentration.

Other metal complexes of thiourea were tried and all were capable of catalysing the reaction. Among these were Co, Ni and Zn complexes of Tu and DM Tu with  $\text{Cl}^-$ ,  $\text{Br}^-$ ,  $\text{I}^-$ ,  $\text{NO}_3^-$  and  $\text{ClO}_4^-$  anions. Comparative rates for some of these complexes will be given in the next section.

A wide range of assorted metal complexes was also tested for catalytic ability in this reaction. Amongst those tried that were effective were:  $\text{Ni}(\text{ClO}_4)_2 \cdot 6\text{H}_2\text{O}$ ,  $\text{RhCl}_3 \cdot \text{XH}_2\text{O}$ ,  $(\text{PPh}_3)_2\text{NiCl}_2$  and  $(\text{PPh}_3)_2\text{Ni}(\text{SCN})_2$ . However  $\text{PPh}_3$  was found to be effective in promoting the reaction. Complexes tried that were ineffective were  $\text{Co}(\text{HBPz})_2$  (cobalt bis-pyrazolylborate) and  $\text{Ni}(\text{ATM})_2$ , (ATM = aminotroponimate). Both of these complexes are very unlikely to dissociate or undergo ligand exchange in acetone solution. When either  $\text{CoCl}_2$  or  $\text{Co}(\text{ClO}_4)_2$  were dissolved in acetone and aniline added an immediate precipitation occurred. These precipitates were the insoluble complexes  $\text{CoAn}_2\text{Cl}_2$  and  $\text{CoAn}_4(\text{ClO}_4)_2$  respectively. The main function of the thiourea therefore seems to be to keep the metal ion in solution but at

the same time to undergo facile ligand exchange. In a related experiment it was noted that while  $\text{Ni}(\text{ClO}_4)_2 \cdot 6\text{H}_2\text{O}$  was a very effective catalyst, addition of 1,10 phenanthroline almost completely destroyed its catalytic properties.

Thus it seems that metal complexes which are capable of undergoing ligand exchange with the solvent or any other potential ligands will function as catalysts. A good catalyst can be rendered ineffective by complexing it with a strong chelating ligand which normally forms inert complexes.

#### (E) Comparison of catalytic efficiencies

In order to obtain some idea of the effectiveness of different metal complexes, a series of  $\text{Co}^{2+}$  and  $\text{Zn}^{2+}$  complexes were used as catalysts in the reaction between p-F aniline and acetone. The compounds used were mostly  $\text{Co}^{2+}$  complexes because the equilibrium constants for the dissociation of these complexes in acetone had been previously determined<sup>(80)</sup>. The reaction was followed after addition of the catalyst by repeatedly integrating the aniline and anil signals in the  $^{19}\text{F}$  NMR spectrum until equilibrium had been reached. The results were plotted as the fraction of anil (i.e.  $\frac{\text{Anil}}{\text{Anil} + \text{Aniline}}$ ) against time elapsed after the addition of catalyst. As all the samples contained the same concentration of aniline the equilibrium position was the same and thus  $t_{1/2}$ , or the time for the fraction of anil to reach one half its final equilibrium value, is a valid measure of the rate. The relative rates, adjusted relative to  $\text{ZnTu}_2\text{Cl}_2$  at the concentration it was used, are given for a series of complexes in table 4.1 along with the equilibrium constants for

Table 4.1

Comparison of the efficiency of various catalysts in the reaction of p-F aniline with acetone

Catalyst	Relative Rate	$K_D (\times 10^4)^*$
$ZnTu_2Cl_2$	1	-
$CoTu_2Cl_2$	3.2	1.46
$Co(DMTu)_2Br_2$	16	2.06
$CoTu_2Br_2$	10	2.82
$CoTu_2I_2$	59	3.86
$CoTu_4(NO_3)_2$	68	14.4
$CoTu_4(ClO_4)_2$	650	53.5

\* from reference (80).

dissociation of these complexes in acetone. For a complex  $MTu_nX_2$  the dissociation constant  $K_D$  is given by

$$K_D = \frac{[MTu_{n-1}AcX_2][Tu]}{[MTu_nX_2]}$$

where Ac represents acetone.

The results collected in table 4.1 show that there is a correlation between the relative rate and the dissociation constant for a complex.

(F) Acid catalysed reaction

Normally reactions of amines with carbonyl compounds are catalysed by acids<sup>(21)</sup> and so the effect of acid on a solution of p-toluidine in acetone was examined.

In figure 4.3 (a) is shown the NMR spectrum of p-toluidine in acetone d-6. The sample was 0.2M in p-toluidine and the spectrum was run at 27°C and 56.4 MHz. The peaks are, going from high to low field, the quintet of the residual  $^1H$  in the deuterated acetone, the para methyl group of the p-toluidine,  $H_2O$ , the amino group of p-toluidine and then the aromatic ortho and meta doublets. Figure 4.3 (b) shows the same sample but now with trifluoroacetic acid added. The sample was 1 M in  $CF_3COOH$  and the spectrum was run immediately after the addition of the anil. There are a number of striking differences from figure 4.3 (a). Firstly the addition of acid has caused the protons in the  $-NH_2$  group and in the water to exchange with the deuterons in the acetone. The intensity of the acetone peak has increased dramatically in about four minutes. Secondly,

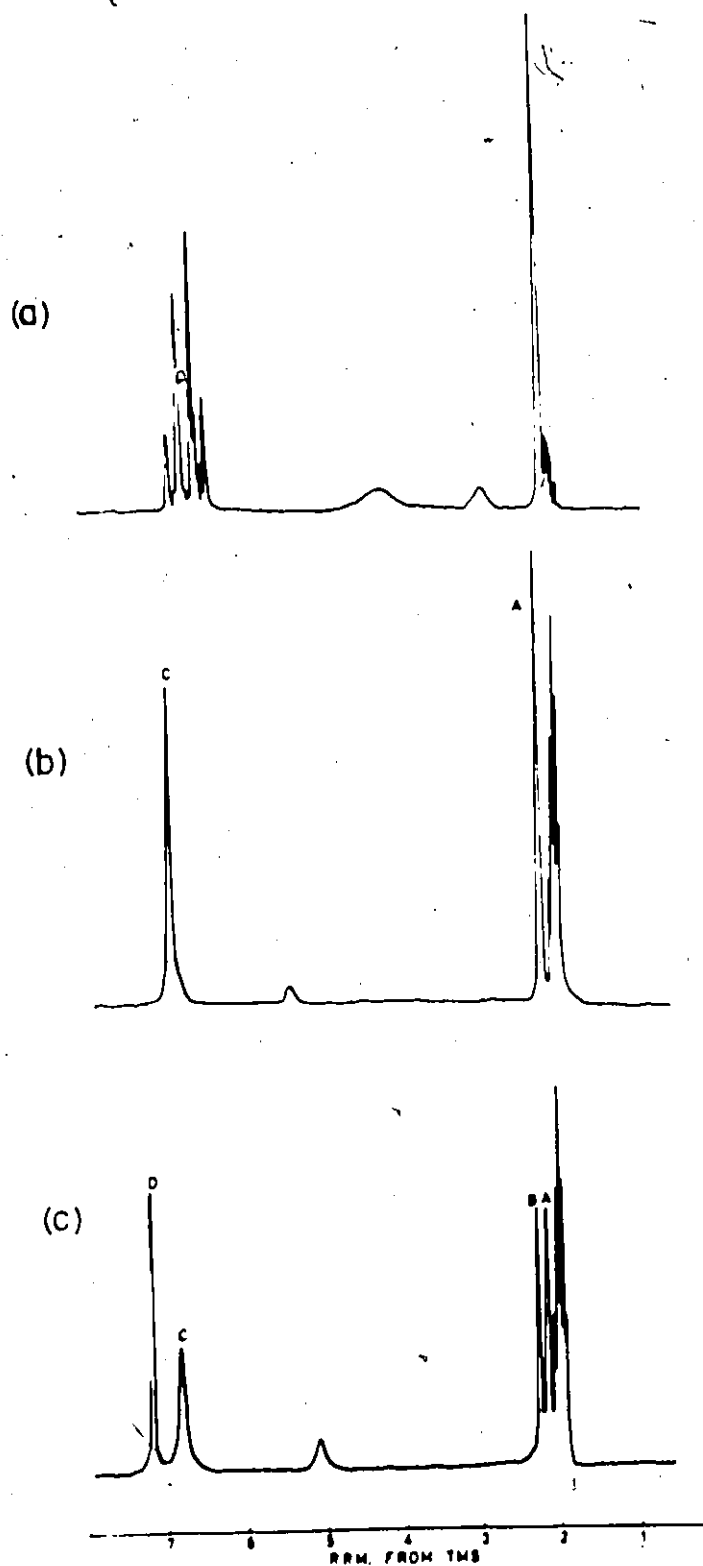


Fig. 4.3 (a) spectrum of p-toluidine in acetone d-6 (at 56.4 MHz)  
(b) as (a) after addition of  $\text{CF}_3\text{COOH}$   
(c) as (b) but 1-1/2 hours later

the para methyl peak (A) has moved downfield about 5 Hz from its position in spectrum (a). Thirdly the aromatic peaks have been reduced to a broad singlet (C). The last two effects are probably due to protonation of the amino group of the p-toluidine.

In figure 4.3(c) is shown the spectrum of the same sample one and a half hours after the acid was added. Two new peaks are present, B in the methyl region and D in the aromatic region. These peaks grow smoothly and as they do, A and C decrease in intensity. Peak B is about 5 Hz downfield from the normal position of the para methyl group signal of the p-toluidine anil. It would be reasonable to assign B and C to the anil because of their slow appearance in conjunction with the disappearance of the p-toluidine peaks and further because the chemical shifts of the peaks were consistent with those of a protonated anil.

The conversion of peak A into peak B was followed by NMR to equilibrium. The value of  $t_{1/2}$  was found to be 26 minutes. This can be compared with a solution which was the same concentration in p-toluidine but was  $4 \times 10^{-4}$  M in  $ZnTu_4(ClO_4)_2$  where  $t_{1/2}$  was 2.25 minutes. Thus on a molar basis the metal complex is about  $10^4$  times as efficient as the acid. Such a comparison is of somewhat dubious value since the acid catalysed reaction will have a different mechanism<sup>(21)</sup> to the metal catalysed one.

## (G) Equilibrium Constant

An attempt was made to determine the equilibrium constant for the reaction:



where K is defined by

$$K = \frac{[\text{Anil}][\text{Water}]}{[\text{Aniline}][\text{Acetone}]}$$

In this experiment  $^{19}\text{F}$  NMR and p-F aniline were used to determine the ratio of aniline to anil.  $^{19}\text{F}$  NMR was employed because acetone h-6 could then be used as a solvent whereas acetone d-6 would have been necessary if  $^1\text{H}$  NMR had been used. As discussed in Chapters 5 and 6 the acetone d-6 contains  $\text{D}_2\text{O}$  and it is difficult to measure its concentration.

First the water content of the acetone h-6 was determined by integrating the  $\text{H}_2\text{O}$  signal against the  $^{13}\text{C}$  sideband of the acetone methyl signal in the  $^1\text{H}$  NMR spectrum. This gave the result that the water content of the acetone was  $1.29 \times 10^{-3}$  (expressed as a fraction by weight). Samples were then prepared by weighing p-F aniline and acetone h-6 into NMR tubes and adding a small quantity of  $\text{ZnTu}_4(\text{ClO}_4)_2$ . When the reaction had reached equilibrium the ratio of aniline to anil was measured in each case by integration of the  $^{19}\text{F}$  NMR spectrum. The concentrations of aniline, anil, acetone and  $\text{H}_2\text{O}$  at equilibrium were then calculated. The results of the experiment are shown in table 4.2 where the "concentrations" are actually listed in moles since the volume terms will cancel in calculating K. The first three of these samples were prepared as indicated above and then, after the measurements had been made, a further



Table 4.2

Composition and equilibrium constant for p-F aniline in acetone

Sample	p-F aniline	acetone	pF anil	H <sub>2</sub> O	K
1	$4.0 \times 10^{-4}$	$5.22 \times 10^{-3}$	$1.63 \times 10^{-4}$	$1.85 \times 10^{-4}$	$1.44 \times 10^{-2}$
2	$1.17 \times 10^{-3}$	$4.08 \times 10^{-3}$	$2.85 \times 10^{-4}$	$3.03 \times 10^{-4}$	$1.81 \times 10^{-2}$
3	$1.71 \times 10^{-3}$	$5.35 \times 10^{-3}$	$4.02 \times 10^{-4}$	$4.26 \times 10^{-4}$	$1.87 \times 10^{-2}$
4	$5.1 \times 10^{-4}$	$5.35 \times 10^{-3}$	$5.55 \times 10^{-4}$	$1.44 \times 10^{-3}$	$2.98 \times 10^{-2}$
5	$1.92 \times 10^{-3}$	$5.55 \times 10^{-3}$	$1.95 \times 10^{-4}$	$1.80 \times 10^{-3}$	$3.29 \times 10^{-2}$

All "concentrations" are in moles.

quantity of water was weighted into two of the samples giving the results listed as Samples 4 and 5.

The first conclusion to be drawn from the results in table 4.2 is that the equilibrium constant  $K$  is obviously not constant. However  $K$  does vary in similar way to the water concentration and gives a fairly good straight line when  $K$  is plotted against water concentration. The trend in  $K$  is not followed by any of the other three species. It would seem that the activity of water in acetone in the range of concentrations studied is not directly proportional to its concentration. This problem will be returned to in Chapter 6.

#### (H) Summary

The metal catalysed reaction of acetone with anilines at room temperature to yield anils has been established. This reaction would seem to have certain definite advantages as a system in which to study the details of homogeneous catalysis. These advantages are:

- (a) the reaction is truly catalytic, not metal ion or complex promoted, and all the potential ligands, including reactants and products, are non-chelating;
- (b) the uncatalysed reaction is extremely slow;
- (c) the reaction can be followed by NMR so that initial rates can be measured;
- (d) the reaction can be studied in both directions, i.e. starting with either the aniline or the anil;
- (e) the dissociation constants for a number of the paramagnetic complexes are known;

- (f) use of paramagnetic compounds could:
  - (i) lead to simplification of the spectra due to the large isotropic shifts,
  - (ii) enable the association constants to be determined for the metal complex with all the ligands and substrates,
  - (iii) combined with low temperatures lead to the measurement of the rates of ligand exchange of the various substrates.
- (h) use of  $^{19}\text{F}$  NMR could drastically simplify spectra;
- (i) having acetone as a solvent as well as a reactant is useful because it freezes at  $\sim -100^\circ\text{C}$  providing a wide temperature range to study ligand exchange reactions;
- (j) since the reaction comes to equilibrium with roughly equal quantities of the aniline and the anil; then it might be possible to study rates of reaction with the system at equilibrium, using spin saturation transfer techniques.

In the following chapters various aspects of the reaction are explored. In Chapter 5 are reported the results of measurements of the initial rate of the reaction in both directions under a variety of conditions. In Chapter 6 the ligand properties are investigated with measurements of equilibrium constants and rates for ligand exchange. In Chapter 7 the results of spin saturation transfer experiments on both cw and FT NMR spectrometers are reported. In the final chapter the results are discussed and a reaction mechanism suggested.

## CHAPTER FIVE

### INITIAL RATE MEASUREMENTS

#### (A) Introduction

As discussed in the previous chapter, the rate of the metal complex catalysed formation of anils could be adjusted by varying the catalyst concentration. This means that "classical" methods may be used to monitor the rate as a function of time, e.g. the use of repeated integration of the NMR spectrum. In this chapter are discussed experiments where the rates of both the forward and backward reactions were measured under various conditions.

In circumstances where the rate law governing a chemical reaction is unknown, but is suspected to involve the concentration of more than one reactant, one of the best methods of proceeding to determine the rate law is that of initial rates. This involves the measurement of the initial rate of the reaction as a function of the initial concentration of each reactant, under conditions where the concentrations of all other possible reactants are kept constant<sup>(21)</sup>.

The measurements were made as described in Chapter 3 Section C. From the experimental data, such as that shown in figure 3.1, the fraction  $\left(\frac{\text{Anil}}{\text{Aniline}+\text{Anil}}\right)$  was calculated using the measured intensities. Since the denominator (Aniline+Anil) is always constant, then the fraction will be independent of small

drifts in the homogeneity of the magnetic field on the NMR spectrometer or in the gain of its amplifier circuits. The fraction  $\left(\frac{\text{Anil}}{\text{Aniline}+\text{Anil}}\right)$  was plotted against the time, and the initial rate evaluated by measuring the slope of the tangent to the curve at the origin. In the case of the back reaction (the hydrolysis of the anil) the fraction  $\frac{\text{Aniline}}{\text{Anil}+\text{Aniline}}$  was plotted against time, but the curve was extrapolated to meet the time axis where the concentration of aniline would be zero. This was necessary because the p-toluidine-anil contained ~ 5% p-toluidine, and the initial rate of formation of the aniline should be determined where the aniline concentration is zero.

A typical plot for the forward reaction, i.e., starting with p-toluidine, is shown in figure 5.1. The slope is evaluated directly as a fraction of anil produced per minute which can easily be converted to moles/l.sec. or any other desired units. In these experiments, p-toluidine and its acetone anil (prepared as described in Chapter 4 Section C(i)) were used due to the suitability of their NMR spectrum for kinetic studies of this kind. The catalysts  $(\text{ZnTuCl}_2)$  and  $(\text{ZnTu}_4(\text{ClO}_4)_2)$  were diamagnetic, and peak heights could then be used in rate calculations. The broadening induced by paramagnetic catalysts precludes use of this method.

#### (B) The Forward Reaction

##### (i) Dependence of rate on concentration of catalyst.

In this experiment, the effect of changing the catalyst concentration on the initial rate of formation of the anil from p-toluidine and acetone was studied. Stock solutions of

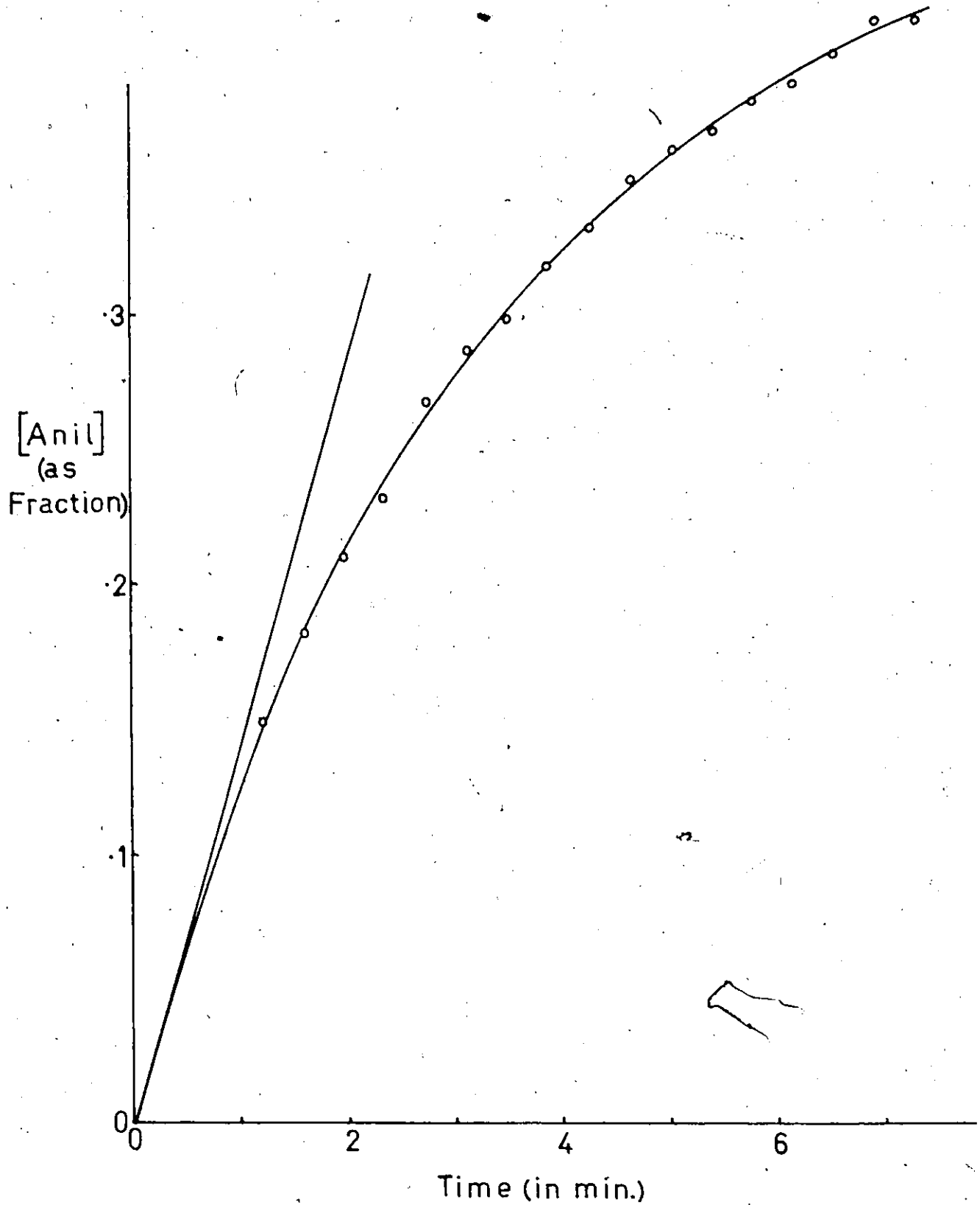


Fig. 5.1 Graphical determination of the initial rate. The fraction  $\frac{\text{Anil}}{\text{Anil} + \text{Aniline}}$  is plotted against the time elapsed (in minutes)

p-toluidine in acetone d-6 and  $\text{ZnTu}_4(\text{ClO}_4)_2$  in acetone d-6 were prepared. Samples were made up by taking 0.30 ml of the p-toluidine solution and adding a quantity of acetone d-6 such that the total sample volume, when the catalyst solution was added, would be 0.50 ml. The samples were 0.19 M in p-toluidine, and the initial rate was studied over a range of catalyst concentrations from  $5 \times 10^{-5}$  M to  $4 \times 10^{-4}$  M. The results are shown in table 5.1, where the initial rate is that of the formation of the p-toluidine anil. The results are plotted in figure 5.2, with the initial rate expressed as the fraction  $\frac{\text{Anil}}{\text{Aniline} + \text{Anil}}$  formed per minute, and the volume of catalyst added in  $\mu\text{l}$ .

The general expression for the dependence of the rate of a catalysed reaction on the catalyst concentration is

$$\text{Rate} = k_o + k_{\text{cat.}} [\text{catalyst}]^n .$$

From figure 5.2 it may be seen that  $k_o$ , or the rate of the uncatalysed reaction, is small in comparison with the catalysed rates. A more accurate measure of the uncatalysed rate was obtained in the manner described in Chapter 4 Section D. From those results, the uncatalysed rate is at least  $10^3$  times smaller than that obtained with the lowest catalyst concentration used in this present experiment. Also, from figure 5.2,  $n$  must be 1 since the graph is linear. A plot of  $\log$  (Initial rate) against  $\log$  (catalyst concentration) has in fact a slope of 0.94 which is the value of  $n$ . The reaction is thus first order in catalyst concentration over the range of concentrations studied.

The data plotted in figure 5.1 are actually from the sample in this experiment where the catalyst concentration was highest,

Table 5.1

Results of experiment on the dependence of the initial rate on the catalyst concentration

Catalyst concentration in moles/l.	Initial rate in moles/l.sec
$5.0 \times 10^{-5}$	$5.8 \times 10^{-5}$
$1.0 \times 10^{-4}$	$1.14 \times 10^{-4}$
$2.0 \times 10^{-4}$	$2.10 \times 10^{-4}$
$3.0 \times 10^{-4}$	$3.05 \times 10^{-4}$
$4.0 \times 10^{-4}$	$4.20 \times 10^{-4}$

The catalyst was  $\text{ZnTu}_4(\text{ClO}_4)_2$  and all samples were 0.19 M in p-toluidine.



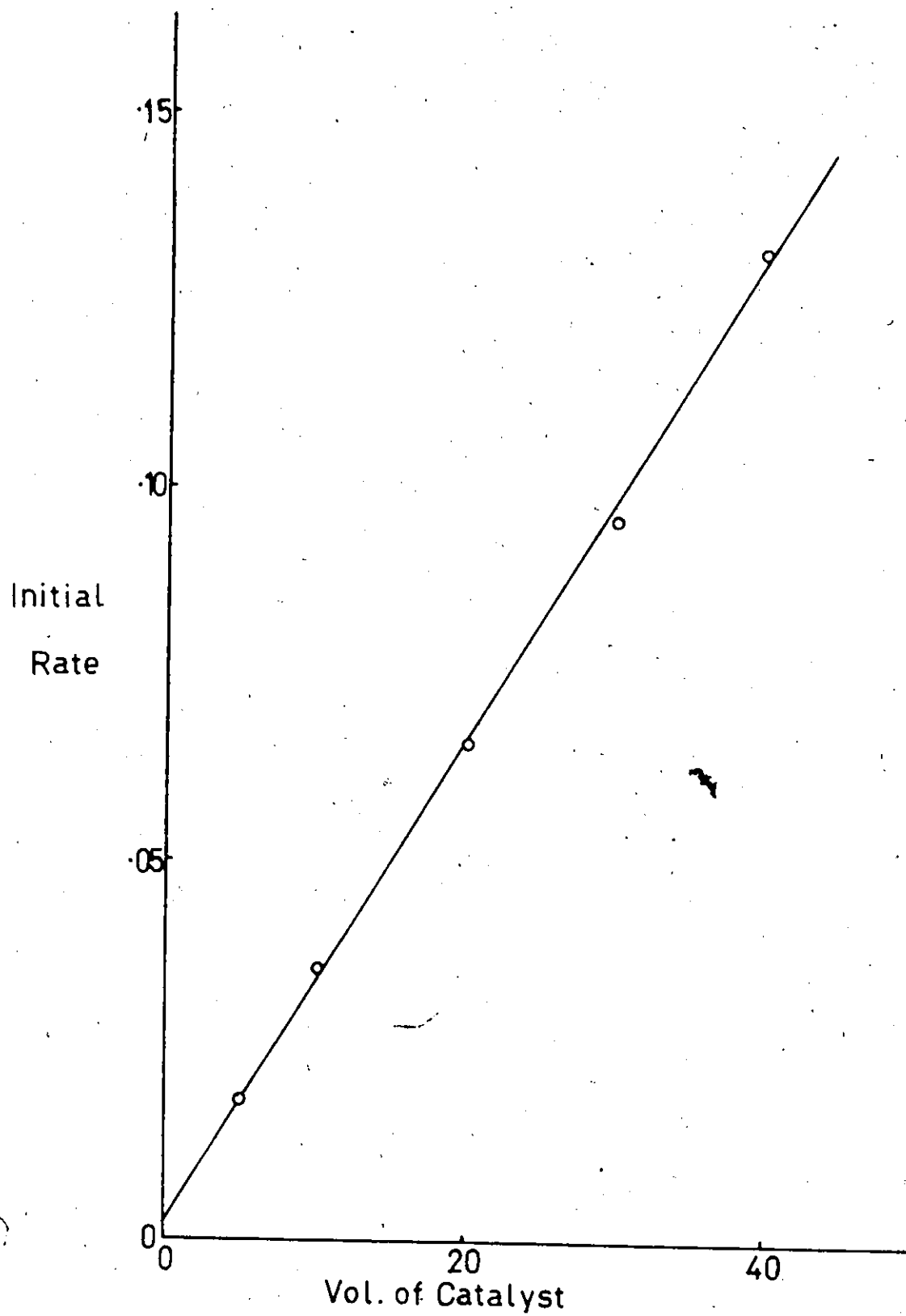


Fig. 5.2 Initial rate of formation of anil (in fraction of anil formed per minute) plotted against the volume of catalyst solution added (in  $\mu\text{l.}$ )

i.e.  $4.0 \times 10^{-4}$  M. The tangent to the curve at the origin yields an initial rate of between .130 and .140, expressed as the fraction of anil formed per minute: the value used was .132. Since the reaction in this experiment had been followed to equilibrium it was possible to check the value of the initial rate by using a computer to fit a curve to the experimental points. The program used was called "A General Nonlinear Curvefitting and Equation Solving Program", and was acquired from the Program Library at Michigan State University Computer Laboratory. A description of the program and its possible uses has been published<sup>(81)</sup>. The program was required to find the best fit of the experimental data to the equation,

$$\frac{d[\text{anil}]}{dt} = k_1[\text{aniline}] - k_2[\text{anil}] \quad (5.1)$$

using  $k_1$  and  $k_2$  as variable parameters. The concentrations of aniline and anil were expressed as fractions of the initial aniline concentration. Equation 5.1 is simply the differential equation to describe two opposing first order reactions. The values of  $k_1$  and  $k_2$  which gave the best fit were 0.136 and 0.159 respectively, with standard deviations of 0.0021 and 0.0032 respectively. The plot of the residuals (i.e. the calculated value from equation (5.1) with  $k_1$  and  $k_2$  optimized less the experimental value) against time was completely random indicating that equation (5.1) does indeed give a good description of the observed data.

The initial rate, which was estimated from the tangent to the curve (0.132), is in good agreement with that (0.136)

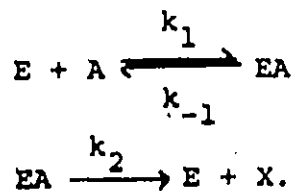
determined by fitting the entire curve by computer. Since this rate is as fast as any measured in the course of experiments described in this chapter, it is fair to consider the initial rates as accurate to  $\pm 10\%$  if not better.

(ii) Dependence of rate on concentration of aniline

The studies of the dependence of the rate on the concentration of p-toluidine were carried out using p-toluidine in which the protons of the amino group had been replaced by deuterons. The necessity for using p-toluidine (d-2) arose from the fact that the acetone d-6, as purchased, contained water which was present as  $D_2O$ . This will be further discussed in Chapter 6, Section (D), but the water content varied from 0.1% to 0.2% by weight. A solution of acetone containing 0.2% by weight of water would be roughly 0.1 M in water. This means that, at the lower concentrations of p-toluidine used, the water and p-toluidine are at about the same concentration. Since the hydrogen or deuterium on the nitrogen of the p-toluidine is in fast exchange with the hydrogen or deuterium in the water, then the p-toluidine will be partly deuterated if there is  $D_2O$  present. The amount of  $D_2O$  is fixed, so, as the concentration of p-toluidine is increased the extent of deuteration will change. If there was a significant kinetic isotope effect for the reaction involving p-toluidine (d-2) or p-toluidine (h-2), then a study of the rate as a function of aniline concentration would be disturbed by the changing extent of deuteration. For this reason, p-toluidine (d-2) was used as the aniline. It was prepared by dissolving p-toluidine in diethyl ether and stirring together with

successive portions of  $D_2O$ . The ether layer was dried with  $Na_2SO_4$ , the solvent removed on a vacuum line, and the p-toluidine (d-2) sublimed in vacuo. It was kept in a glove bag under a nitrogen atmosphere. By integration of the NMR spectrum of a concentrated solution of this p-toluidine (d-2) in  $CDCl_3$ , the compound was found to be 95% deuterated.

The experiment was carried out using  $ZnTu_4(ClO_4)_2$  as the catalyst. The p-toluidine (d-2) was weighed into the NMR sample tubes, 0.50 ml of acetone d-6 added by syringe together with a few drops of TMS to provide a locking signal. The catalyst solution was added by syringe, 15  $\mu$ l in each case, making each sample  $1.21 \times 10^{-4}$  M in catalyst. The results are given in table 5.2 and plotted in figure 5.3(a) as rate versus p-toluidine concentration. The shape of the curve in figure 5.3(a) is very reminiscent of those obtained for the reaction rate as a function of substrate concentration in studies of enzyme catalysed reactions. The simplest system which will give this hyperbolic curve is described by the Michaelis-Menten equation<sup>(82)</sup>. This system consists of a catalyst or enzyme E, and a substrate A, which form a complex EA, and then react to yield E and X, where X is the product.



The net reaction is thus  $A \rightarrow X$ . If the first equilibrium or pre-equilibrium is fast, i.e.  $k_1 \gg k_2$ , then the rate of reaction

Table 5.2

Results for dependence of initial rate on p-toluidine (d2) concentration with  $\text{ZnTu}_4(\text{ClO}_4)_2$  as catalyst.

Concentration of p-toluidine (d-2) in moles/l.	Initial rate of formation of anil in moles/l.sec.
$6.70 \times 10^{-2}$	$4.23 \times 10^{-5}$
$1.18 \times 10^{-1}$	$6.40 \times 10^{-5}$
$1.73 \times 10^{-1}$	$8.38 \times 10^{-5}$
$2.31 \times 10^{-1}$	$1.15 \times 10^{-4}$
$2.83 \times 10^{-1}$	$1.31 \times 10^{-4}$
$4.71 \times 10^{-1}$	$1.96 \times 10^{-4}$
$6.01 \times 10^{-1}$	$1.86 \times 10^{-4}$
$7.80 \times 10^{-1}$	$2.52 \times 10^{-4}$

All samples were  $1.2 \times 10^{-4}$  M in catalyst.

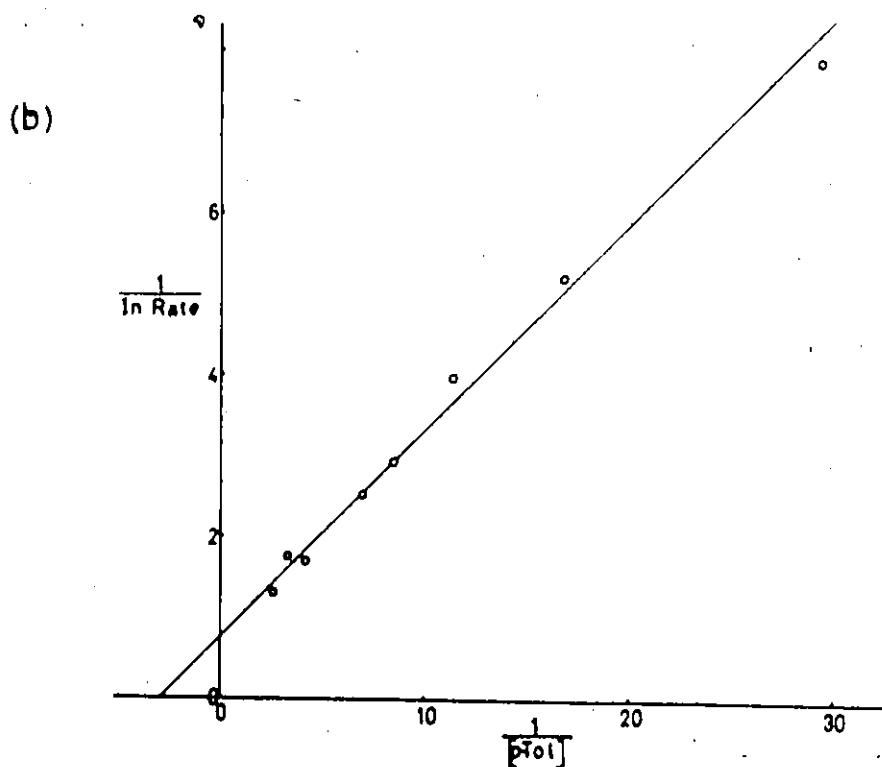
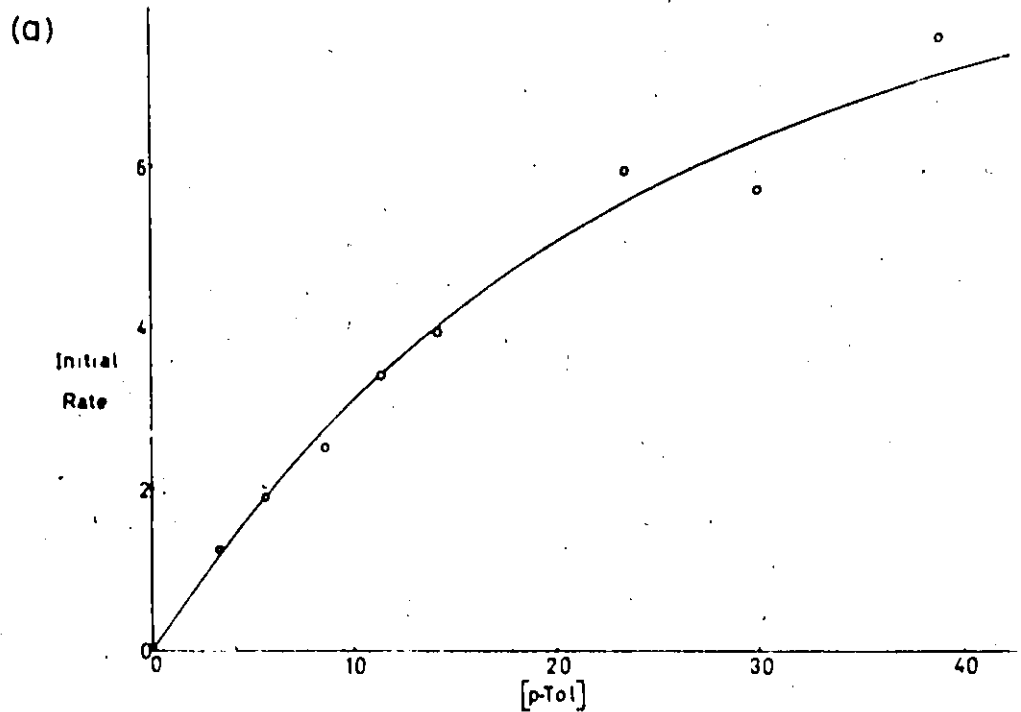


Fig. 5.3 (a) Initial rate of formation of anil (in moles/min. $\times 10^6$ ) plotted against the concentration of p-toluidine (d-2) in moles $\times 10^{-5}$   
 (b) (Initial rate) $^{-1}$  (in min./mole $\times 10^{-5}$ ) plotted against [p-toluidine] $^{-1}$  in moles $^{-1}\times 10^{-3}$

(v) may be written as

$$v = \frac{k_2 [E]_0 [A]}{K_A + [A]} \quad (5.2)$$

Here,  $[E]_0$  is the total concentration of the catalyst which is equal to  $[E] + [EA]$ . The constant  $K_A$  is the Michaelis constant and is written for the term  $(\frac{k_{-1} + k_2}{k_1})$ .

The equation (5.2) can be recast in the form;

$$\frac{1}{v} = \frac{K_A}{V} \cdot \frac{1}{[A]} + \frac{1}{V} \quad (5.3)$$

where  $V = k_2 [E]_0$  which is the limiting rate at very high values of  $[A]$ . A plot of  $\frac{1}{v}$  against  $\frac{1}{[A]}$  should give a straight line with a slope of  $\frac{K_A}{V}$  and an intercept of  $\frac{1}{V}$  on the  $\frac{1}{v}$  axis. Such a graph is known as a Lineweaver-Burk or double reciprocal plot. The intercept on the  $\frac{1}{[A]}$  axis is  $-\frac{1}{K_A}$  and, if  $k_1 \gg k_2$ , then  $K_A$  is the association constant for A with the catalyst or enzyme.

In figure 5.3(b), the data of table 5.2 is plotted in a Lineweaver-Burk plot. This gives a very reasonable straight line with an intercept on the  $\frac{1}{[p\text{-tol.}]}$  axis of  $-1.50 \text{ l./mole}$ . This would seem to indicate that the reaction followed Michaelis-Menten kinetics or some more complex scheme which reduces to the same general form.

A similar experiment was carried out using  $ZnTu_2Cl_2$  as a catalyst. In this case, the samples were 0.022 M in  $ZnTu_2Cl_2$  and the measurements were made with p-toluidine (d-2) in the same way as before. The experimental results are given in table 5.3. The double reciprocal plot for this experiment is shown in figure 5.4, and again a good straight line was obtained with an intercept on the  $[p\text{-tol.}]^{-1}$  axis of  $-2.0 \text{ l./mole}$ .

Table 5.3

Results for dependence of initial rate on p-toluidine (d-2) concentration with  $\text{ZnTu}_2\text{Cl}_2$  as catalyst.

Concentration of p-toluidine (d-2) in moles/l.	Initial rate of formation of anil in moles/l.sec.
$6.42 \times 10^{-2}$	$7.43 \times 10^{-5}$
$1.17 \times 10^{-1}$	$1.21 \times 10^{-4}$
$1.61 \times 10^{-1}$	$1.44 \times 10^{-4}$
$2.13 \times 10^{-1}$	$1.67 \times 10^{-4}$
$2.92 \times 10^{-1}$	$2.24 \times 10^{-4}$
$6.20 \times 10^{-1}$	$3.31 \times 10^{-4}$

All samples were  $2.2 \times 10^{-2}$  M in  $\text{ZnTu}_2\text{Cl}_2$



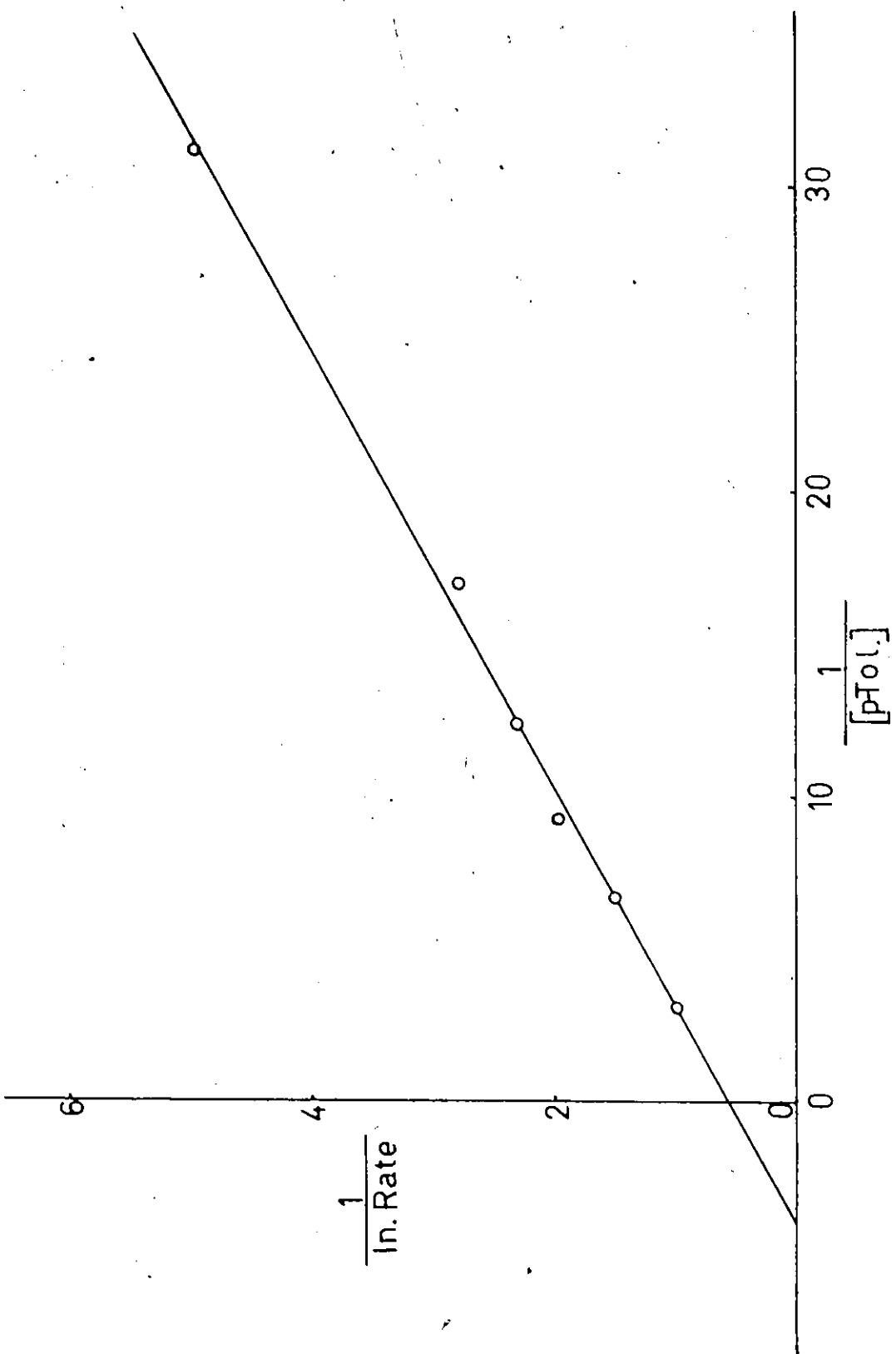


Fig. 5.4 Double reciprocal plot for the formation of anil from p-toluidine (d-2) with  $\text{ZnTu}_2\text{Cl}_2$  as catalyst. (Initial rate) $^{-1}$  in (min/moles $\times 10^{-5}$ ) is plotted against [p-toluidine] $^{-1}$  in moles $^{-1}\times 10^{-3}$ .

(iii) Overall concentration dependence

Since the forward rate obviously depended on both the concentration of catalyst and of aniline, it was desirable to find a way of determining whether it also depended on the acetone concentration, i.e. to determine the order in acetone. This was difficult because acetone was the solvent, and it was necessary to have a large excess of acetone present to produce the anil owing to the small value of the equilibrium constant for the overall reaction (Chapter 4 Section G). The experiment decided upon involved running a series of initial rate measurements on samples prepared from a stock solution of p-toluidine in acetone d-6 which was progressively diluted with  $\text{CCl}_4$ . Carbon tetrachloride was chosen as a diluent because it should be an "inert" solvent, i.e. it should be an extremely poor ligand, and this should not perturb the relative concentrations of all the possible mixed ligand species in solution. The same quantity of catalyst was used in each run which made all the samples  $1.0 \times 10^{-4}$  M. in  $\text{ZnTu}_4(\text{ClO}_4)_2$ . The experimental results are presented in table 5.4. This shows that the initial rate of formation of the anil in moles/l.sec. is quite independent of the degree of dilution with  $\text{CCl}_4$ .

At this stage, it is of interest to examine the predicted behaviour of the initial rate as a function of dilution with an "inert" solvent for two likely mechanisms. These can be denoted as the "one site" and "two site" mechanisms. In the one site mechanism only one of the two substrates, acetone or aniline, need be coordinated to the metal, whereas for the two site mechanism

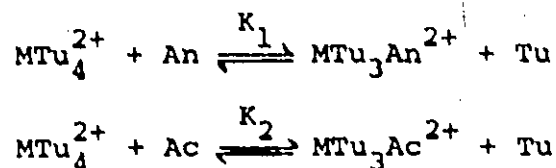
Table 5.4

Results for dependence of initial rate of formation of anil on dilution with  $\text{CCl}_4$

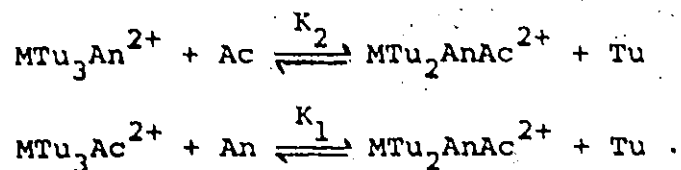
Sample No.	$\text{CCl}_4$ as a fraction of sample volume	Catalyst conc. in moles/l.	p-toluidine conc. in moles/l.	Initial rate in moles/l. sec
1	0	$1.0 \times 10^{-4}$	$2.38 \times 10^{-1}$	$1.43 \times 10^{-4}$
2	$\frac{1}{5}$	$1.0 \times 10^{-4}$	$1.91 \times 10^{-1}$	$1.44 \times 10^{-4}$
3	$\frac{2}{5}$	$1.0 \times 10^{-4}$	$1.43 \times 10^{-1}$	$1.34 \times 10^{-4}$
4	$\frac{3}{5}$	$1.0 \times 10^{-4}$	$0.95 \times 10^{-1}$	$1.45 \times 10^{-4}$

$\text{ZnTu}_4(\text{ClO}_4)_2$  was the catalyst used.

both need to be coordinated. The equilibria for ligand exchange with  $ZnTu_4(ClO_4)_2$  are:



where An and Ac represent aniline and acetone, respectively. Assuming that the equilibrium constant for replacing a second Tu ligand is the same as for the first, then:



The concentration of the species  $MTu_2AnAc^{2+}$  is given by:

$$[MTu_2AnAc^{2+}] = \frac{K_1 K_2 [An] [Ac] [MTu_4^{2+}]}{[Tu]^2}$$

For a two site mechanism the rate of reaction will be proportional to  $[MTu_2AnAc^{2+}]$ , or

$$\begin{aligned} \text{Rate} &= k [MTu_2AnAc^{2+}] \\ &= \frac{k K_1 K_2 [An] [Ac] [MTu_4^{2+}]}{[Tu]^2} \end{aligned}$$

If the solution is now diluted with some "inert" solvent so that the volume is  $V$  times what it was, then all the concentrations will be reduced by the factor  $\frac{1}{V}$ . If the diluting solvent is truly "inert", it will not change the ratio  $[MTu_4^{2+}]/[Tu]^2$ .

The rate is now given by:

$$\text{Rate}_1 = kK_1k_2 \frac{[\text{Ac}]}{V} \cdot \frac{[\text{An}]}{V} \cdot \frac{[\text{MTu}_4^{2+}]}{V} \cdot \frac{V^2}{[\text{Tu}]^2}$$

$$\therefore \text{Rate} = \frac{kK_1K_2[\text{Ac}][\text{An}] \cdot [\text{MTu}_4^{2+}]}{[\text{Tu}]^2} \cdot \frac{1}{V}$$

So, for a two site mechanism the rate will be proportional to  $\frac{1}{V}$ .

For a single site mechanism, e.g. where acetone is coordinated, the rate =  $k'[\text{An}][\text{MTu}_3\text{Ac}^{2+}]$

$$\therefore \text{Rate} = k'K_2[\text{An}][\text{Ac}] \frac{[\text{MTu}_4^{2+}]}{[\text{Tu}]}$$

On dilution to  $V$  times the original volume with an "inert" solvent, the rate is given by:

$$\text{Rate} = k'K_2 \frac{[\text{An}]}{V} \cdot \frac{[\text{Ac}]}{V} \cdot \frac{[\text{MTu}_4^{2+}]}{V} \cdot \frac{V}{[\text{Tu}]}$$

$$\therefore \text{Rate} = k'K_2[\text{An}][\text{Ac}] \frac{[\text{MTu}_4^{2+}]}{[\text{Tu}]} \cdot \frac{1}{V^2}$$

For a single site mechanism then, the rate will be proportional to  $\frac{1}{V^2}$ .

In the actual experiment carried out, the acetone and aniline concentrations were reduced by dilution with  $\text{CCl}_4$  but the  $\text{ZnTu}_4(\text{ClO}_4)_2$  concentration was kept constant. The reaction is known to be first order in catalyst in the range studied, so, if the catalyst had been diluted along with the acetone and aniline, the observed rate would have been reduced by a factor  $\frac{1}{V}$ . The observed rate is, in fact, a constant and independent of  $V$ ; so, if the experiment had been performed by diluting aniline, acetone and

catalyst, the result would have been that the rate was proportional to  $V^{-1}$ . This is the expected behaviour for a two site mechanism. However, the interpretation of this result will be discussed in more detail in Chapter 8.

(iv) Dependence of rate on Thiourea concentration

Since the Tu ligands on the catalyst complexes are known to dissociate, and since the results of the initial rate experiments already discussed indicate that complexation of acetone and/or aniline is a prerequisite for reaction, then Tu should inhibit the reaction. This was investigated by measuring the initial rate of formation of anil for a series of samples containing different amounts of Tu. The complex  $ZnTu_4(ClO_4)_2$  was used as a catalyst. The results of the experiment are given in table 5.5, and are presented graphically in figures 5.5(a) and 5.5(b). Figure 5.5(a), where the initial rate is plotted against the added Tu, shows that Tu does inhibit the reaction. The added Tu concentration ranges from 10 times to over 100 times the total Tu concentration available from the  $ZnTu_4(ClO_4)_2$ . Thus, to a good approximation, the total Tu concentration is that of the added Tu. In figure 5.5(b) the initial rate of formation of anil is plotted against the reciprocal of the Tu added. A smooth curve may be drawn through the points and the origin, indicating that the rate at infinite Tu concentration would be zero. No catalysis by Tu itself was noted in these samples.

Table 5.5

Results of dependence of initial rate of formation of anil on added Tu concentration.

Tu added (in moles)	Initial rate in moles/l.sec.
0	$1.57 \times 10^{-2}$
$4.08 \times 10^{-6}$	$1.24 \times 10^{-2}$
$9.08 \times 10^{-6}$	$1.01 \times 10^{-2}$
$1.65 \times 10^{-5}$	$8.46 \times 10^{-3}$
$2.58 \times 10^{-5}$	$6.73 \times 10^{-3}$
$5.61 \times 10^{-5}$	$5.19 \times 10^{-3}$

All samples were .188 M in p-toluidine and  $2.0 \times 10^{-4}$  M  $ZnTu_4(ClO_4)_2$ .

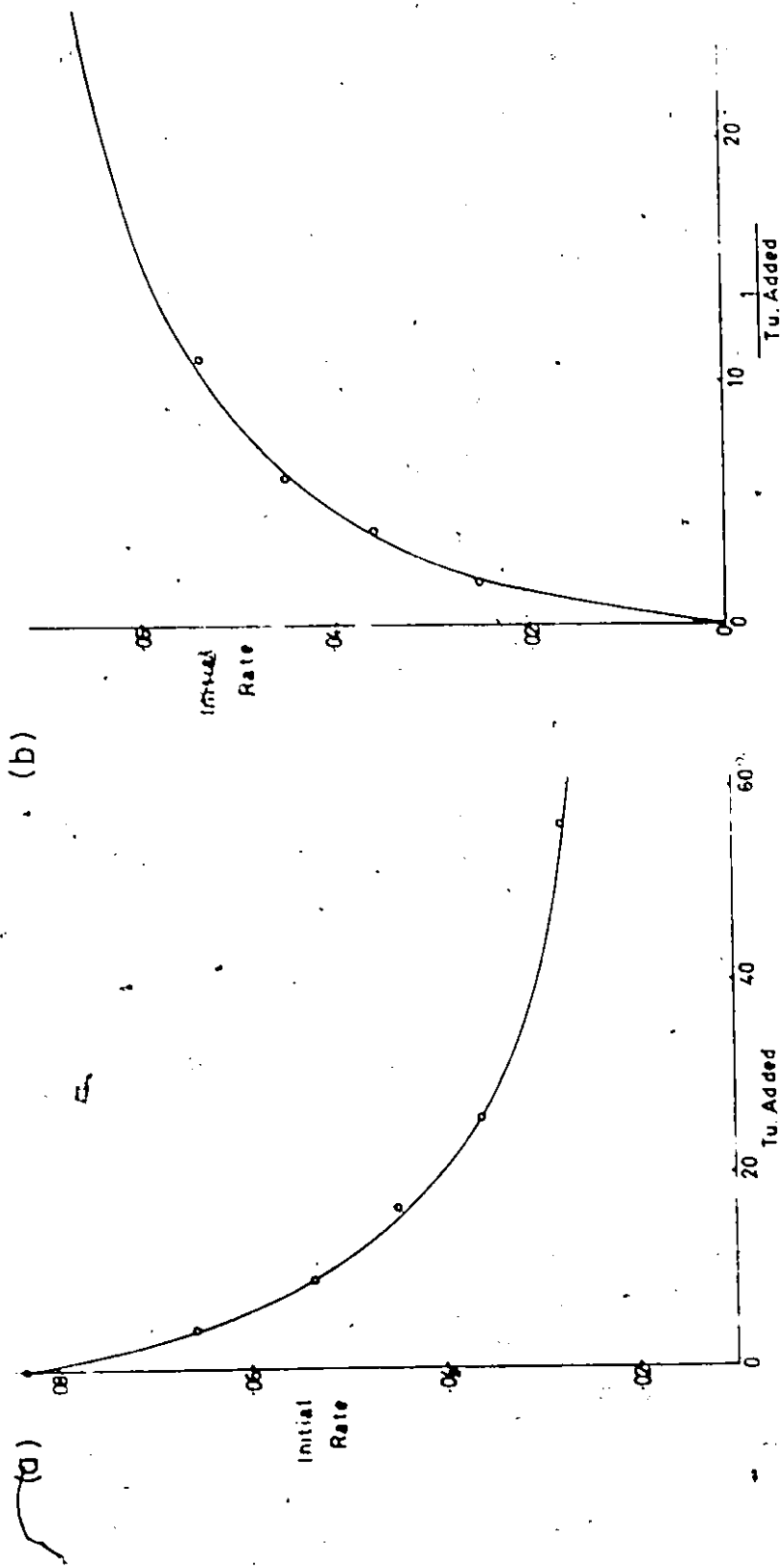


Fig. 5.5 Dependence of initial rate on added [Tu].  
 (a) Initial rate (as fraction of anil formed per minute) plotted against Tu added (in moles  $\times 10^6$ )  
 (b) Initial rate (as fraction of anil formed per minute) plotted against  $(Tu \text{ added})^{-1}$  in moles  $\times 10^{-4}$



(C) The Back Reaction

(i) Dependence on anil concentration

The back reaction is the hydrolysis of the anil to yield aniline and acetone. The dependence of the back reaction on catalyst concentration should be the same as the forward reaction, and so the dependence of the initial rate of the back reaction on the concentrations of anil and water was determined.

The acetone anil of p-toluidine was prepared as described in Chapter 4 Section C(i). The material used in this experiment had only about 5% of p-toluidine present as an impurity. The anil was added by syringe and acetone d-6 with a little (2.5  $\mu$ l per 0.5 ml sample) D<sub>2</sub>O added was used as a solvent. Since the density of the anil is not known, the results presented in table 5.6 are in units of  $\mu$ l. The results are plotted in figure 5.6(a) and a double reciprocal plot is shown in figure 5.6(b). Here, a straight line is not obtained, but the graph curves upwards at high anil concentration. This is very similar to the appearance of the double reciprocal plot when there is inhibition by substrate itself<sup>(82)</sup>. This is normally explained for single substrate reactions by invoking the formation of a species EA<sub>2</sub> which reacts more slowly than EA. However, similar behaviour might be expected for a two site mechanism requiring the formation of a species MAB. As the concentration of A is increased, some MA<sub>2</sub> will be formed which is inactive. Thus inhibition at high concentrations of A would be expected.

Table 5.6

Results of dependence of initial rate of formation of p-toluidine on the concentration of the p-toluidine-anil

Anil added in $\mu$ l.	Initial rate [(fraction/sec.) $\times$ (anil added ( $\mu$ l))]
4	$7.73 \times 10^{-3}$
7.5	$1.15 \times 10^{-2}$
10	$1.61 \times 10^{-2}$
20	$2.02 \times 10^{-2}$
35	$2.67 \times 10^{-2}$

All samples were  $6.4 \times 10^{-4}$  M in  $ZuTu_4(ClO_4)_2$ .

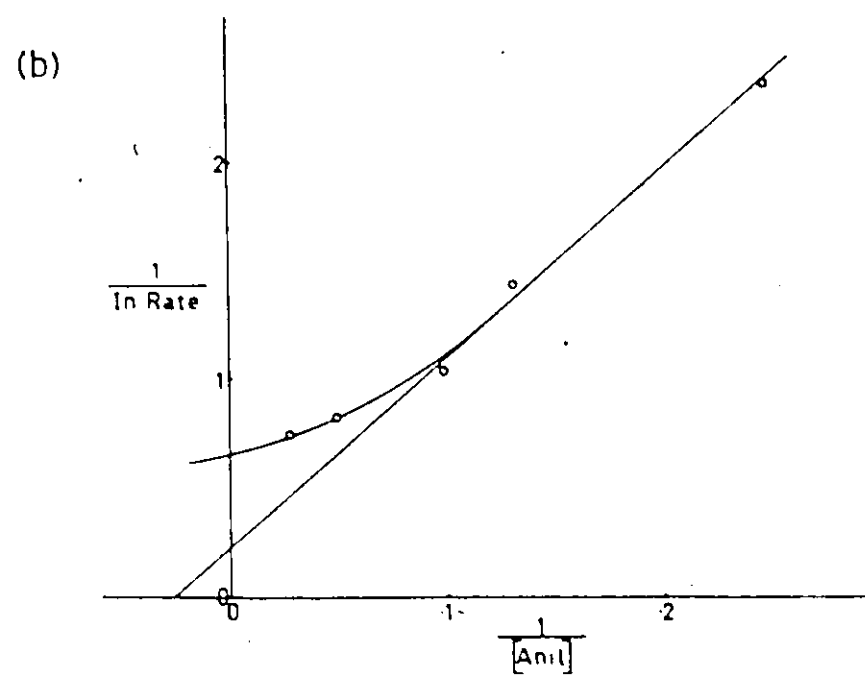
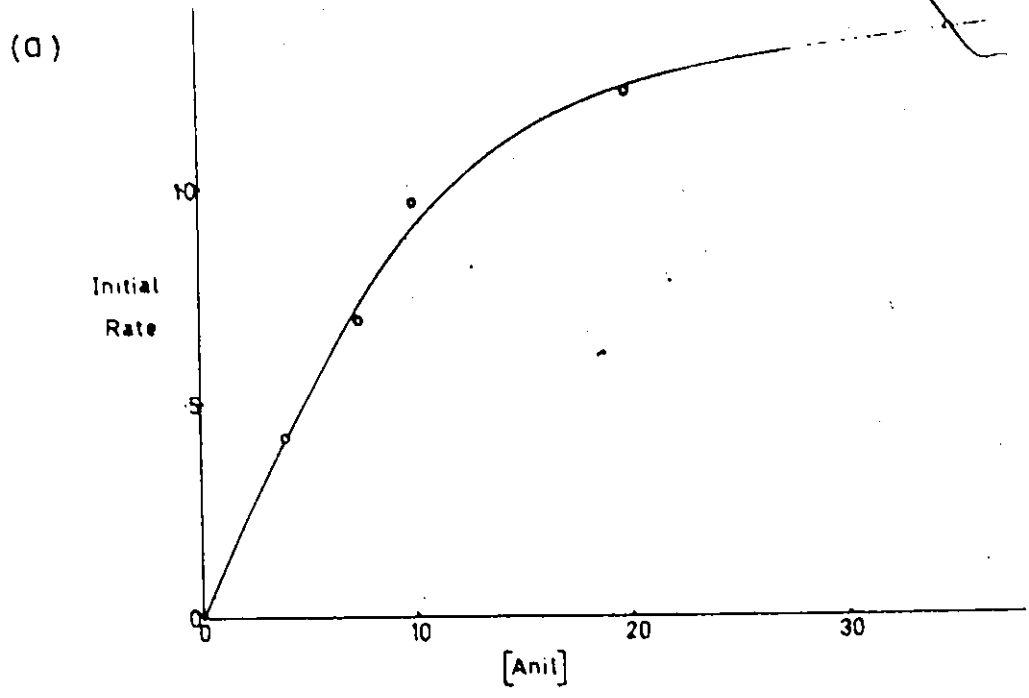


Fig. 5.6 Dependence of initial rate of formation of p-toluidine on the concentration of its acetone-anil. (a) Initial Rate (as fraction/minute X anil added in  $\mu\text{l}$ ) plotted against the anil added in  $\mu\text{l}$ , (b) (Initial rate) $^{-1}$ , units as in (a), plotted against (anil added) $^{-1}$  in  $\mu\text{l}^{-1}$

(ii) Dependence on water concentration

Since the acetone used already contained  $D_2O$ , the dependence of the initial rate of formation of aniline by hydrolysis of the anil was studied by adding different quantities of  $D_2O$ . The experimental results are collected in table 5.7 and plotted in figures 5.7(a) and 5.7(b). In figure 5.7(a), the usual hyperbolic dependence of the initial rate on the water added was observed. The curve in figure 5.7(a) should really not go through the origin since there is some  $D_2O$  already present in the acetone d-6. By studying the position of the final equilibrium attained in these samples, the water concentration originally present in the acetone d-6 was judged to be slightly less than 0.1% by weight. This is equivalent to 0.4 mg in each sample, compared to the 2, 4 and 8 mg added. The added quantities, thus, to fairly good approximation, represent the total water concentration. In figure 5.7(b) the double reciprocal plot for the above data is given and is a reasonable straight line.

(iii) Dependence of initial rate on overall concentration

As in the case of the forward reaction, the effect of diluting the reactants with an "inert" solvent,  $CCl_4$ , was examined. In this experiment all the species involved, the anil, acetone, catalyst and water (since its sole source is the acetone d-6) were progressively diluted with  $CCl_4$  while keeping their relative proportions exactly the same. A stock solution of anil in acetone d-6 (with a little  $D_2O$  added) was prepared and diluted with  $CCl_4$  to make up the five samples. The catalyst solution,  $ZnTu_4(ClO_4)_2$  in acetone d-6, was added by syringe keeping the relative concentrations of anil and catalyst constant in all samples. In table

Table 5.7

Dependence of initial rate of formation of p-toluidine on water concentration.

Water added (mg)	Initial rate (moles/l.sec)
2	$2.2 \times 10^{-4}$
4	$3.7 \times 10^{-4}$
8	$5.2 \times 10^{-4}$

Samples were 0.14 M in p-toluidine-anil and  $6.4 \times 10^{-4}$  M in  $\text{ZnTu}_4(\text{ClO}_4)_2$ .

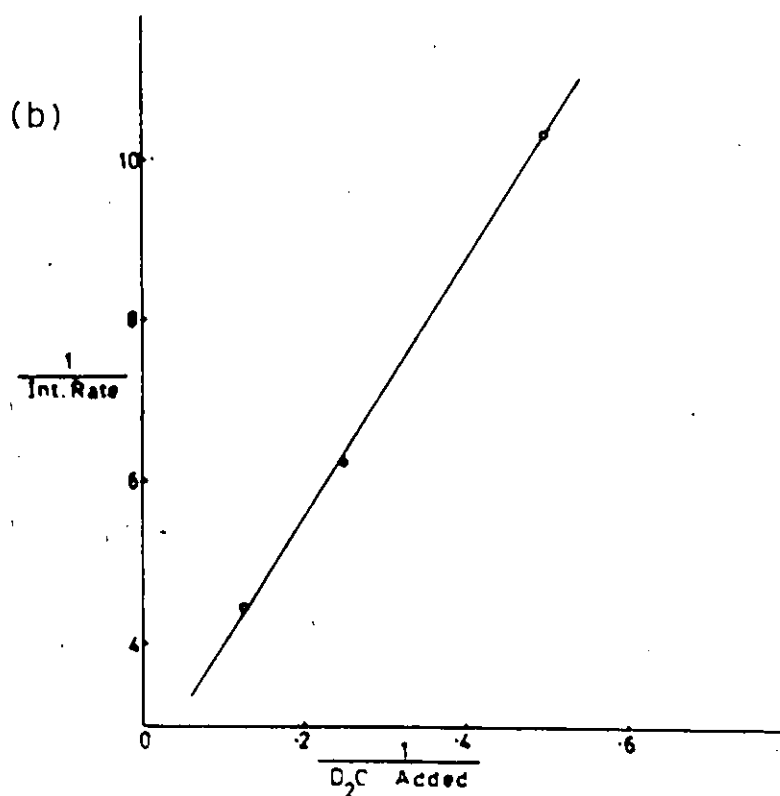
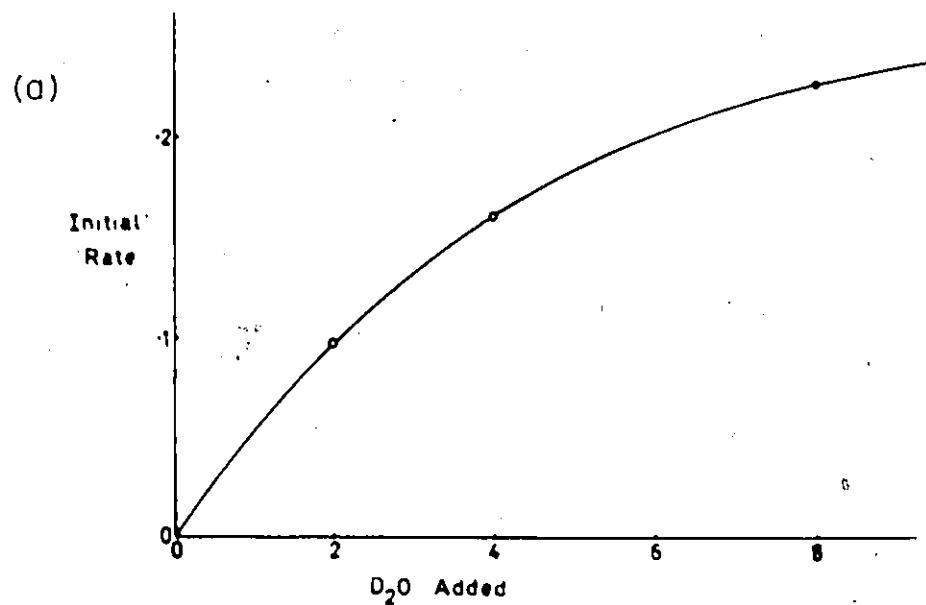


Fig. 5.7 Dependence of initial rate of formation of *p*-toluidine on the water concentration. (a) Initial Rate (as fraction of *p*-toluidine/minute) plotted against D<sub>2</sub>O added (in mg.) (b) (Initial Rate)<sup>-1</sup> (min/fraction) against [D<sub>2</sub>O added]<sup>-1</sup> in mg<sup>-1</sup>

5.8 the results are presented giving the rates and concentrations relative to the undiluted sample. The rates were expressed in moles/l.sec. rather than the fraction per unit time. The results are plotted in figure 5.8, and the graph is a good straight line passing through the origin. The rate is thus proportional to  $V^{-1}$ , where  $V$  is the factor by which the stock solution was diluted with carbon tetrachloride.

(D) The Kinetic Isotope Effect

It has frequently been observed that the rate of reaction, in a system where hydrogen is transferred from one atom to another, can be reduced by replacing that hydrogen with deuterium<sup>(21)</sup>. The ratio of the rate constants,  $\frac{k_H}{k_D}$ , for the reaction with the normal and the deuterated material is known as the magnitude of the kinetic isotope effect. Frequently, in studies of chemical reactions, kinetic isotope effects are measured and used as evidence for or against the occurrence of hydrogen transfer in the rate determining step of a reaction. In the reaction of aniline and acetone to form anil it is possible that transfer of a hydrogen atom, or two, could be important in the rate determining step. An experiment was therefore designed to determine the kinetic isotope effect for the forward reaction. This experiment is complicated by the presence of  $D_2O$  in the acetone as discussed earlier in this chapter. Any p-toluidine (h-2) added will very quickly become partly deuterated on the amino group due to exchange between protons on the amino group and deuterons in the water. The samples in the experiment were therefore made up in pairs, one containing p-toluidine (A) and

Table 5.8

Dependence of initial rate of formation of p-toluidine on degree of dilution with  $\text{CCl}_4$

Relative concentration of anil, acetone, $\text{D}_2\text{O}$ and catalyst	$\text{CCl}_4$ as a fraction of the volume	Relative initial rate
1	0	1.00
$\frac{4}{5}$	$\frac{1}{5}$	.72
$\frac{3}{5}$	$\frac{2}{5}$	.57
$\frac{2}{5}$	$\frac{3}{5}$	.41
$\frac{1}{5}$	$\frac{4}{5}$	.18

The initial solution was 0.27 M in p-toluidine-anil and  $1.1 \times 10^{-3}$  M in  $\text{ZnTu}_4(\text{ClO}_4)_2$ .



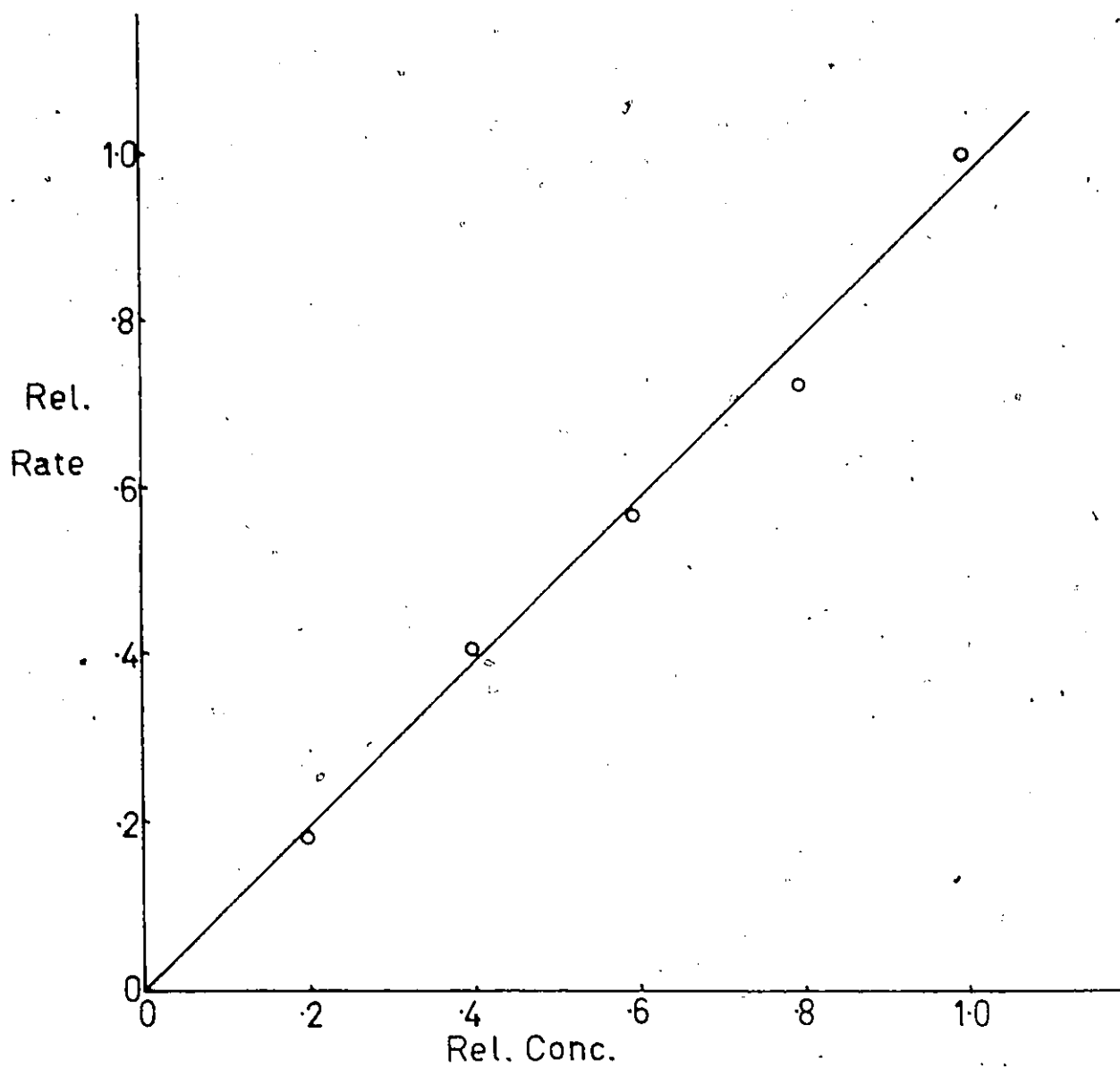


Fig. 5.8 Dependence of initial rate of formation of p-toluidine on dilution with  $\text{CCl}_4$ . Relative initial rate is plotted against the relative concentration

and the other an equal concentration of p-toluidine(d-2) (B). The p-toluidine (d-2) was deuterated to the extent of 95% on the amino group. The initial rate of formation of the anil was then studied over a range of p-toluidine concentrations. For each concentration the ratio of the initial rates, i.e.  $\frac{\text{rate A}}{\text{rate B}}$ , was calculated. In table 5.9 the values of  $\frac{\text{rate A}}{\text{rate B}}$  are listed for the concentrations of p-toluidine and p-toluidine (d-2) used. The results are plotted in figure 5.9. The ratio  $\frac{\text{rate A}}{\text{rate B}}$  increases as the p-toluidine concentration increases. This is due to the fact that, at low p-toluidine concentrations, the p-toluidine (h-2) is partially deuterated, but, as the concentration is increased, the fraction deuterated decreases. Thus, the true value of the kinetic isotope effect will be the ratio  $\frac{\text{rate A}}{\text{rate B}}$  in the limit of infinite p-toluidine concentration. This limit was obtained by fitting a curve to the points in figure 5.9. The ideal form of the curve in figure 5.9 may be simply derived. Let X be the value of the ratio  $\frac{\text{rate A}}{\text{rate B}}$ , Y be the p-toluidine concentration and  $X_{\infty}$  the value of X when  $Y = \infty$ .

For sample A then,

$$\text{rate A} = \text{rate H}(f_H) + \text{rate D}(f_D)$$

where rate H is the rate of reaction of the p-toluidine (h-2), rate D is the rate of reaction of the p-toluidine (d-2), and  $f_H$  and  $f_D$  are the fractions of p-toluidine in sample A which are protonated and deuterated respectively. For sample B, assumed to be 100% deuterated,

$$\begin{aligned} \text{rate B} &= \text{rate D}(f_D) \\ &= \text{rate D.} \end{aligned}$$

Table 5.9

Determination of the kinetic isotope effect for the forward reaction.

p-toluidine concentration in moles/l.	$\frac{\text{rate A}}{\text{rate B}}$
$0.68 \times 10^{-1}$	1.148
$1.20 \times 10^{-1}$	1.245
$1.77 \times 10^{-1}$	1.269
$2.36 \times 10^{-1}$	1.329
$2.88 \times 10^{-1}$	1.424
$4.81 \times 10^{-1}$	1.456
$6.11 \times 10^{-1}$	1.500

All samples were  $1.21 \times 10^{-4}$  M in  $\text{ZnTu}_4(\text{ClO}_4)_2$  and were made up with acetone (d-6) from the same lot.

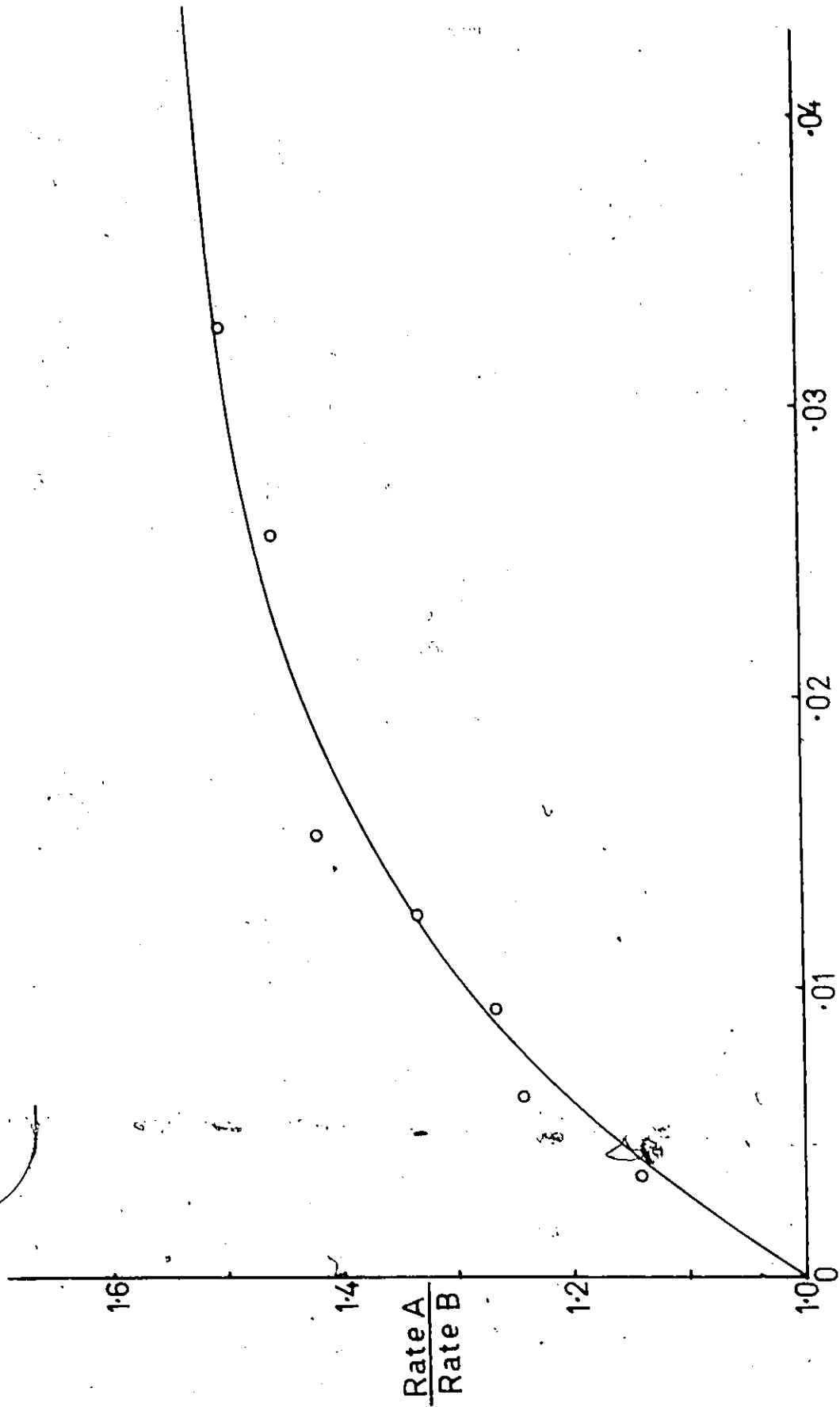


Fig. 5.9 The kinetic isotope effect. The ratio  $\frac{\text{rate H}}{\text{rate D}}$  plotted against the p-toluidine added (in grams)

$$\frac{\text{rate A}}{\text{rate B}} = X = \frac{\text{rate H}(f_H) + \text{rate D}(f_D)}{\text{rate D}}$$

$$X = \frac{\text{rate H}}{\text{rate D}} (f_H) + f_D$$

$$= \frac{\text{rate H}}{\text{rate D}} (1 - f_D) + f_D$$

When the concentration of p-toluidine in samples A and B is infinite, then the fraction deuterated in sample A would be negligible and  $X_\infty = \frac{\text{rate H}}{\text{rate D}}$

$$X = X_\infty (1 - f_D) + f_D$$

$$\frac{X - X_\infty}{1 - X_\infty} = f_D$$

Now, as  $f_D$  must be 1 when Y is zero and must be 0 when Y is infinity, then  $f_D$  may be represented as a function of Y by  $f_D = e^{-kY}$ .

$$\frac{X - X_\infty}{1 - X_\infty} = e^{-kY} \quad (5.4)$$

also  $\ln\left(\frac{X - X_\infty}{1 - X_\infty}\right) = -ky \quad (5.5)$

Therefore, a plot of  $\ln\left(\frac{X - X_\infty}{1 - X_\infty}\right)$  against Y should be a straight line through the origin with a slope of k. For a series of values of  $X_\infty$  the experimental values of X and Y were used in equation (5.5), and a least squares fit was carried out for each  $X_\infty$  value. The values of the slope (k) and the standard deviation ( $\sigma$ ) obtained for k are listed in table 5.10. In figure 5.10, the standard deviation ( $\sigma$ ) is plotted against  $X_\infty$ , and it may be seen that  $\sigma$  is a minimum when  $X_\infty = 1.55$ . The curve drawn in figure 5.9 is calculated from equation (5.4), using  $X_\infty = 1.55$  and  $k = 74.53$ . From this experiment

Table 5.10

Determination of best value for  $X_{\infty}$  by linear regression

$X_{\infty}$	k(slope)	$\sigma$ (standard deviation)
1.530	85.15	3.5296
1.540	79.27	3.2970
1.545	76.79	3.2660
1.550	74.53	3.2610
1.555	72.48	3.2676
1.560	70.57	3.2827
1.570	67.16	3.3189

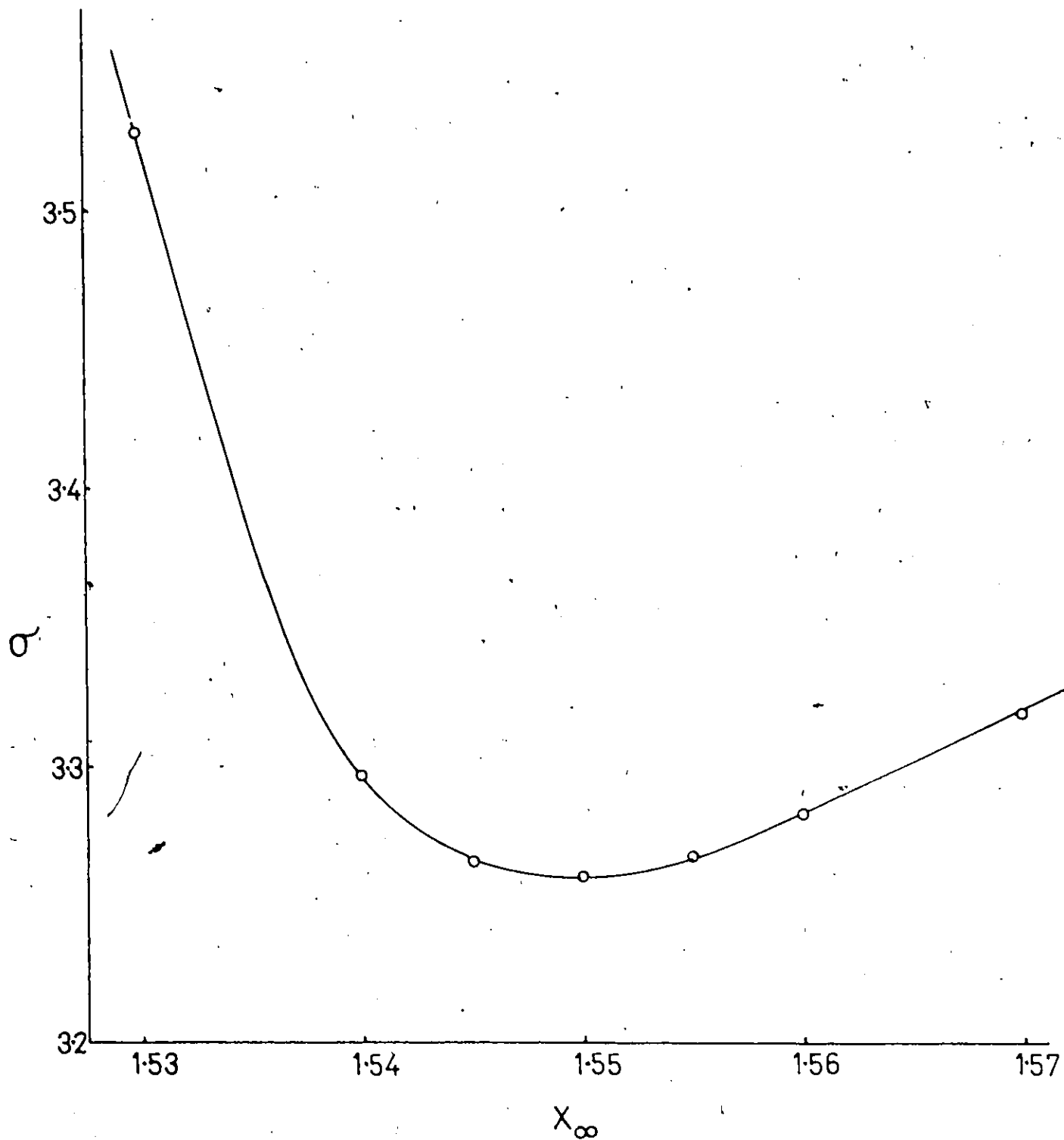


Fig. 5.10 The kinetic isotope effect. The standard deviation ( $\sigma$ ) plotted against  $X_\infty$ .

the value of  $\frac{\text{rate H}}{\text{rate D}}$  is found to be 1.55. This is not the true kinetic isotope effect which would be the ratio of the rate constants  $\frac{k_H}{k_D}$ , as the observed rates probably contain equilibrium constants which could also be effected by isotopic substitution. However, these effects are likely to be small compared to the effect on the rate constant itself (21).

(E) Summary

In this chapter measurements of the initial rate of reaction for the formation and hydrolysis of p-toluidine-anil have been discussed. The following are the results obtained.

- (a) The forward reaction is first order in catalyst (with  $\text{ZnTu}_4(\text{ClO}_4)_2$  as the catalyst).
- (b) The form of the dependence of the initial rate of reaction on the aniline, anil and water concentrations is a hyperbolic curve. When the data for these substates is plotted in a double reciprocal, or Lineweaver-Burk plot, a straight line is obtained.
- (c) For both the forward and back reactions, dilution with  $\text{CCl}_4$  causes the rate (in moles/l.sec) to vary as  $\frac{1}{V}$  where V is the factor by which the original solution was diluted.
- (d) Addition of Tu inhibits the rate of the forward reaction.
- (e) The isotope effect on the rates  $\left(\frac{\text{rate H}}{\text{rate D}}\right)$  was found to be 1.55 for the forward reaction of p-toluidine (h-2) and p-toluidine (d-2) with acetone d-6.



CHAPTER SIX  
LIGAND EXCHANGE

(A) INTRODUCTION

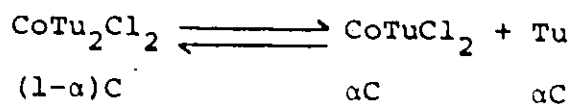
As mentioned in Chapter Four it is most desirable, when studying a metal complex catalysed reaction, to know both the equilibrium constants for complexing the various substrates with the metal and the rates of these ligand exchange processes. The equilibrium constants are most commonly determined using spectrophotometry, for example see reference 34. Ligand exchange rates have been much studied with the bulk of this work falling into two main areas<sup>(12)</sup>. One of these is concerned with complexes of Cr(III), Co(III) and Pt(II) for which the exchange rates are fairly slow and can be studied by simple spectrophotometry. The other main area is the labile complexes of Ni(II) and non-transition metals in aqueous solution, where ligand exchange has been studied using temperature-jump techniques<sup>(83)</sup>. The use of NMR has opened up a third and growing area, that of moderate exchange rates which are amenable to line broadening studies. In the specific area of Schiff bases or imines as ligands, little work seems to have been done on the measurement of ligand exchange rates. There is a report<sup>(84)</sup> of an NMR study of aqueous pyridoxal-alanine-Zn(II) and Al(III) systems in which it was found that exchange between free and complexed aldimine, or Schiff base, was fast (on the NMR time scale) in the Zn(II)

case, whereas in the Al(III) case exchange was slow. In a temperature-jump study<sup>(85)</sup> the kinetics of ligand and exchange reactions of a Cu(II) complex were studied. It was found that protonated histamine replaced coordinated serine via an apparent "dissociative" path and an associative one. The "dissociative" path almost certainly involves an aquated intermediate.

In this chapter are reported the results of NMR experiments which were designed to determine the equilibrium constants and rates of ligand exchange for systems closely related to those for which the initial rate measurements have been carried out.

#### (B) THIOUREA AS A LIGAND IN ACETONE SOLUTION

In the course of an extensive study<sup>(80,86)</sup> of metal thiourea complexes in acetone solution, Dr. K. Zaw of this laboratory measured the dissociation constant and the exchange rates of thiourea in the complex  $\text{CoTu}_2\text{Cl}_2$  in acetone solution. These measurements depend critically on the large isotropic shift exhibited by complexed Tu. At room temperature there is fast exchange (on the NMR time scale) between free and complexed Tu, but this may be "frozen out" at  $-80^\circ\text{C}$ , giving separate signals for free and for complexed Tu. The complex  $\text{CoTu}_2\text{Cl}_2$  is slightly dissociated in acetone solution, and its dissociation constant  $K_D$  may be defined from the equilibrium (ignoring solvent for the moment)



where C = concentration of complex in moles/l

and  $\alpha$  = degree of dissociation of the complex.

Then

$$K_D = \frac{[\text{CoTuCl}_2][\text{Tu}]}{[\text{CoTu}_2\text{Cl}_2]} = \frac{\alpha^2 C}{1-\alpha}$$

If  $\alpha$  is very small, then  $K_D = \alpha^2 C$  or  $\alpha = \sqrt{\frac{K_D}{C}}$ . If the free and complexed thiourea are in fast exchange, then the observed shift  $\Delta v_{\text{obs}}$  will be given by

$$\Delta v_{\text{obs}} = \Delta v_c (f_c) + \Delta v_f (1-f_c),$$

where  $\Delta v_c$  is the shift of the complex ligand,  $\Delta v_f$  is the shift of free ligand, and  $f_c$  the fraction of thiourea which is complexed. If the shifts are measured from the free ligand signal, then  $\Delta v_f = 0$  and

$$\Delta v_{\text{obs}} = \Delta v_c (f_c)$$

The fraction of Tu which is complexed ( $f_c$ ) is  $1 - \frac{\alpha C}{2C} = 1 - \frac{\alpha}{2}$ ,

$$\Delta v_{\text{obs}} = \Delta v_c \left(1 - \frac{\alpha}{2}\right) = \Delta v_c \left(1 - \frac{1}{2} \sqrt{\frac{K_D}{C}}\right) \quad (6.1)$$

Therefore, a plot of  $\Delta v_{\text{obs}}$  against  $\frac{1}{\sqrt{C}}$  should be a straight line and give  $\Delta v_c$  as the intercept.  $K_D$  may be evaluated from the slope. For  $\text{CoTu}_2\text{Cl}_2$  in acetone d-6 Zaw<sup>(80)</sup> found  $\Delta v_c = 2167$  Hz at 56.4 MHz and  $K_D = 1.5 \times 10^{-4}$  at 27°C. The graph of  $\Delta v_{\text{obs}}$  against  $\frac{1}{\sqrt{C}}$  was a good straight line.

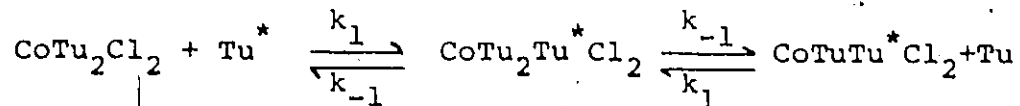
The rates of ligand exchange for complexes of thiourea in acetone were determined using NMR line broadening measurements<sup>(86,69)</sup>. The line broadening studies were carried out in the fast exchange region where the linewidth of the observed signal is given by:

$$\frac{1}{T_2} = \frac{P_C}{T_{2C}} + \frac{P_F}{T_{2F}} + P_C^2 P_F^2 (\omega_C - \omega_F)^2 (\tau_C + \tau_F)$$

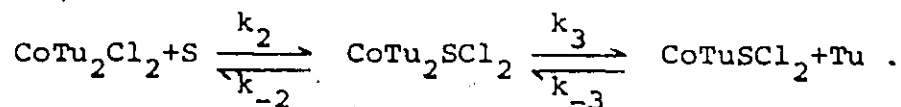
where  $P_C$  and  $P_F$  are the fractions of complexed and free Tu, and  $\frac{1}{T_{2C}}$  and  $\frac{1}{T_{2F}}$  are the linewidths of the complexed and free Tu signals. The chemical shift between the two peaks is  $(\omega_C - \omega_F)$ , and  $\tau_C$  and  $\tau_F$  are the lifetimes of complexed and free thiourea respectively. The terms  $\frac{1}{T_{2F}}$ ,  $P_C$ ,  $P_F$ ,  $(\omega_C - \omega_F)$  are easily determined once  $K_D$  is known as a function of temperature. The problem is to find  $\frac{1}{T_{2C}}$ , and extrapolation from the linewidth of the low temperature "frozen out" complexed ligand peak is a notably dangerous process<sup>(69)</sup>. Reliable values of  $\frac{1}{T_{2C}}$  were obtained by extrapolation of the plot of linewidth against  $\frac{1}{\sqrt{C}}$  to the point where  $\frac{1}{\sqrt{C}} = 0$ , i.e. where there is no free Tu. The linewidths were studied as a function of temperature and free ligand concentration.

The results<sup>(86,69)</sup> indicated that two mechanisms must be considered;

(a) a direct associative mechanism,

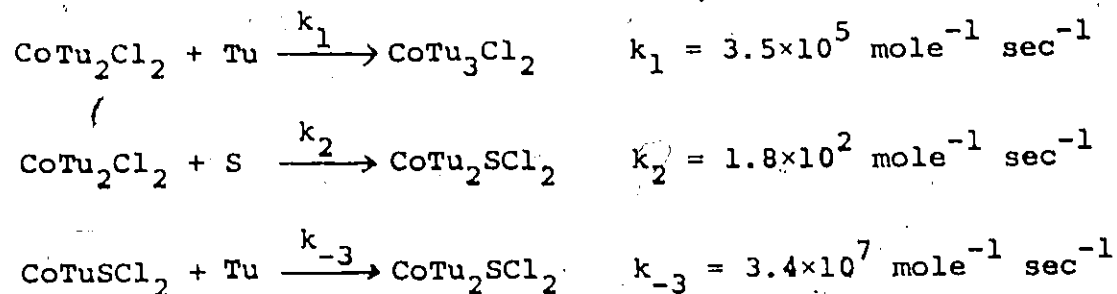


(b) a 'dissociative' mechanism, which is really exchange via a solvated intermediate:



The formation of the five-coordinate intermediate is rate determining in each case and the three rate constants for this

step determined for  $\text{CoTu}_2\text{Cl}_2$  at  $27^\circ\text{C}$  were:



The enthalpies and entropies of activation were also determined and support the description of mechanism (b) as going via an associative formation of a solvated intermediate, rather than a true dissociative process.

#### (C) THIOUREA AS A LIGAND IN ACETONITRILE SOLUTION

Anilines cannot be studied alone in acetone solutions of  $\text{CoTu}_2\text{Cl}_2$  because of interference from the anil which will be formed. The metal thiourea complexes are only soluble in a few solvents<sup>(69)</sup>; some other ketones, DMSO, acetonitrile and nitromethane. Acetonitrile seemed to be the one most suitable and similar to acetone, and so a study of  $\text{CoTu}_2\text{Cl}_2$  in acetonitrile was undertaken. The free and complexed thiourea were in fast exchange at room temperature, and remained that way until the solvent froze at  $-45^\circ\text{C}$ . The limiting shift was determined using the same method as described in the previous section. The shift of the Tu signal was measured as described in Chapter 3 Section (C). The plot of  $\Delta\nu_{\text{obs}}$  (in Hz from  $\text{CH}_3\text{CN}$  at 100 MHz) against  $\frac{1}{\sqrt{c}}$ , where  $c$  is the concentration of  $\text{CoTu}_2\text{Cl}_2$  in moles/l, is shown

in figure 6.1. The extrapolation to  $\frac{1}{\sqrt{c}} = 0$  gives an intercept of 4013 Hz. Measured from the free Tu signal this gives  $\Delta\nu_c = 3534$  Hz. The value of  $\Delta\nu_c$  for  $\text{CoTu}_2\text{Cl}_2$  in acetone is 3842 at 100 MHz.

Unlike the plot obtained by Zaw<sup>(80)</sup>, figure 6.1 shows a deviation from the predicted straight line as  $\frac{1}{\sqrt{c}}$  becomes small or as  $c$  becomes large. However, the deviation is only noticeable when the value of  $\frac{1}{\sqrt{c}}$  is less than  $3.0 \text{ l}^{1/2} \text{ mole}^{-1/2}$ . There is no data on  $\text{CoTu}_2\text{Cl}_2$  in acetone in this region. To investigate this deviation further, the dependence of the shift on  $\text{CoTu}_2\text{Cl}_2$  concentration was measured at higher concentrations. The results are plotted in figure 6.2, where the highest value of  $c$  is now 1.0 mole/l. The graph now shows a marked deviation at high values of  $c$  with the shift ( $\Delta\nu_{\text{obs}}$ ) eventually decreasing as  $c$  is increased. One possible explanation is that the  $\text{CH}_3\text{CN}$  peak, which is used as a reference, is in fact shifting as a function of  $c$ . This could be caused by the complexing of  $\text{CH}_3\text{CN}$  inducing an isotropic shift of the protons in the methyl group. This was checked by measuring the shift of  $\text{CH}_3\text{CN}$  from TMS as a function of  $\text{CoTu}_2\text{Cl}_2$  concentration. When the solution was 1.0 M in  $\text{CoTu}_2\text{Cl}_2$ , which corresponds to the most concentrated solution shown in figure 6.2, the  $\text{CH}_3\text{CN}$  signal had only shifted 15 Hz (at 100 MHz) from its position with no  $\text{CoTu}_2\text{Cl}_2$  added. This shift was to high field and the correction would only increase the deviations observed at high  $\text{CoTu}_2\text{Cl}_2$  concentrations. As a further check, the magnetic susceptibility was measured as a function of the  $\text{CoTu}_2\text{Cl}_2$ . This

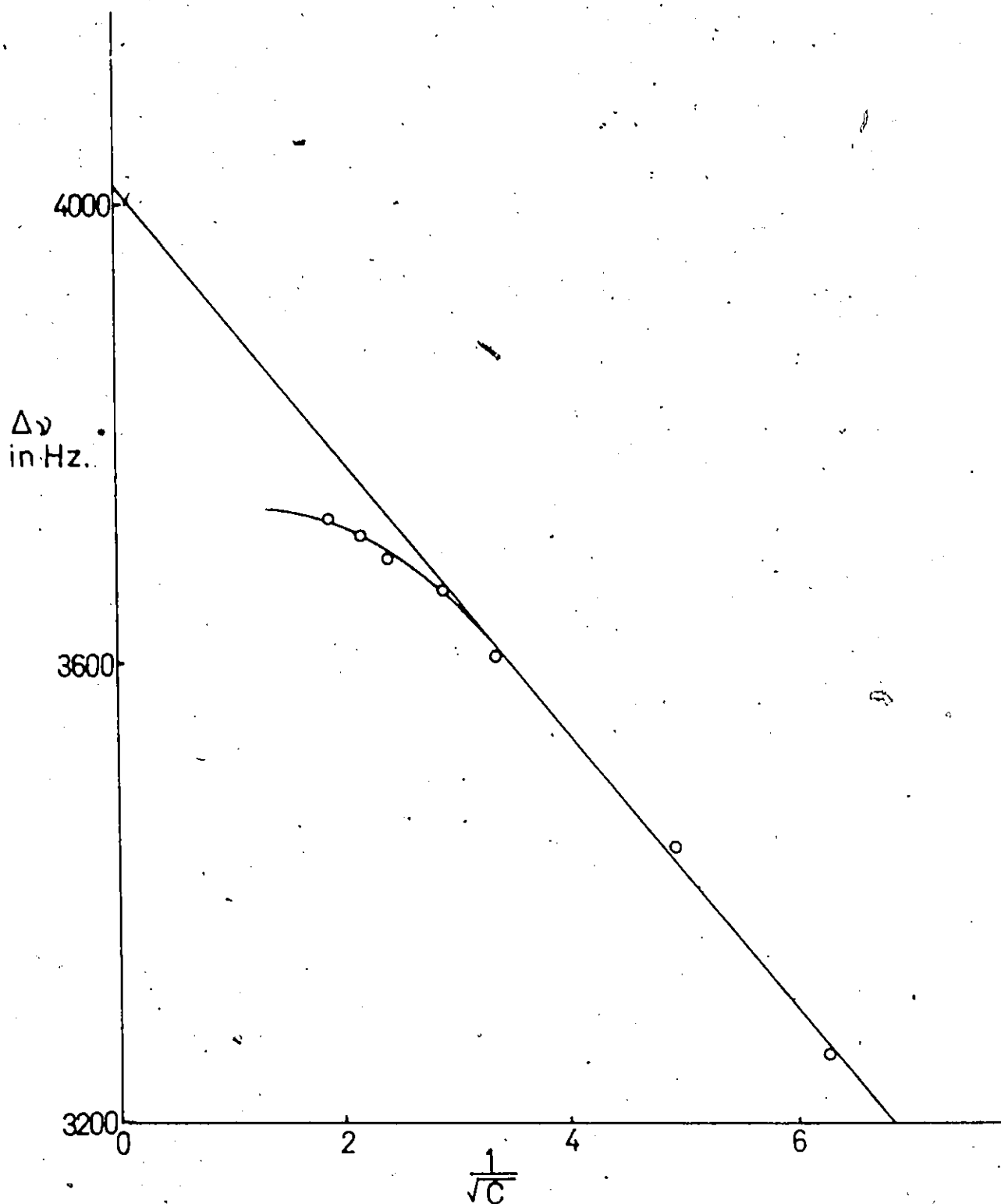


Fig. 6.1  $\text{CoTu}_2\text{Cl}_2$  in  $\text{CH}_3\text{CN}$ . A plot of  $\Delta\nu_{\text{obs}}$  (in Hz at 100 MHz measured from the  $\text{CH}_3\text{CN}$  signal) against  $1/\sqrt{c}$  (where  $c$  is the concentration of  $\text{CoTu}_2\text{Cl}_2$  in moles/l)

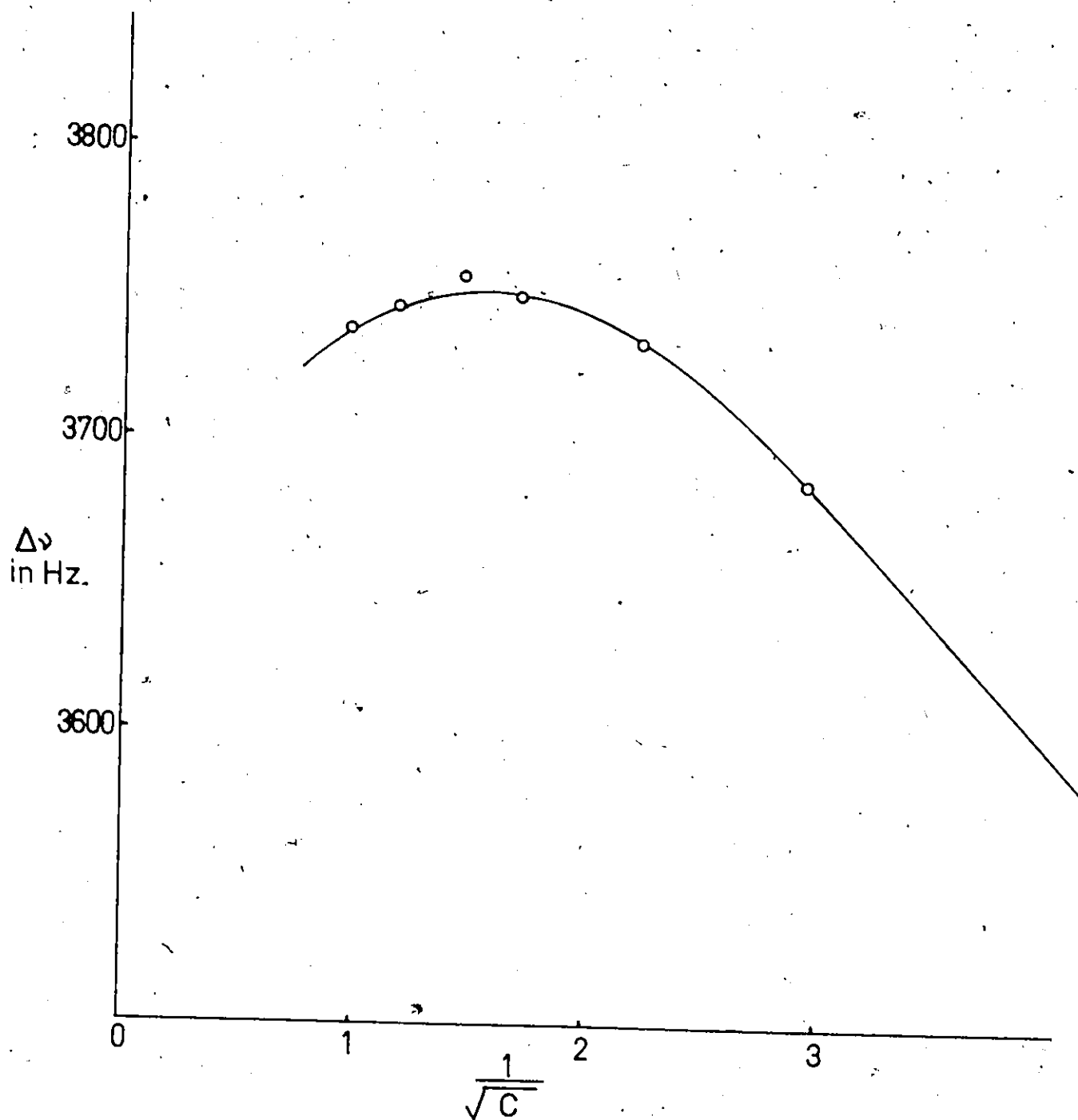


Fig. 6.2  $\text{CoTu}_2\text{Cl}_2$  in  $\text{CH}_3\text{CN}$ . A plot of  $\Delta\nu_{\text{obs}}$  (in Hz at 100 MHz measured from the  $\text{CH}_3\text{Cn}$  signal) against  $1/\sqrt{C}$  (where  $C$  is the concentration of  $\text{CoTu}_2\text{Cl}_2$  in moles/l)



was done by Evan's method<sup>(87)</sup> which involves measuring the shift in Hz between the signal of a reference compound in the paramagnetic solution and the same peak in a coaxial capillary of a diamagnetic solution. The susceptibility of the paramagnetic solute is given by

$$\chi = \frac{3}{2\pi m} \cdot \frac{\Delta f}{f_0} + \chi_0$$

where  $\Delta f$  is the shift in Hz,  $f_0$  is the operating frequency of the spectrometer,  $m$  is the mass (in grams) of the solute in 1 ml and  $\chi_0$  is the susceptibility of the solvent. In figure 6.3, the observed shift difference for  $\text{CH}_3\text{CN}$  internal and  $\text{CH}_3\text{CN}$  external ( $\Delta\nu$ ) is plotted against the mole fraction of  $\text{CoTu}_2\text{Cl}_2$ . The straight line obtained indicates no reduction in the susceptibility, which could result from such interactions as dimer formation. The deviations in figures 6.1 and 6.2 remain puzzling, but could be due to a slight shift of the magnetic axes caused by the changes in the second coordination sphere as the concentration of metal complex is increased. Such effects at high concentration will not affect the usefulness of the equilibrium constant reported provided it is applied to solutions where the  $\text{CoTu}_2\text{Cl}_2$  concentration is less than 0.1 moles/l.

(D) WATER AS A LIGAND

(i) Water concentration

Water is always present in acetone to a certain extent. If all the water is known to be present as  $\text{H}_2\text{O}$ , then its concentration in acetone h-6 may be simply determined by measuring

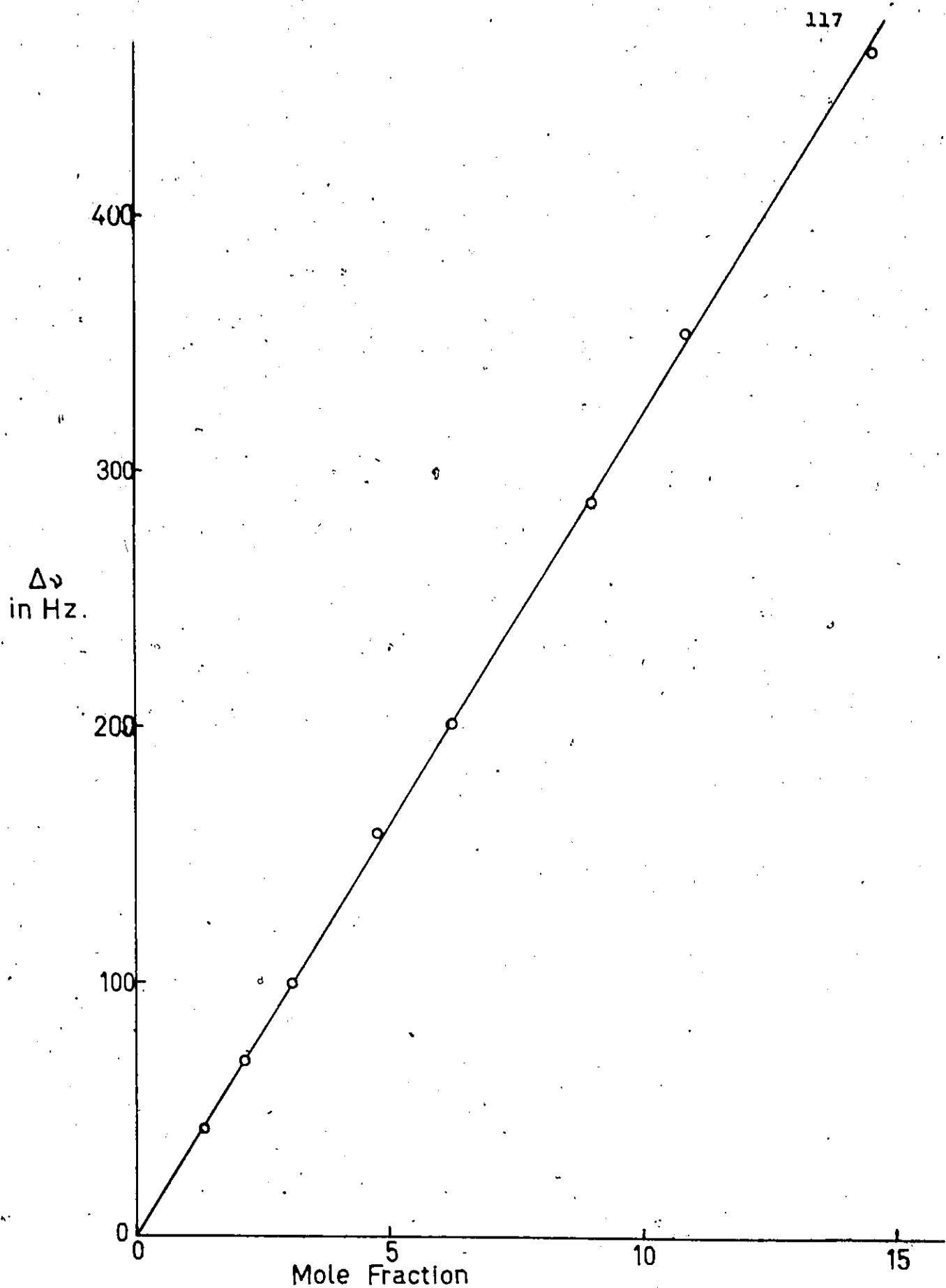
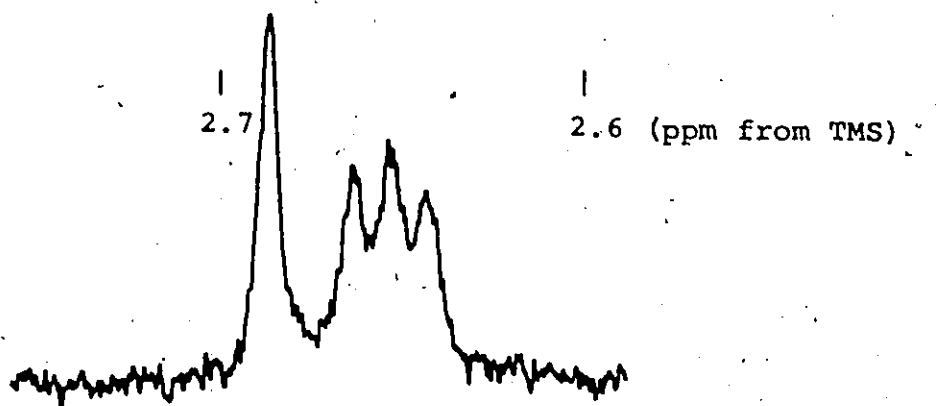


Fig. 6.3 Susceptibility of  $\text{CoTu}_2\text{Cl}_2$  in  $\text{CH}_3\text{CN}$ . A plot of  $\Delta\nu$  (shift in Hz at 100 MHz between the internal and external  $\text{CH}_3\text{CN}$  signals) against the mole fraction of  $\text{CoTu}_2\text{Cl}_2 \times 10^3$

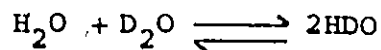
the area of the  $\text{H}_2\text{O}$  signal in the NMR spectrum and comparing this to the area of the nearby  $^{13}\text{C}$  satellite of the acetone signal. This method was used to find the concentration of  $\text{H}_2\text{O}$  in acetone  $\text{d}-6$  as described in Chapter 4 Section (G). However, when part of the water is suspected to be present as  $\text{HDO}$  or  $\text{D}_2\text{O}$ , the situation is more difficult. This is the case for the water in commercially supplied acetone  $\text{d}-6$ . According to the manufacturers, the acetone  $\text{d}-6$  contains between 0.1% and 0.2% of water. The H to D ratio in this water is the same as in the acetone  $\text{d}-6$ , i.e. the water should contain 99.5% D and 0.5% H. The water can then be considered to be present as  $\text{D}_2\text{O}$ . Various methods were considered for measuring the heavy water concentration, e.g. mass spectrometry, density measurements and infrared spectroscopy. A method using NMR was finally decided upon. This was based on the observation of the NMR of acetone  $\text{d}-6$  as  $p$ -toluidine was added. Pure acetone  $\text{d}-6$ , when handled under  $\text{N}_2$  and placed in a dried NMR sample tube, has an extremely weak  $^1\text{H}$  signal in the water region. This consists of three peaks of approximately equal intensity spaced 1 Hz apart. As  $p$ -toluidine is added, the three peaks increase in intensity and broaden slightly. With further quantities of  $p$ -toluidine, a singlet appears downfield from the triplet and grows in intensity at the expense of the triplet. The  $^1\text{H}$  from the amino group of the  $p$ -toluidine is presumably exchanging with the D in the water producing  $\text{HDO}$  and  $\text{H}_2\text{O}$ . The triplet is due to  $\text{HDO}$ , with the H coupling to the D

nucleus ( $I=1$ ), and the singlet is due to  $H_2O$ <sup>(88)</sup>. A typical spectrum with both signals present is shown below,



The NMR spectra thus confirm that initially virtually all the water present in acetone d-6 is there as  $D_2O$ .

The measurement of the  $D_2O$  concentration was carried out by weighing pure sublimed p-toluidine and dissolving it in 0.50 ml of acetone d-6 in an NMR sample tube. The  $H_2O$ , HDO and para methyl peaks were integrated several times and the average areas calculated. The equilibrium constant  $K$  for the equilibrium



is given by

$$K = \frac{[HDO]^2}{[H_2O][D_2O]}$$

This constant  $K$ , which would be 4.0 by statistical methods, was found to be  $3.94 \pm 0.12$  at  $20^\circ C$  by an NMR method<sup>(88)</sup> similar

to the one used in this experiment. Thus, knowing  $K$ ;  $[H_2O]$  and  $[HDO]$  it is possible to evaluate the term  $[D_2O]$ . The total water concentration in the sample is therefore known. The average of several determinations using different amounts of p-toluidine yielded the  $D_2O$  concentration as  $0.21(\pm 0.02)\%$  by weight for a particular sample of acetone d-6.

(ii) Equilibrium constant for water as a ligand

Once the concentration of water in the acetone d-6 was known, it was possible to determine the equilibrium constant for the complexing of water with  $CoTu_2Cl_2$ .

The experiment was carried out by weighing  $CoTu_2Cl_2$  and dissolving it in 0.50 ml of acetone d-6. This acetone d-6 was from the same sample as that in which the concentration of water was measured as described above. The NMR spectrum was run and the position of the Tu resonance was measured. This resonance was monitored as  $H_2O$  was added in 2  $\mu$ l. portions from a 20  $\mu$ l. syringe. Altogether 20  $\mu$ l. of water were added. The initial water content of the acetone d-6 was roughly 1  $\mu$ l. of water. The shift of the Tu peak, relative to the free Tu peak position, is listed in table 6.1 for a series of values of the total water concentration. The shift of the Tu peak ( $\Delta\nu_{obs}$ ) yields the concentration of free Tu from the equation:

$$\frac{\Delta\nu_{obs}}{\Delta\nu_c} = 1 - f_F$$

where  $\Delta\nu_c$  is the shift of complexed Tu and  $f_F$  is the fraction of

Table 6.1

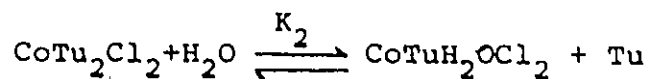
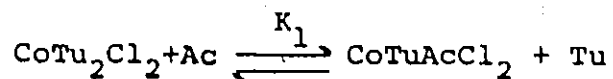
Shift of Tu peak of  $\text{CoTu}_2\text{Cl}_2$  as a function of  
water concentration

Water concentration in moles/l	Shift of Tu from free Tu in Hz
0.11	3346
0.33	3309
0.56	3291
0.78	3258
1.00	3212
1.22	3183
1.44	3131
1.67	3065
1.89	3024
2.11	2990
2.33	2956

Measurements made at 90 MHz

Solution was .040 M in  $\text{CoTu}_2\text{Cl}_2$

Tu which is free in solution. There are only two potential ligands to replace Tu, acetone and water. The equilibria possible for the case of a small degree of dissociation of the metal complex, which is certainly the case here, are



$$K_1 = \frac{[\text{CoTuAcCl}_2][\text{Tu}]}{[\text{CoTu}_2\text{Cl}_2][\text{Ac}]}$$

$$K_2 = \frac{[\text{CoTuH}_2\text{OCl}_2][\text{Tu}]}{[\text{CoTu}_2\text{Cl}_2][\text{H}_2\text{O}]}$$

where Ac represents acetone.

If M is the initial concentration of  $\text{CoTu}_2\text{Cl}_2$  added, in moles/l. Then

$$M = [\text{CoTu}_2\text{Cl}_2] + [\text{CoTuAcCl}_2] + [\text{CoTuH}_2\text{OCl}_2].$$

The total concentration of Tu is 2M;

$$2M = 2[\text{CoTu}_2\text{Cl}_2] + [\text{Tu}] + [\text{CoTuAcCl}_2] + [\text{CoTuH}_2\text{OCl}_2].$$

If the total water concentration is W moles/l, then

$$W = [\text{H}_2\text{O}] + [\text{CoTuH}_2\text{OCl}_2].$$

The total acetone concentration which is 13.7 moles/l will not be affected by the small fraction of acetone complexed and is left as C.

There are thus five unknowns and five equations, the two equilibria and the three mass balance equations. It is possible to rearrange the equations and to write a cubic

equation in only one variable. The coefficients are listed below for such a polynomial with  $[\text{CoTu}_2\text{Cl}_2]$  as the variable, i.e.  $A[\text{CoTu}_2\text{Cl}_2]^3 + B[\text{CoTu}_2\text{Cl}_2]^2 + C[\text{CoTu}_2\text{Cl}_2] + D = 0$

where

$$A = 1 - K_2$$

$$B = -3M - K_1C + 2MK_2 + K_1K_2C - K_2W$$

$$C = 3M^2 + K_1MC - K_2M^2 + K_2WM$$

$$D = -M^3$$

Thus, knowing  $K_1$ ,  $K_2$ ,  $M$ ,  $C$  and  $W$ , the concentrations of all species in solution may be determined. In this particular case  $K_1$ ,  $M$ ,  $C$  and  $W$  are known and  $[\text{Tu}]$  is also known. The value of  $K_2$  was determined by computing the value of  $[\text{Tu}]$  for a variety of values of  $K_2$  until agreement with the experimental value of  $[\text{Tu}]$  was obtained. This was done for a number of concentrations of water and  $K_2$  was determined for each concentration. In figure 6.4 is a graph where  $K_2$  is plotted against the water concentration ( $W$ ). The most obvious point is that  $K_2$  is not a constant, but rather depends strongly on water concentration. Assuming that  $K_1$  is not affected strongly by water concentration this means that the relative ability of water and thiourea to act as ligands is dependant on water concentration, at least for dilute solutions. The highest concentration of water in figure 6.4 corresponds to 5% water by weight in acetone d-6. The water appears to behave as a progressively better ligand towards  $\text{Co(II)}$  in  $\text{CoTu}_2\text{Cl}_2$  as the water concentration increases. Similar



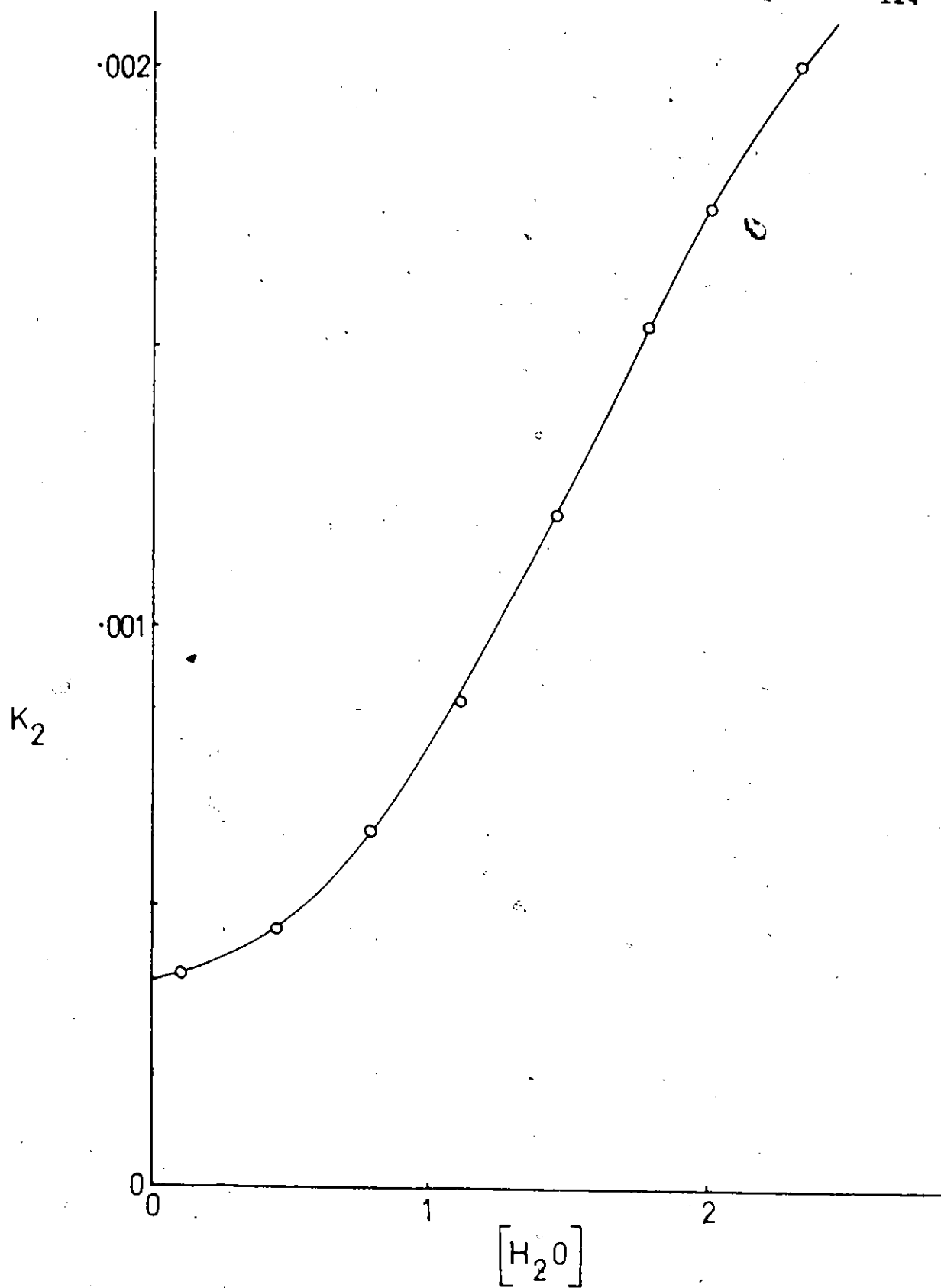


Fig. 6.4 Dependence of  $K_2$ , the equilibrium constant for association of water with  $CoTu_2Cl_2$  in acetone on  $[H_2O]$  in moles/l

qualitative conclusions were reached by Eaton and Zaw<sup>(80)</sup> for  $\text{CoTu}_2\text{Cl}_2$  and  $\text{CoTu}_4(\text{ClO}_4)_2$  in acetone by observing the shift of the  $\text{H}_2\text{O}$  peak as a function of water concentration. Also, in an electrochemical study of the stability of metal thiourea complexes in aqueous acetone, Shul'man et al<sup>(89)</sup> found that the relative complexing abilities of Tu and  $\text{H}_2\text{O}$  depended on the dielectric constant of the solution.

The result obtained in this experiment, and the one described in Chapter 4 Section (G) where the "equilibrium constant" for the formation of anil was found to depend on water concentration, would suggest that the activity of water in dilute solution in acetone is not a linear function of its concentration.

#### (E) ANILINES AND ANILS AS LIGANDS

##### (i) NMR Spectra

As has been discussed in Chapter 4, anilines will react with acetone in the presence of thiourea complexes of Co and Zn to produce anils. In Figure 6.5 are the 100 MHz proton NMR spectra obtained from p-toluidine in acetone d-6 solution under various experimental conditions. Spectrum A is that of a freshly prepared solution of p-toluidine in acetone d-6. The peaks present are, starting from the high field end: the quintet of the residual  $^1\text{H}$  in the acetone d-6, the methyl peak of p-toluidine, the HDO and  $\text{H}_2\text{O}$  resonances, the amino group signal and the ortho and meta doublets of the aromatic protons.

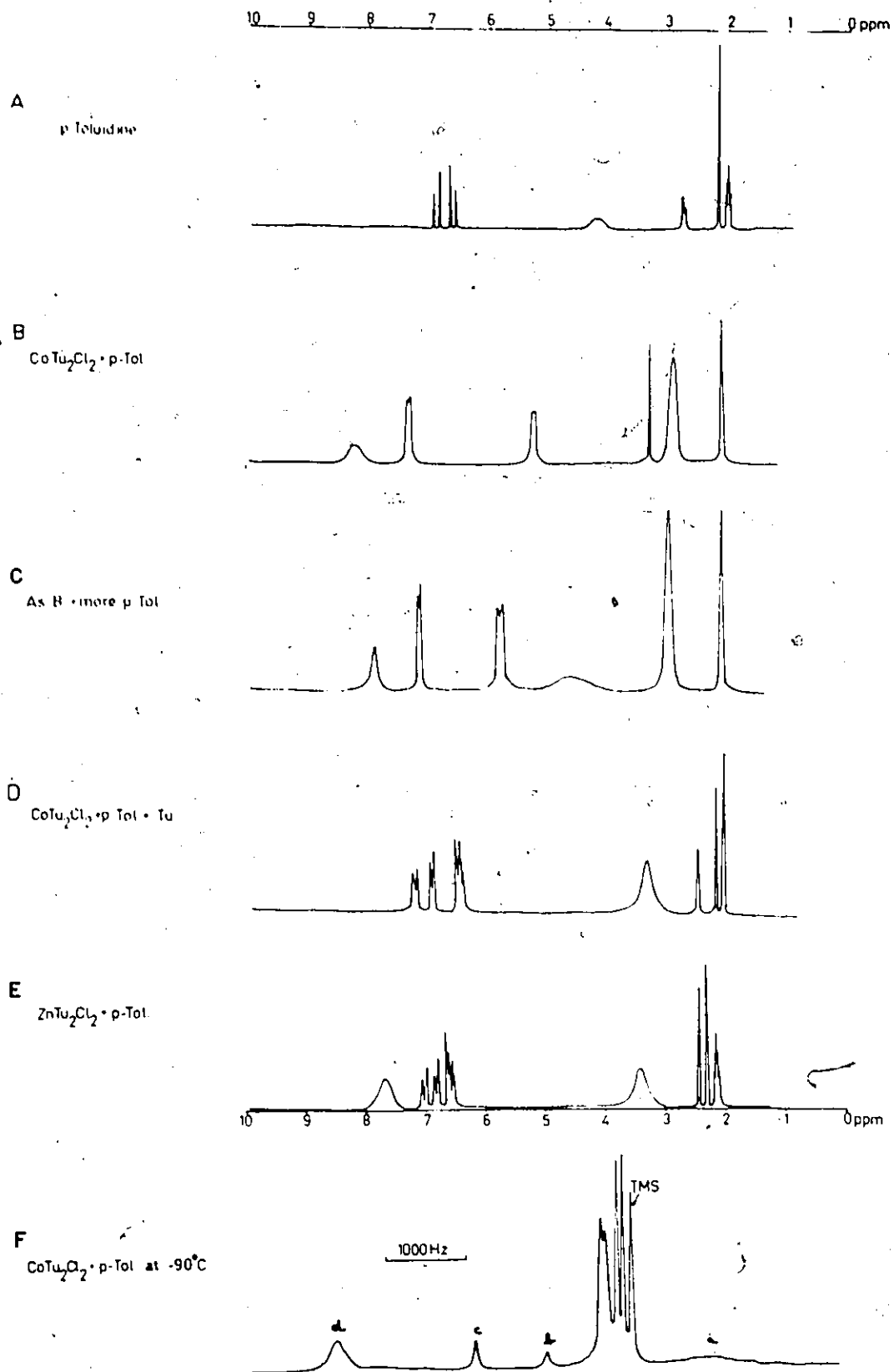


Fig. 6.5 100 MHz <sup>1</sup>H NMR spectra with p-toluidine in acetone (d-6)

Spectrum B was obtained by adding  $\text{CoTu}_2\text{Cl}_2$  to the sample of p-toluidine in acetone d-6. Addition of more p-toluidine yielded spectrum C. If Tu was then added (to saturation), spectrum D was obtained. This spectrum D bears a marked resemblance to that shown in E which was produced by adding  $\text{ZnTu}_2\text{Cl}_2$  to a solution of p-toluidine in acetone d-6. By comparison with the spectrum of the acetone-anil of p-toluidine (Chapter 4 section (C)) the peaks in spectrum E can be assigned as follows: acetone quintet, para methyl of p-toluidine, para methyl of p-toluidine anil,  $\text{H}_2\text{O}/\text{HDO}$ /amino group in fast exchange, ortho protons of p-toluidine and the anil (overlapped), meta doublet of p-toluidine, meta doublet of the anil and the signal due to the  $\text{NH}_2$  groups of thiourea in  $\text{ZnTu}_2\text{Cl}_2$ . The peaks observed in D may be assigned by comparison with spectrum E where the chemical shifts are quite similar. Addition of  $\text{CoTu}_2\text{Cl}_2$  to acetone d-6 solutions of p-toluidine thus produces the anil (virtually instantaneously at the metal complex concentrations used). Both the p-toluidine and its anil undergo ligand exchange with the Tu on the meta complex. This is demonstrated by the shifting of the peaks from their diamagnetic positions due to the interaction with the paramagnetic metal. That the exchange is fast is shown by the dependence of the shifts on the p-toluidine to metal complex concentration ratio and also on the Tu concentration. The shift of a peak in fast exchange is given by:

$$\Delta\nu_{\text{obs}} = \Delta\nu_{\text{C}}f_{\text{C}} + \Delta\nu_{\text{F}}f_{\text{F}}$$

where  $\Delta\nu_{\text{C}}$  and  $\Delta\nu_{\text{F}}$  are the chemical shifts of the free and complexed ligands, respectively, and  $f_{\text{F}}$  and  $f_{\text{C}}$  are the fractions of ligand which are free and complexed. Thus, as Tu is added it replaces both the p-toluidine and the anil as ligands, reducing  $f_{\text{C}}$  in each case, and bringing the observed shifts closer to  $\Delta\nu_{\text{F}}$  as was observed in spectrum D. On complexing with the Co(II) the meta and para methyl resonances of both the p-toluidine and its anil shift downfield, whereas the ortho protons shift upfield. The degree of broadening induced by coordination roughly follows the observed shift, as may be seen from a comparison of spectra B and C which contain the same concentration of metal complex. In spectrum F of figure 6.5 is shown the NMR spectrum obtained when a sample similar to that in B is cooled to  $-90^{\circ}\text{C}$ . This spectrum will be discussed below.

In figure 6.6 are some  $^{19}\text{F}$  NMR spectra obtained from solutions of p-F aniline in acetone under various conditions. Spectrum A is that of p-F aniline alone in acetone. If  $\text{ZnTu}_2\text{Cl}_2$  is added, as in spectrum B, a second signal is observed with the same fine structure due to coupling to the ring protons. By comparison with spectra obtained from the synthesized p-F anil (Chapter 4 section (C)), the second peak in spectrum B can be assigned to the acetone anil of p-F aniline. If  $\text{CoTu}_2\text{Cl}_2$  is added instead of  $\text{ZnTu}_2\text{Cl}_2$ , spectrum C is obtained with both the aniline and anil peaks shifted downfield from the free ligand positions. If the sample in C (run at  $+27^{\circ}\text{C}$ ) is cooled then spectra D, E and F are obtained. In D, run at  $-20^{\circ}\text{C}$ , the anil

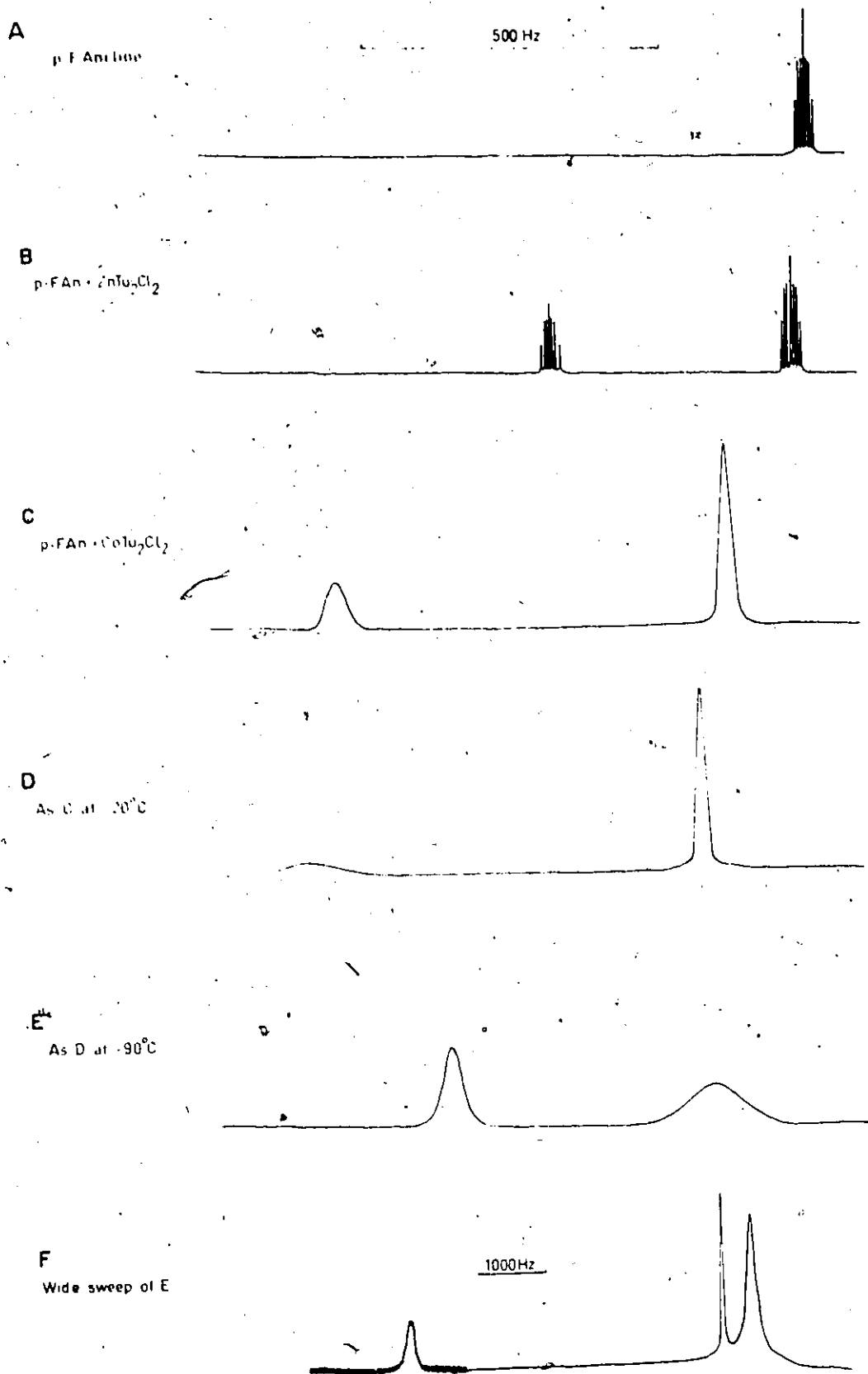


Fig. 6.6  $56.4 \text{ MHz } ^{19}\text{F}$  NMR spectra with p-F aniline in acetone

resonance is much broader than in C, whereas the aniline signal has the same linewidth. As cooling is continued, the anil resonance broadens further, then disappears, and at roughly  $-70^{\circ}\text{C}$  a signal in approximately the same position as the free anil resonance appears. In spectrum E, run at  $-90^{\circ}\text{C}$ , this signal, which is assigned to free anil, is shown. The exchange between free and complexed anil is now slow and the anil signal appears at a position close to that of the free anil at the same temperature. By using a much wider sweep, and by increasing the spectrometer gain, a weak broad peak may be observed some 5000 Hz downfield in the same sample at  $-90^{\circ}\text{C}$ , as shown in spectrum F. This is assigned as the signal due to the para fluorine in the complexed anil. This has been shifted from the free ligand position by an isotropic shift (Chapter 2 section (B)) induced by the paramagnetism of the cobalt atom. The exchange between free and complexed anil has been slowed by reducing the temperature, and they are now in "slow exchange" (Chapter 2 section (C)) or the exchange has been "frozen out" and the separate signals are visible at  $-90^{\circ}\text{C}$ . The aniline signal in spectra E and F is broadening at  $-90^{\circ}\text{C}$ , but the separate free and complexed signals were never observed for p-F aniline with  $\text{CoTu}_2\text{Cl}_2$ , although many attempts were made to observe them.

Returning to the spectra of figure 6.5, a similar effect was noted if, for example, the sample used for spectrum B was cooled. At about  $-30^{\circ}\text{C}$ , the signal due to the meta protons of

the anil was so broad as to be undetectable. However, on further cooling to about  $-70^{\circ}\text{C}$  two broad lines appeared far downfield. These are shown at  $-90^{\circ}\text{C}$  in spectrum F. The peaks in spectrum F are assigned as follows:

- (a) very broad signal from Tu in  $\text{CoTu}_2\text{Cl}_2$ . The exchange between free and complexed Tu is slow at this temperature<sup>(80)</sup>
- (b) the meta signal of the complexed anil
- (c) the para methyl signal of the complexed anil
- (d) second signal from Tu in  $\text{CoTu}_2\text{Cl}_2$  (see ref. 5)

The assignment of the two complexed anil peaks is based on the following information:

- (i) under fast exchange conditions with  $\text{CoTu}_2\text{Cl}_2$ , the meta and para methyl peaks of the anil shift downfield, and that of the ortho protons shifts upfield. Thus, for complexed anil two peaks would be expected in the downfield region.
- (ii) the expected intensity ratio for the meta peak to the para methyl peak of complexed anil is 2/3.
- (iii) with the peaks assigned as above, the ratio of the slow exchange shift to the fast exchange shift is the same for the meta and the para methyl peaks.

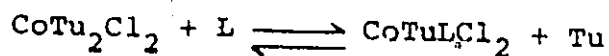
At  $-90^{\circ}\text{C}$  the p-toluidine peaks are broadened, but at the lowest temperatures attainable before the solvent freezes ( $\sim -105^{\circ}\text{C}$ ) it was still not possible to observe separate resonances



for free and complexed p-toluidine.

(ii) Determination of equilibrium constants

In acetone solutions of  $\text{CoTu}_2\text{Cl}_2$  with p-toluidine present, there are five potential ligands: acetone, water, thiourea, p-toluidine and p-toluidine-anil. In solutions which are concentrated in both  $\text{CoTu}_2\text{Cl}_2$  and p-toluidine the most important ligands will be thiourea, p-toluidine and its anil. In such a solution it is possible to obtain a measure of the equilibrium constants for the equilibria:

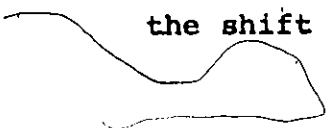


where L may be p-toluidine or p-toluidine-anil.

Among the prerequisites for such a calculation are the chemical shifts for two of the three ligands when they are complexed. For Tu, this is obtained by plotting the observed Tu chemical shift against  $\frac{1}{\sqrt{C}}$  (C is the  $\text{CoTu}_2\text{Cl}_2$  concentration in moles/l.) as described in section B of this chapter. For the remaining two ligands the situation is more complex since they cannot be studied separately or in the absence of Tu. The solution is to extrapolate the shifts observed for complexed anil at low temperatures to the temperature at which the equilibrium constants are measured (27°C). This was done for the meta signal of the p-toluidine-anil, labelled (b) in spectrum F of figure 6.5. The meta signal was chosen over the para methyl signal because, in fast exchange, the methyl signal is sometimes overlapped with other signals (for example, spectrum C of figure 6.5). In figure

6.7 is a plot of the observed chemical shift of the meta peak of the complexed anil  $\Delta\nu_c$  (measured from the free ligand position) against  $T^{-1}$  (T in °K). The measurements were made at 56.4 MHz and the temperature ranged from -110°C to -70°C. At -70°C the peak is quite broad and has started to shift towards the fast exchange signal position. This last point was ignored for the extrapolation. The plotted points are each the average of six values obtained in three cycles over the temperature range. The four points used do give a reasonable basis for extrapolation to 27°C. An extrapolation of this sort obviously requires some evidence that the isotropic shift is likely to follow Curie Law, i.e. to give a linear plot against  $\frac{1}{T}$ . This evidence is supplied by the observation that, for Tu in  $\text{CoTu}_2\text{Cl}_2$ , the shift ( $\Delta\nu_c$ ) gives a very good linear plot against  $\frac{1}{T}$  from 27°C to -65°C<sup>(80)</sup>. It is therefore reasonable to assume that the complex  $\text{CoTu}(\text{anil})\text{Cl}_2$  will exhibit similar behaviour. From the extrapolation in figure 6.7 the shift of the meta protons of the p-toluidine-anil in  $\text{CoTu}(\text{anil})\text{Cl}_2$  at 27°C would be 264 Hz (at 56.4 MHz).

The samples were made up by weighing the  $\text{CoTu}_2\text{Cl}_2$  and p-toluidine into an NMR sample tube and adding the acetone d-6 by syringe. The shifts of the metaresonances of both the anil and the p-toluidine were then carefully measured, as was the position of the Tu signal which lies downfield of TMS. If the shift of the Tu resonance ( $\Delta\nu_{\text{obs}}$ ) is measured from the free



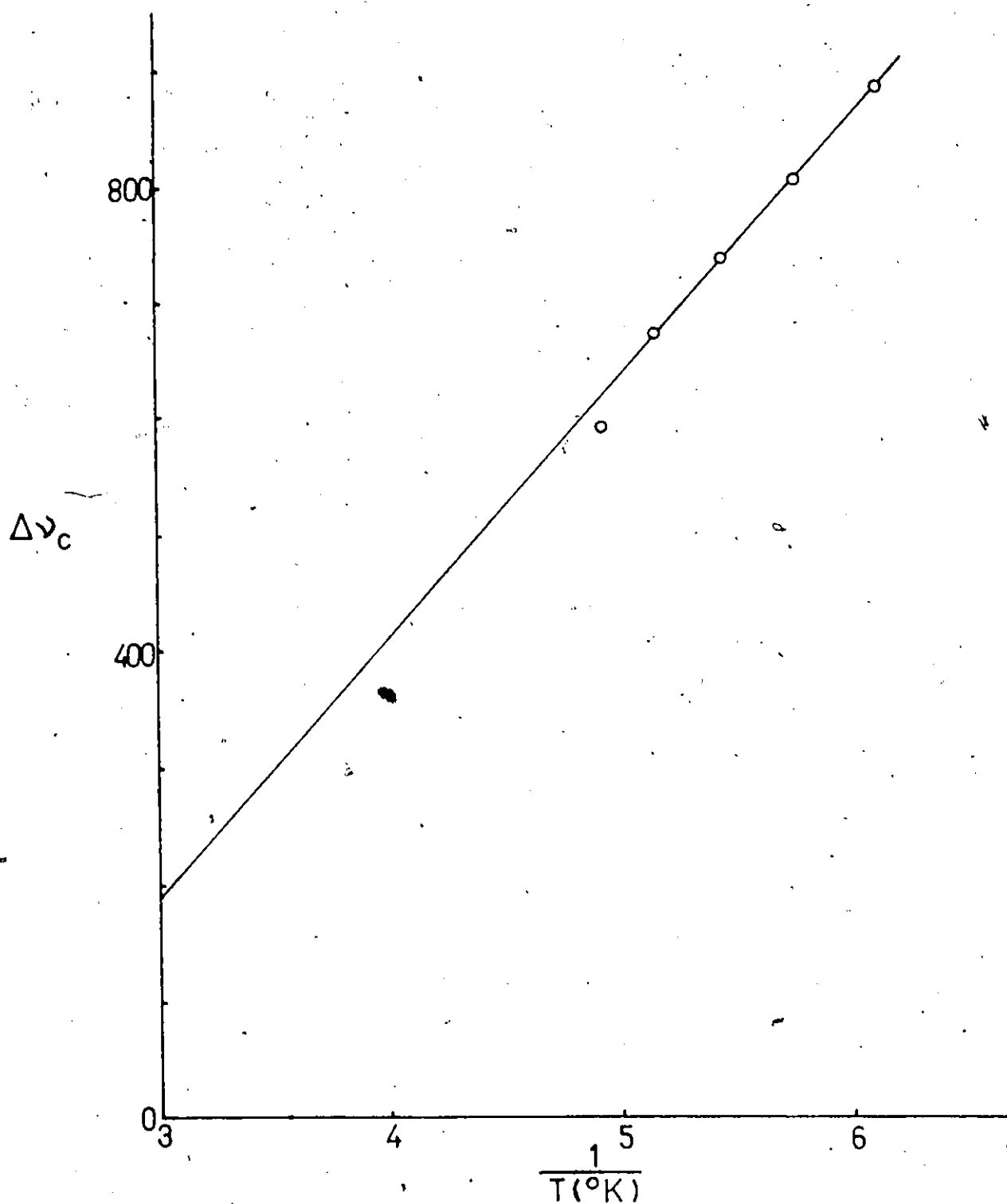


Fig. 6.7 A plot of  $\Delta\nu_c$  (shift in Hz of the meta peak of complexed anil from its diamagnetic position) against  $1/T$  ( $T$  in  $^{\circ}\text{K}$ )

ligand signal then

$$\Delta\nu_{\text{obs}} = \Delta\nu_{\text{c}} \cdot f_{\text{c}}$$

so that  $f_{\text{c}}$  may be determined. This means that the amount of Tu replaced by other ligands in solution is known. From a similar expression the amount of anil which is complexed may be calculated, since  $\Delta\nu_{\text{c}}$  is known from extrapolation. The assumption now made is that only p-toluidine and the anil are responsible for displacing the Tu. Therefore the fraction of aniline complexed  $f_{\text{c}}$  is known. The equilibrium constants ( $K_{\text{p-tol}}$  and  $K_{\text{anil}}$ ) may be calculated since all the concentration terms are now known. The results for two samples containing the same initial  $\text{CeTuCl}_2$  concentration, but having different initial p-toluidine concentrations, are given in Table 6.2. The values obtained for  $K_{\text{p-tol}}$  and  $K_{\text{anil}}$  are roughly independent of the initial p-tol/complex concentration ratio. Another test of the assumptions used is to calculate the expected shift of complexed p-toluidine. In both cases this expected shift is 415 Hz and this tends to confirm the appropriateness of the method.

### (iii) Kinetics

No attempt has been made in this work to accurately measure the rates of ligand exchange of p-toluidine or of p-toluidine-anil with any of the metal complexes. However, variable temperature studies with some of the paramagnetic complexes have served to place lower limits on the exchange rates. As discussed in part (i) of this section, the NMR spectra, both  $^1\text{H}$  and  $^{19}\text{F}$ , demonstrate that exchange between free and complexed

Table 6.2

	Sample A	Sample B
Initial weight of $\text{CoTu}_2\text{Cl}_2$	$9.8 \times 10^{-3}$ g.	$1.0 \times 10^{-2}$ g.
Initial weight of p-toluidine	$1.92 \times 10^{-2}$ g.	$4.3 \times 10^{-2}$ g.
Acetone d-6 added	0.40 ml	0.40 ml
Ratio $\frac{[\text{Anil}]}{[\text{p-tol}]}$ (by integration)	0.45	0.38
Shift of Tu peak from free ligand position	1675 Hz	1512 Hz
Shift of p-toluidine meta signal*	17 Hz	10 Hz
Shift of anil metal signal*	51 Hz	34 Hz
Fraction of Tu in $\text{CoTu}_2\text{Cl}_2$ displaced	0.237	0.302
Fraction of anil complexed	0.193	0.129
Fraction of p-toluidine complexed	0.041	0.024
Calculated value of $\Delta\nu_c$ for p-toluidine	415 Hz	415 Hz
$K_{\text{anil}}$	$2.0 \times 10^{-1}$	$2.2 \times 10^{-1}$
$K_{\text{ptol}}$	$3.5 \times 10^{-2}$	$3.8 \times 10^{-2}$

\*Measured from the corresponding peaks in a solution with  $\text{ZnTu}_2\text{Cl}_2$  replacing  $\text{CoTu}_2\text{Cl}_2$ .

Experiment carried out at  $27^\circ\text{C}$  and at 56.4 MHz.

anil may be slowed down and "frozen out" in the case where the metal complex is  $\text{CoTu}_2\text{Cl}_2$ . A very crude estimate of the lifetime for exchange at one temperature may be obtained by using the formula shown below, which gives the lifetime for exchange at the "coalescence" temperature<sup>(37)</sup>:

$$\tau = \frac{1}{2\pi(\nu_A - \nu_B)} \quad (6.1)$$

where  $\tau$  is the lifetime of the exchanging species in either site A or site B and  $\nu_A$  and  $\nu_B$  are the chemical shifts of the sites A and B respectively. This formula holds for a system with two equally populated sites A and B and where the transverse relaxation time  $T_2$  is the same for both sites. The "coalescence" temperature is that where the two separate peaks just merge to form a single broad line. This formula may be applied to the case of p-toluidine-anil which is in exchange between free and complexed sites in the presence of  $\text{CoTu}_2\text{Cl}_2$ . The "coalescence temperature" in this case must be between  $-35^\circ$  and  $\sim -50^\circ\text{C}$  for the meta proton resonance. Using figure 6.7, at  $-40^\circ\text{C}$  the shift of the complexed resonance measured from the free ligand signal would be approximately 460 Hz (at 56.4 MHz). This would give an exchange lifetime of  $3.5 \times 10^{-4}$  seconds, using equation 6.1. The conditions for the use of the coalescence temperature formula are, of course, not fulfilled in this case, i.e. neither the populations nor the transverse relaxation times are equal. However, it would seem reasonable to assume that at  $30^\circ\text{C}$  the exchange lifetime would not be longer than  $10^{-4}$  sec.

The exchange between free and complexed aniline is even faster since it is not "frozen out," even at  $-100^{\circ}\text{C}$ . The shift at that temperature of the meta resonance of the complexed p-toluidine is likely to be  $\sim 1000$  Hz (at 56.4 MHz) from the free ligand signal. This figure is obtained from the calculated shift for the meta resonance of complexed p-toluidine at  $27^{\circ}\text{C}$  as obtained in Section E(ii) of this chapter, i.e. 415 Hz, and by assuming that the slope of the plot of  $\Delta\nu_{\text{C}}$  versus  $\frac{1}{T}$  will be the same as that in figure 6.7. The lifetime for the exchange of p-toluidine between the free ligand and complexed ligand sites should therefore be less than  $10^{-5}$  seconds at  $30^{\circ}\text{C}$ .

(iv) General considerations

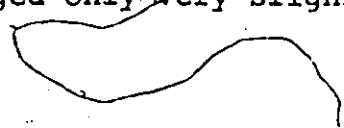
The large isotropic shifts experienced by ligands in  $\text{Co}^{\text{II}}$  complexes are very useful in determining the equilibrium constants for ligand association and also in observing the rates of ligand exchange. The complexing of a ligand to a diamagnetic Zn(II) atom on the other hand produces only small shifts and this makes studies of ligand exchange very difficult. For example, an experiment was carried out wherein a concentrated solution of  $\text{ZnTu}_4(\text{ClO}_4)_2$  in acetone d-6 was progressively diluted with more solvent. This experiment was designed to measure the equilibrium constant for replacing Tu by acetone by means of a plot of the Tu signal against  $\frac{1}{\sqrt{C}}$  where C was the  $\text{ZnTu}_4(\text{ClO}_4)_2$  concentration in moles/l. However, instead of shifting towards the free ligand position as expected, the Tu peak shifted very slowly in the other direction, i.e. further

downfield. This may possibly be explained by the increased degree of hydrogen bonding occurring as the solution is diluted.

The low temperature studies with Co(II) complexes and aniline/anil mixtures sometimes gave rise to a proliferation of peaks with large isotropic shifts. In the case of p-F aniline using  $^{19}\text{F}$  NMR, the situation is not confused by the presence of Tu or solvent signals. With  $\text{CoTu}_2\text{I}_2$  and p-F aniline in acetone a single isotropically shifted resonance was observed if the p-F aniline concentration was low. As the concentration was increased, a series of peaks appeared in the far downfield region, i.e. about 3000 Hz to 6000 Hz from the free p-F aniline resonance. A smooth series was observed with peaks decaying and others increasing as the p-F aniline concentration was increased. Similar behaviour was noted for other Co(II) complexes. The tendency to produce multiple peaks increased in the order  $\text{CoTu}_2\text{Cl}_2 < \text{CoTu}_2\text{Br}_2 < \text{CoTu}_2\text{I}_2 < \text{Co}(\text{DMTu})_2\text{Br}_2$ . It is possible that the peaks are due to the formation of species with a coordination number greater than four.

#### (F) ACETONE IN MIXED LIGAND SOLUTIONS

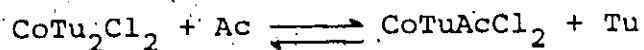
Although the equilibrium constant for the displacement of Tu by acetone may be determined as outlined in section B of this chapter, it would be useful to have a means of direct observation of complexed acetone. Experiments showed that the chemical shift of the methyl signal of acetone h-6 or acetone d-6 in the  $^1\text{H}$  NMR changed only very slightly upon addition of





paramagnetic Co(II) complexes to the solution. For a solution almost saturated in  $\text{CoTu}_2\text{Cl}_2$ , the shift of the solvent signal is only a couple of Hz from the signal in the pure solvent. The  $^{13}\text{C}$  NMR spectra of solutions of Co(II) complexes in acetone were also run. Using a HA-100 operating in cw mode at 26 MHz no shift of the carbonyl carbon resonance was detected on addition of  $\text{CoTu}_2\text{I}_2$ . Using a Bruker WH90 observing  $^{13}\text{C}$  at 22.6 MHz in the FT mode, shifts of the carbonyl and methyl group signals were detected. However, the largest shift, with the solution almost saturated with  $\text{CoTu}_4(\text{ClO}_4)_2$ , was  $\sim 15$  Hz for both the carbonyl and methyl carbons. In the presence of other ligands, the fraction of acetone complexed will be reduced still further; and so observation of chemical shifts, either  $^1\text{H}$  or  $^{13}\text{C}$ , does not afford a method of directly determining that fraction.

Another possible probe is the relaxation time  $T_1$  of the acetone. Since the equilibrium constant for the process



is known then the fraction of acetone complexed at any concentration of complex or Tu may be calculated. If the spin-lattice relaxation time  $T_1$  was measured at a series of different Tu concentrations, then the relationship of  $T_1$  to the fraction of aniline complexed could be determined. This could then be used in more complex solutions to evaluate the fraction of acetone complexed from a measurement of  $T_1$ . To investigate the usefulness of an approach of this nature, the spin-lattice

relaxation time  $T_1$  of the  $^1\text{H}$  signal of acetone d-6 was measured under various conditions. The measurements were carried out at  $32^\circ\text{C}$ , observing  $^1\text{H}$  at 56.4 MHz and decoupling  $^2\text{H}$  with an rf field at 8.664646 MHz. This resulted in a single sharp peak for the acetone d-6 resonance. A small quantity of benzene was added and this signal was used for the field frequency lock. The relaxation time was measured by the "saturation-recovery technique" <sup>(71)</sup> as described in Chapter 3 Section D. An example of a plot of  $\ln (M_0 - M_z(t))$  against  $t$  is shown in figure 6.8. This was obtained with a sample of acetone d-6, with a little benzene added, and the relaxation time  $T_1$  was found to be 5.9 sec. When a little  $\text{CoTu}_2\text{Cl}_2$  was added the value of  $T_1$  dropped to 2.9 seconds. When the sample was then saturated with Tu the value of  $T_1$  was found to be 2.8 seconds. Thus use of  $T_1$  as a probe of the fraction of complexed acetone is not practical. The assumption on which most studies of this nature are based is that any changes in the relaxation time are produced solely by those solvent molecules which are in the first coordination sphere of the metal complex, and that the relaxation time of all the bulk solvent is unaffected. The above result suggests that in the present system this does not hold, but rather that there is an important contribution to the relaxation time from solvent molecules other than those in the first coordination sphere. This may well be due to acetone which is in the second coordination sphere of the metal complex from which it is not replaced by Tu, unlike that in the first coordination sphere.

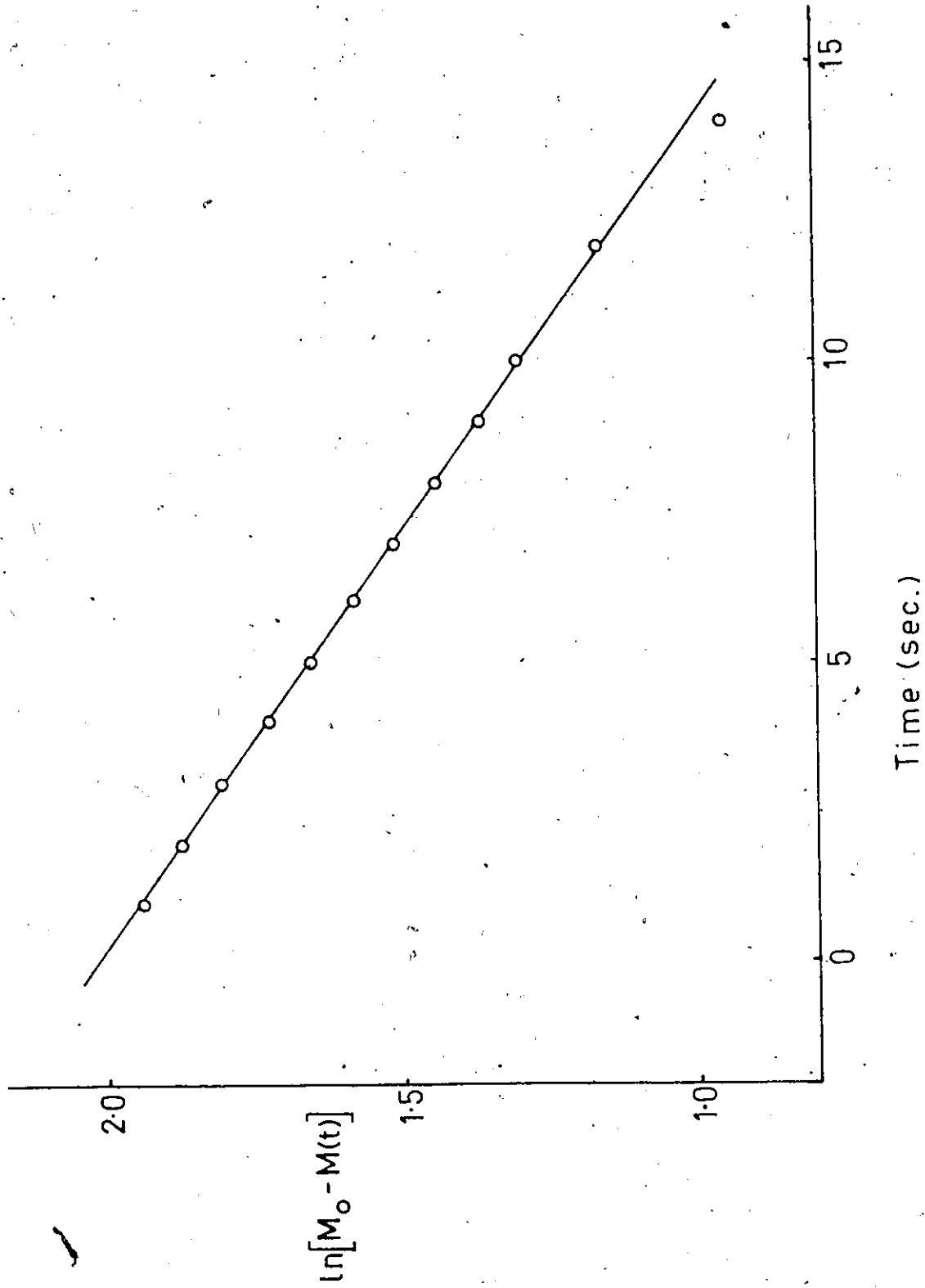


Fig. 6.8 Plot of  $\ln[M_0 - M(t)]$  (arbitrary units) against  $t$  in seconds for a "saturation recovery" experiment to determine  $T_1$

## (G) ANILINES IN ACETONITRILE

As has been frequently mentioned during the preceding sections of this chapter, the formation of anils can make the study of ligand exchange of anilines difficult when acetone is used as the solvent. For this reason, acetonitrile ( $\text{CH}_3\text{CN}$ ) was used as the solvent in an experiment designed to determine the equilibrium constants for ligand exchange of Tu in  $\text{CoTu}_2\text{Cl}_2$  with a series of para substituted anilines. A known quantity of  $\text{CoTu}_2\text{Cl}_2$  was dissolved in 5.0 ml of acetonitrile and this was used as a stock solution. The position of the Tu resonance was measured in this stock solution. Samples were prepared from the stock solution and quantities of the various anilines so that all samples were 0.20 M in aniline. The position of the Tu resonance was then measured for each sample. By using the value of  $\Delta\nu_c$  determined for  $\text{CoTu}_2\text{Cl}_2$  in  $\text{CH}_3\text{CN}$  as described in section C of this chapter, the concentration of free Tu may then be calculated in each case.

From the first sample a value of the equilibrium constant for association of the solvent may be determined, since the concentration of the complex containing coordinated  $\text{CH}_3\text{CN}$  is known from the free Tu concentration. With this piece of information, the equilibrium constants for the anilines may be simply determined by solving a quadratic equation for each case.

The derivation of the equations used is contained in Appendix

A. The free Tu concentration is given by

$$[\text{Tu}] = [\text{MTuAn}] + [\text{MTuAc}] + 2[\text{MAN}_2] + 2[\text{MAC}_2] + 2[\text{MANAc}]$$

Using the expressions from Appendix A this may be re-written:

$$[\text{Tu}] = \frac{M(2K_1K_3[\text{Tu}][\text{An}] + 2K_1K_2[\text{Tu}][\text{Ac}] + 2K_3^2[\text{An}]^2 + 2K_2^2[\text{Ac}] + 4K_2K_3[\text{An}][\text{Ac}])}{(K_1[\text{Tu}] + K_2[\text{Ac}] + K_3[\text{An}])^2} \quad (6.2)$$

where  $K_1$ ,  $K_2$  and  $K_3$  are the equilibrium constants for replacement of Tu as a ligand by Tu, Ac(etone) and An(iline) respectively, and M is total amount of metal complex originally added as  $\text{MTu}_2\text{Cl}_2$ . For the case where there is no aniline present equation (6.2) may be rewritten

$$\frac{[\text{Tu}]}{M} (aK_2 + b)^2 = cK_2^2 + dK_2$$

where  $a = [\text{Ac}]$

$$b = K_1[\text{Tu}]$$

$$c = 2[\text{Ac}]^2$$

$$d = 2K_1[\text{Tu}][\text{Ac}]$$

This is a quadratic equation in  $K_2$ , and, when solved with the observed  $[\text{Tu}]$  value, yielded  $K_2 = 1.37 \times 10^{-4}$ .

When there is the third ligand (aniline) present equation (6.2) may be written:

$$\frac{[\text{Tu}]}{M} = (aK_3 + b)^2 = cK_3^2 + dK_3 + e$$

where  $a = [\text{An}]$

$$b = [\text{Tu}] + K_2[\text{Ac}]$$

$$c = 2[\text{An}]^2$$

$$d = 2K_1[\text{Tu}][\text{An}] + 4K_2[\text{An}][\text{Ac}]$$

$$e = 2K_1K_2[\text{Tu}][\text{Ac}] + 2K_2^2[\text{Ac}]^2$$

The equilibrium constants for the anilines,  $K_3$ , may thus be determined from the observed free Tu concentrations. The results of this experiment were tabulated in Table 6.3. The observed values of  $K_3$  for the anilines vary from  $340 \times 10^{-4}$  for p-anisidine to  $2.8 \times 10^{-4}$  for p-nitroaniline. In figure 6.9,  $\log K_3$  is plotted against the Hammett  $\sigma$  value<sup>(90)</sup> for the various anilines. As might be expected, a good correlation is observed. This is in contrast to a study by Rakshys<sup>(91)</sup> in which the relative stability constants for a series of (substituted aniline)<sub>2</sub>Ni(acac)<sub>2</sub> complexes were determined by measuring the isotropic NMR shifts. In this case poor Hammett plots were obtained.

#### (H) EXCHANGE REACTIONS

In the solutions used to study the formation and hydrolysis of the anils there are three species with "exchangeable" hydrogen atoms. These are thiourea (amino groups), aniline (amino group) and water. "Exchangeable", in this sense, means that these hydrogen atoms are usually considered to be very much more labile than those on carbon atoms. Fairly slow exchanges can be detected by adding the deuterated form of one component, e.g. D<sub>2</sub>O, and then monitoring the system as it comes to equilibrium. Faster exchanges may be followed by using line-broadening techniques as outlined in Chapter 2 Section (Cii).

A simple example is illustrated by the <sup>1</sup>H NMR spectra shown in figure 6.10. Spectrum 6.10(a) was obtained from

Table 6.3

Determination of the equilibrium constants for various anilines with  $\text{CoTu}_2\text{Cl}_2$  in  $\text{CH}_3\text{CN}$

Aniline	Aniline concentration moles/l.	Shift of Tu*	Free [Tu]	$K_3$
none	0.0	3046	0.0161	-
p-toluidine	0.203	2817	0.0237	$1.7 \times 10^{-2}$
p-anisidine	0.198	2666	0.0287	$3.4 \times 10^{-2}$
p- $\text{NO}_2$ aniline	0.199	3041	0.0163	$2.8 \times 10^{-4}$
p-Cl aniline	0.198	2986	0.0181	$3.7 \times 10^{-3}$
p-Br aniline	0.201	3009	0.0173	$2.2 \times 10^{-3}$
Aniline	0.202	2937	0.0197	$7.06 \times 10^{-3}$

All samples were  $5.8 \times 10^{-2}$  M in  $\text{CoTu}_2\text{Cl}_2$  and the measurements were carried out at  $35^\circ\text{C}$ .

\*In Hz at 100 MHz measured from the free ligand position.

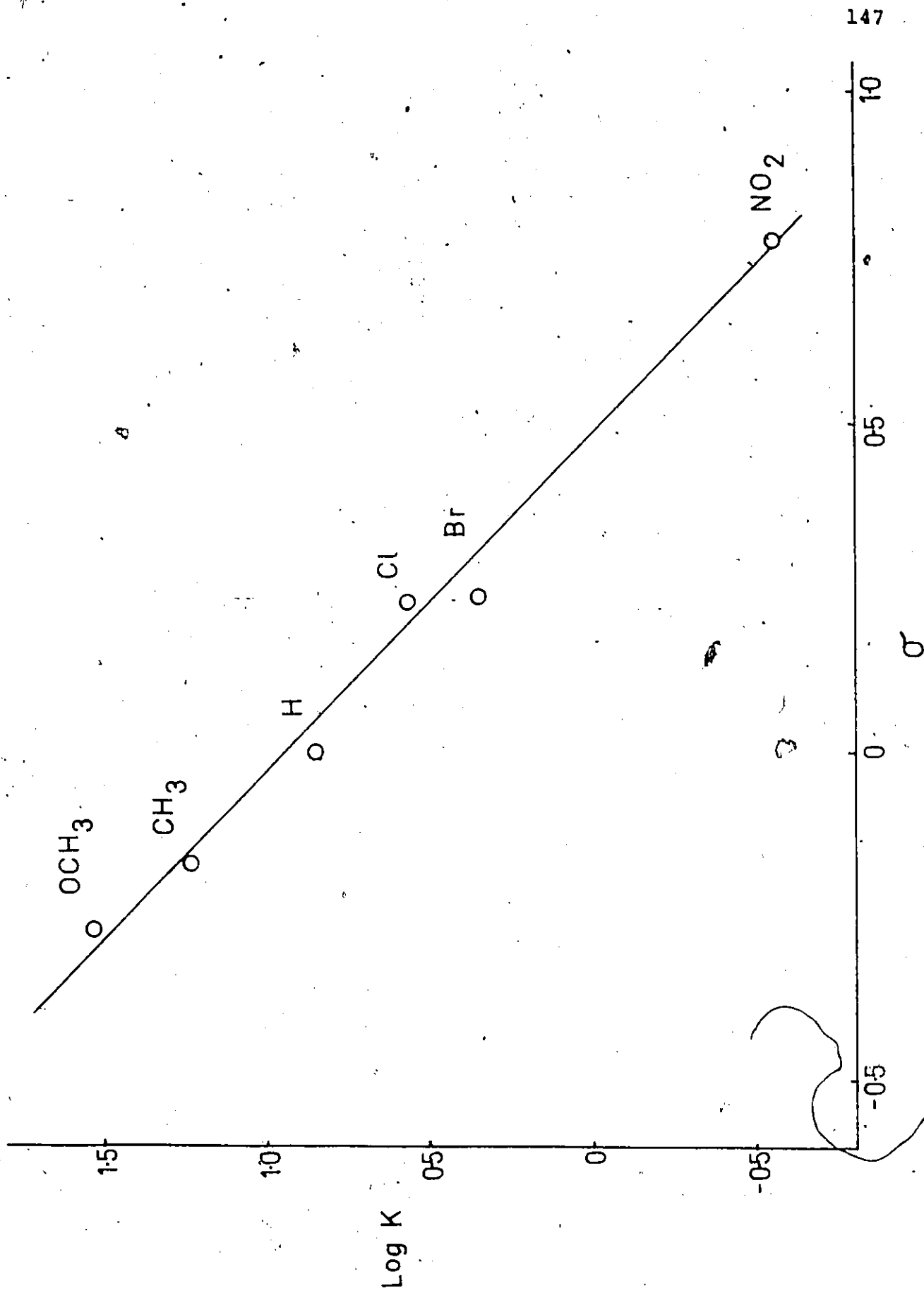


Fig. 6.9 A plot of  $\log K$  against the Hammett  $\sigma$  value for a series of para substituted anilines.  $K$  is the equilibrium constant for association of the aniline with  $\text{CoCl}_2 \cdot 2\text{Cl}_2$  in acetonitrile.



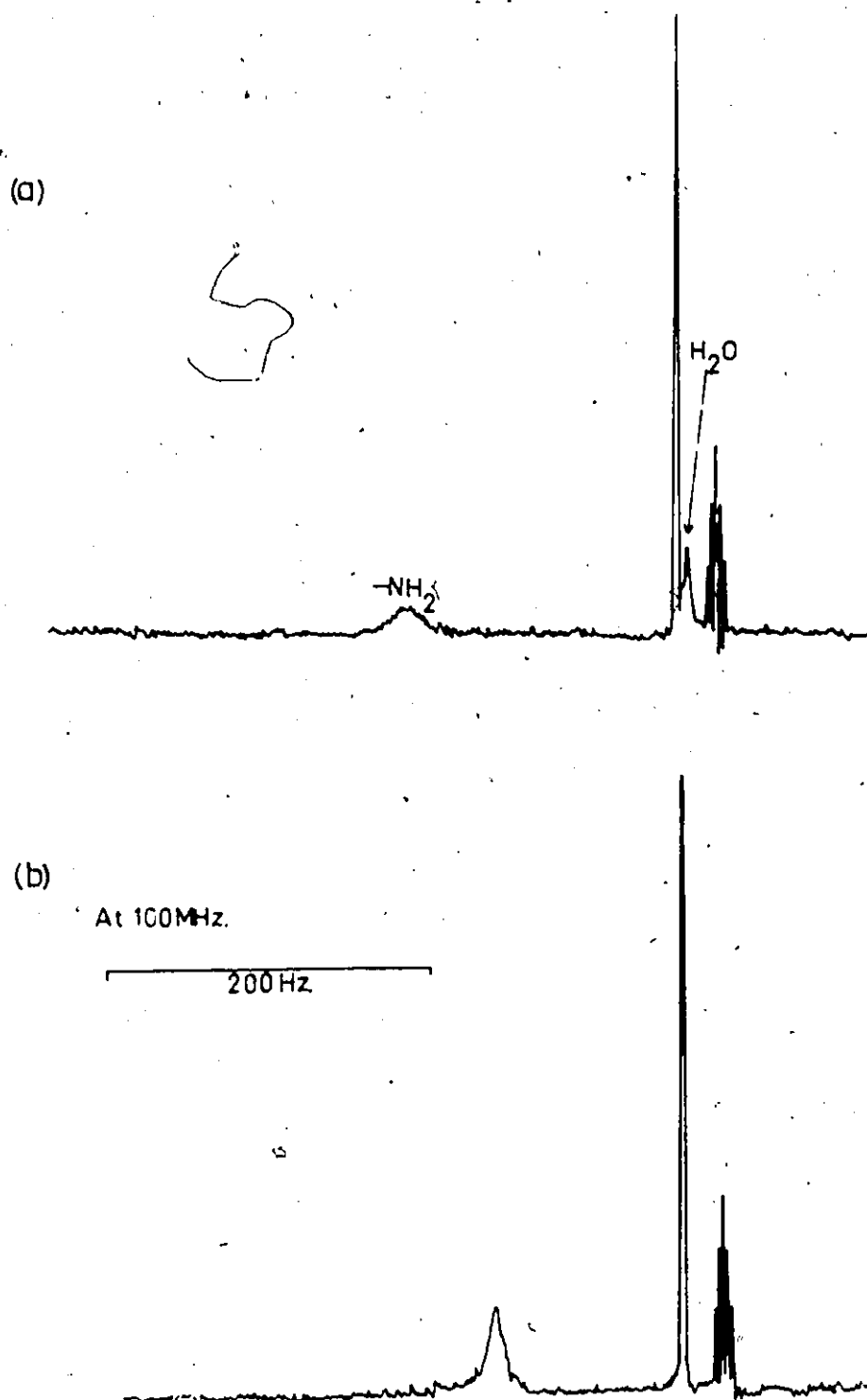


Fig. 6.10 (a)  $^1\text{H}$  spectrum of p-toluidine in acetone d-6  
(b) as (a) after addition of  $\text{ZnTu}_4(\text{ClO}_4)_2$

a sample of acetone d-6 which was 0.2 M in p-toluidine and  $\sim 0.1$  M in  $H_2O$ . The peaks due to the water and the amino group of the p-toluidine are labelled. Addition of  $ZnTu_4(ClO_4)_2$  to make the solution  $\sim 10^{-5}$  in catalyst gave spectrum (b). The hydrogen atoms of water and p-toluidine are now in fast exchange. Application of the coalescence formula (equation 6.1) leads to a value for the maximum lifetime for the protons in either water or aniline of  $10^{-3}$  sec. The lifetime may well be much less than this upper limit.

For the case of thiourea, fast exchange was never detected between the hydrogen on thiourea and either water or aniline. This includes cases with thiourea metal complexes in solution and with large excesses of Tu. The exchange between aniline and water is metal complex catalysed and both bind to the metal with the atom on which the hydrogens are attached. Thiourea, on the other hand, coordinates to metal ions via the sulphur atom. The difference in exchange rates is therefore not surprising.

Three interesting exchange processes are observed when initial rate measurements are carried out on the hydrolysis of the p-toluidine-anil as described in Chapter 5 Section (C). These three processes may be observed in the methyl region of the spectrum, and take place on three different time scales. Firstly, there is the conversion of the anil methyls into acetone (h-6). This process proceeds at the same rate as the conversion of p-toluidine-anil into p-toluidine, i.e.

hydrolysis. Secondly, and slower, is the incorporation of  $CD_3$  groups into the methyl groups of the anil caused by formation of anil between acetone (d-6) and p-toluidine. This process is slower because the rate of formation of anil is initially zero. The third process, and one which is much slower, is the exchange of hydrogen and deuterium as noted by the increase in intensity of the acetone d-6 quintet. This reaction is very slow, and is distinguished from the second process by the fact that there,  $CD_3$  is exchanged for  $CH_3$ , whereas here,  $CD_3$  is converted to  $CD_2H$ .

This last process, the catalysed exchange of hydrogen atoms in water or amino groups with acetone (d-6) to give  $CD_2H$  groups has been observed frequently during the course of this work. It is a very slow process requiring large catalyst concentrations and was not detected during initial rate studies. This is in marked contrast to the case where acid catalysis was used, and where the exchange was found to be virtually instantaneous (Chapter 4, Section (F)).

#### (I) SUMMARY

In this chapter, various aspects of ligand exchange are reported using  $CoTu_2Cl_2$ , taking advantage of its paramagnetism. The equilibrium constants for complexing of thiourea in acetone and in acetonitrile solution have been determined. The concentration of water in acetone d-6 was measured and its association with  $CoTu_2Cl_2$  was studied. For p-toluidine and its acetone-anil, the equilibrium constants and approximate

exchange lifetimes were measured. Finally, the equilibrium constants for ligand exchange of a series of para substituted anilines with  $\text{CoTu}_2\text{Cl}_2$  in acetonitrile have been determined.



## CHAPTER SEVEN

### SPIN SATURATION TRANSFER EXPERIMENTS

#### (A) INTRODUCTION

The theory applicable to spin saturation transfer (SST) experiments in the presence of chemical exchange has been discussed in Chapter 2 Section (C). The necessary equipment and experimental methods have been described in Chapter 3 Section (D). In this chapter the results of such experiments using both cw and FT spectrometers will be discussed.

#### (B) EXPERIMENTS USING $^{19}\text{F}$ NMR

As may be seen from spectrum B of figure 6.6 the  $^{19}\text{F}$  NMR signals from p-F aniline and its acetone anil are  $\sim 400$  Hz apart at 56.4 MHz. This large separation makes the system suitable for SST experiments on a cw instrument since the direct effect of the saturating field at the observing frequency will be minimal. The initial experiments attempted to establish if spin saturation transfer was detectable, i.e. to check whether the lifetime for exchange or reaction was of the same order of magnitude as the spin lattice relaxation time  $T_1$  of the  $^{19}\text{F}$  nucleus. It was found that in the presence of either  $\text{ZnTu}_2\text{Cl}_2$  or  $\text{ZnTu}_4(\text{ClO}_4)_2$  a decrease in intensity of the anil resonance was noted when a saturating field was applied at the frequency of the aniline resonance.

Furthermore the greater the metal complex concentration the larger was the decrease in intensity observed in the anil signal on switching on the saturating field. Thus it is established that the system is suitable for SST experiments.

In order to remove systematic errors and to simplify and automate data collection, the developments and improvements described in Chapter 3 Section (D) were carried out. The desirable strength of the saturating field was determined with an exchanging, i.e. catalysed sample. As the strength of the field is increased at peak A, the intensity of B decreases due to the transfer of non-equilibrium magnetisation. When A is fully saturated the intensity of B will remain constant as the strength of the field at A is further increased. Eventually peak B will decrease in intensity again due to direct saturation from the field centred at A. The actual strengths of the saturating fields used were close to the minimum required to produce full saturation as further increases may produce Bloch-Siegert<sup>(36)</sup> shifts at peak B. Shifts of this nature would lead to errors in the results derived from the recovery or decay of the magnetisation at peak B. Under the conditions used no Bloch-Siegert shift at peak B could be observed. A further check showed no effect on the intensities of peaks A and B when the saturating field was set midway between A and B.

With the equipment available it was possible to determine the relaxation times  $T_1$  of both the anil and the aniline signals from the decay of the magnetisation of one peak when the satura-

ting field was applied to the other peak. From equations (2.14) and (2.15)

$$M_z^A(t) - M_\infty^A = M_0^A \left( \frac{\tau_{1A}}{\tau_A} \right) e^{-\frac{t}{\tau_{1A}}} \quad (7.1)$$

Therefore a plot of  $\ln(M_z^A(t) - M_\infty^A)$  versus  $t$  will yield a value of  $\tau_{1A}$  from its slope. Use of equation (2.10) will then give a value of  $T_{1A}$ . The relaxation time  $T_1$  may also be determined from the recovery of magnetisation after removal of the saturating field at the second peak as discussed at the end of Chapter 3. The condition that the recovery be a simple exponential with a characteristic time of  $T_{1A}$  is that  $\tau_{1A} > 2T_{1A}$  <sup>(23)</sup>. This may be simply satisfied by adding an appropriate quantity of catalyst.

When  $\ln[M_z^A(t) - M_\infty^A]$  was plotted against  $t$  very good straight lines were usually obtained, showing that the conditions were being satisfied. The recovery method has the advantage that  $T_1$  is determined directly from the slope of the logarithmic plot without any measurement of the rate as is required if  $T_1$  is determined from the decay of the magnetisation. Some experiments were carried out in which the relaxation times were measured both by the decay and by the recovery technique.

A third method used to measure relaxation times was the "saturation recovery" technique. The experimental method has been discussed in Chapter 3 Section (D). This technique was used to measure the spin lattice relaxation time for the  $^{19}\text{F}$  nucleus in p-F aniline. The samples were approximately 10% p-F aniline in acetone and no special precautions were taken to remove oxygen.

The protons were decoupled to give a single sharp line in the  $^{19}\text{F}$  spectrum. The values obtained for  $T_1$  were quite consistent ranging from 2.7 sec to 3.2 sec with an average value of 3.0 sec. Values of  $T_1$  are not usually considered reliable to more than  $\pm 10\%$  (37).

The values of  $T_1$  for p-F aniline, determined from the decay and recovery of magnetisation, however, varied over a much wider range. In general, the values of  $T_1$  were longer than 3.0 sec and varied up to 10 seconds. Initially the  $T_1$  values were determined from the logarithmic plots of the decay of magnetisation. Using this method the results were usually consistent within a particular experiment, for example those given in Table 7.1 for two consecutive experiments on a sample containing p-F aniline, the acetone-anil and  $\text{ZnTu}_4(\text{ClO}_4)_2$  in acetone. The relaxation times  $T_1$  are in good agreement with each other but not with the value of 3.0 sec determined by the saturation recovery technique. Also the test of the method, i.e. the comparison of the value of  $\tau_A/\tau_B$  with the value of  $\frac{M_A^O}{M_B^O}$  obtained by integration is not particularly satisfactory. These problems combined with the one mentioned in Chapter 3, i.e. the inability of the frequency generators to maintain their set frequency to  $\pm 0.1$  Hz or better, finally led to the abandoning of efforts to actually measure  $T_1$  in the presence of chemical exchange on a cw spectrometer. The alternative method was to take the  $T_1$  value from a saturation recovery experiment and to determine  $M_O^A/M_\infty^A$  as outlined in Chapter 3 Section (D). Some experiments were conducted using this approach.



Table 7.1  
 $^{19}\text{F}$  SST results

Sample; p-F aniline (A), p-F anil. (B) and  $\text{ZnTu}_4(\text{ClO}_4)_2$   
 in acetone

	1st experiment	2nd experiment
$T_{1A}$	8.5 sec.	9.5 sec
$T_{1B}$	8.0 sec	8.0 sec
$\tau_A$	1.4 sec	1.5 sec
$\tau_B$	0.5 sec	0.5 sec
$\tau_A/\tau_B$	2.7	3.3
$M_O^A/M_O^B$	3.8	3.7

One such experiment involved measuring the rate of exchange between p-F aniline and its acetone anil in the presence of  $ZnTu_4(ClO_4)_2$  as a function of added Tu concentration. The Tu decreased the rate as expected for a metal complex catalysed process involving coordination of reacting substrates.

Another experiment involved adding  $Ni(ClO_4)_2 \cdot 6H_2O$  to p-F aniline in acetone and observing a fast reaction by SST as indicated by the value of  $M_O^A/M_\infty^A$ . Adding ortho-phenanthroline or terpyridine dramatically reduced the value of  $M_O^A/M_\infty^A$ . Since the addition of either of these two compounds is not likely to change the value of  $T_1$  greatly, the conclusion is that o-phenanthroline and terpyridine inhibit the activity of  $Ni^{2+}$  as a catalyst in this system. On the other hand  $\alpha, \alpha$ -dipyridyl was found to be ineffective as an inhibitor.

A third experiment involved measuring how the rate of reaction or exchange changed with time due to possible deterioration of the catalyst. The method used was to determine  $M_O^A/M_\infty^A$  by weighing the cutouts of the peaks. The sample was p-F aniline and  $ZnTu_4(ClO_4)_2$  in acetone. The values of  $M_O^A/M_\infty^A$  as a function of time are listed in Table 7.2. The results indicate a slow decrease in the rate of exchange but this is not fast enough to interfere with the rate measurements reported elsewhere in this thesis.

### (C) EXPERIMENTS USING $^1H$ NMR

In order to be able to carry out an SST experiment to measure the exchange rate of aniline and anil using  $^1H$  NMR there

Table 7.2  
Time dependence of  $M_O^A/M_\infty^A$

Time after adding catalyst in minutes	$M_O^A/M_\infty^A$ (anil)
17	2.65
35	2.62
55	2.87
72	2.76
108	2.70
129	2.54
225	2.63
245	2.44
1 week later	<1.0

Sample: p-F aniline, p-F anil,  $ZnTu_4ClO_4$  in acetone.  
Measurements of anil resonance with ( $M_\infty^A$ ) and  
without ( $M_O^A$ ) saturation of aniline resonance.

are a number of conditions which need to be satisfied. Firstly a suitable peak for use as a probe must be chosen. This should ideally be a singlet, i.e. there should be no spin-spin coupling to any other nuclei in the molecule. The methyl peak of p-toluidine would be satisfactory from this point of view since there is only a small (usually unresolved) coupling to the aromatic protons. The second condition is that the selected nucleus or group of nuclei should have different chemical shifts in the anil and in the parent aniline. In the case of p-toluidine the difference in chemical shift between the para methyl group in p-toluidine itself and its acetone anil is 10.4 Hz at 100 MHz. For p-anisidine and m-toluidine the situation is very similar. Using the available equipment on the HA100 it was not possible to carry out SST experiments on peaks that close together. The "beats" generated by the observing and saturating fields together with the modulation due to the sample spinning frequency tended to obscure a region of roughly 15 to 20 Hz on each side of the saturated peak. This eliminated any possibility of measuring exchange rates for aniline/anil systems using CW spectrometers observing  $^1\text{H}$ .

It was however possible to measure another exchange rate using  $^1\text{H}$  NMR and SST. This was the rate of exchange of the two methyl groups of the anil. In Figure 4.1 is the  $^1\text{H}$  spectrum of the acetone anil of p-F aniline in  $\text{CD}_3\text{CN}$ . The two methyl resonances are 38 Hz apart at 100 MHz. It was noted that on addition of  $\text{ZnTu}_4(\text{ClO}_4)_2$  to such a solution the methyl resonances were slightly broadened. This suggested that the rate of exchange of

the two peaks, either with each other or with acetone, would be amenable to a study using SST. This must be carried out in a solvent other than acetone d-6 to avoid rapid deuteration of the anil methyl peaks. Acetonitrile is a suitable alternative solvent and in  $\text{CD}_3\text{CN}$  residual  $^1\text{H}$  signals are conveniently located between the two isopropylidene resonances.

Initial experiments indicated that only weak fields were required to saturate the very sharp isopropylidene signals and that at those fields there was usually little "beat" activity in the vicinity of the other signal. In Figure 7.1 are shown some  $^1\text{H}$  NMR spectra obtained at 100 MHz with a sample of N-isopropylidene p-F aniline in acetonitrile d-3. In each case the methyl region of the spectrum is shown and the weak quintet is due to the residual  $^1\text{H}$  in the  $\text{CD}_3\text{CN}$ . The weak sharp peak labelled Ac is due to acetone. Spectrum A shows the normal spectrum. In B the high field methyl peak of the anil has been saturated using an external oscillator. The other methyl signal shows only a very slight change in intensity. Spectrum C is obtained when a small quantity of  $\text{ZnTu}_4(\text{ClO}_4)_2$  is added to the solution and a slight broadening of the anil methyl peaks can be observed. Now, as shown in spectrum D, when a saturating field is applied at the high field methyl peak there is a marked decrease in intensity of the other methyl signal. However the acetone signal is completely unaffected by the saturation of one of the anil methyl peaks. The conclusion here is that there

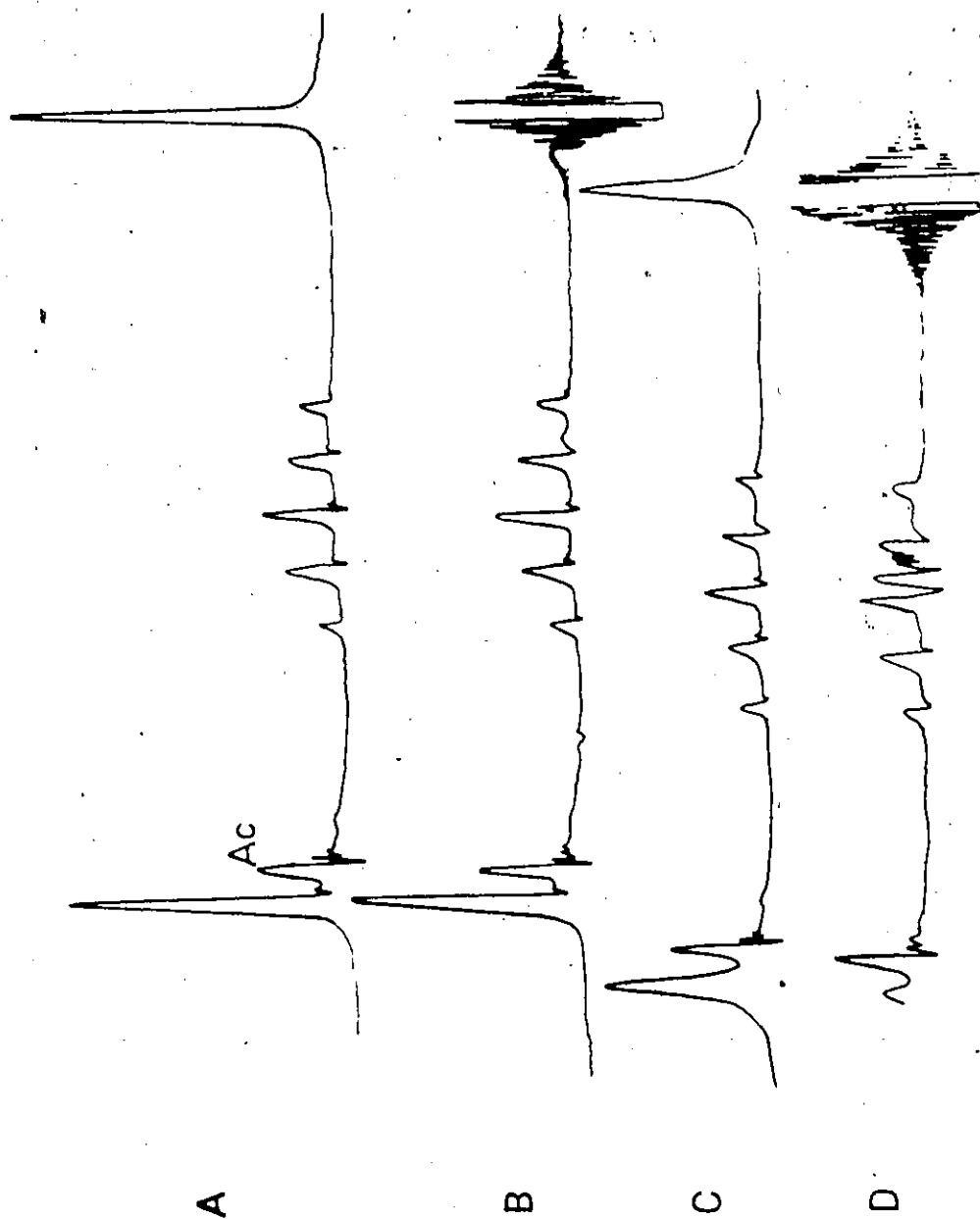


Fig. 7.1  $^1\text{H}$  NMR SST experiment with the acetone anil of p-F aniline in  $\text{CD}_3\text{CN}$ .

is a process which interchanges the anil methyl groups which does not involve the acetone.

A possible explanation for the observed exchange is that the anil on coordination to the metal has its  $>C=N$ -bond weakened due to the participation of  $M+\bar{N}-\overset{\oplus}{C}$ . This would lower the activation energy necessary for rotation about the C-N bond and thus facilitate the interchange of the two methyl groups. For the compound N-isopropylidene aniline in the absence of catalyst the temperature at which the two methyl peaks coalesce was found to be  $126^\circ\text{C}$  <sup>(79)</sup>. Since the above experiments were carried out at room temperature the observed interchange is obviously a catalysed process. This is confirmed by the absence of an SST effect in the absence of catalyst.

As in the case of SST in  $^{19}\text{F}$  NMR attempts were made to automate measurements and to determine  $T_1$  values in the presence of exchange. Similar stability problems were encountered in the present experiments. Also slight irregularities in the NMR sample tubes were found to produce "beats" in the vicinity of the observed peaks when the saturating field was switched on. For these reasons no quantitative experiments were carried out using automated techniques. However the qualitative SST experiment described above does establish that there is some metal complex catalysed process responsible for interchanging the anil methyl groups which is faster than the dynamic equilibrium involving the formation and hydrolysis of the anil.

(D) COMPARISON OF  $^1\text{H}$  AND  $^{19}\text{F}$  SST LIFETIMES

Following the observation of the catalysed exchange of the methyl groups of the acetone anil of p-F aniline it seemed desirable to compare the rate of aniline/anil exchange as monitored by  $^{19}\text{F}$  NMR with the rate of exchange of the two methyl groups of the anil using  $^1\text{H}$  NMR.

The experiments were carried out on both the DP60 and HA100 spectrometers with both probe temperatures set to 27°C. The sample consisted of p-F aniline and p-F anil (an ~50/50 mixture) dissolved in  $\text{CD}_3\text{CN}$ . The p-F anil was prepared as described in Chapter 4 Section (C). The SST experiments were designed to determine the ratio  $M_{\text{O}}^{\text{A}}/M_{\infty}^{\text{A}}$  by measuring the intensity of a peak A with a saturating field at B and again with the saturating field at some position remote from both A and B. The A, B pairs were the  $^{19}\text{F}$  signals of p-F aniline and its acetone anil and the two methyl signals of the anil.

The following measurements were carried out:

- (a) the  $^{19}\text{F}$  spectrum was integrated
- (b) SST experiments were performed on both  $^{19}\text{F}$  and  $^1\text{H}$
- (c) the catalyst  $\text{ZnTu}_4(\text{ClO}_4)_2$  was added and when equilibrium was established the SST experiments were repeated.
- (d) the sample was then split into two portions. To one half was added a small quantity of acetone h-6 and the intensity of the acetone and anil methyl peaks was monitored for one hour. To the other portion of the sample was added a small quantity of water and the same peaks were observed for an hour.



The information from (a) allowed calculation of the concentrations of both the p-F aniline and the p-F anil present in the solution. The intensity measurements in (b) showed that there was no effect caused by the saturating field in the  $^{19}\text{F}$  case and a small ( $\sim 10\%$ ) decrease in intensity in the  $^1\text{H}$  case. After the addition of the  $\text{ZnTu}_4(\text{ClO}_4)_2$  the SST experimental results shown in Table 7.3 were obtained. The  $T_1$  values needed to calculate the exchange lifetimes were measured independently. The value of 3.0 sec for  $T_1$  of  $^{19}\text{F}$  in p-F aniline was obtained from a series of "saturation recovery" measurements as described in section (B) of this chapter. The  $T_1$  value used in interpreting the  $^1\text{H}$  results was that obtained for acetone in a  $\text{CD}_3\text{CN}$  containing 0.2 moles/l. of p-toluidine and with a  $\text{ZnTu}_4(\text{ClO}_4)_2$  concentration approximately equal to that used in the above experiment. The value obtained and used was 4.8 seconds.

From Table 7.3 it may be seen that the lifetime calculated for the anil as measured by  $^{19}\text{F}$  NMR is approximately half that obtained for the interchange of the two anil methyl groups.

The second half of the experiment consisted of monitoring the effect of adding acetone and water to separate portions of the catalysed sample. The acetone or water would be expected to displace the position of the equilibrium



and the return to the new equilibrium position could be observed. This is a "concentration jump" experiment<sup>(92)</sup>. The change in the equilibrium position was followed by measuring the ratio of

Table 7.3

$^1\text{H}$  results for low field anil Me signal

$$M_{\text{O}}^{\text{A}} = 4.8 \text{ cm (average of 4 scans)}$$

$$M_{\infty}^{\text{A}} = 1.17 \text{ cm (average of 7 scans)}$$

$$T_{1\text{A}} = 4.8 \text{ sec}$$

$$\tau_{1\text{A}} = T_{1\text{A}} \frac{M_{\infty}^{\text{A}}}{M_{\text{O}}^{\text{A}}} = 1.17 \text{ sec}$$

$$\therefore \tau_{\text{A}} = 1.55 \text{ sec.}$$

$^{19}\text{F}$  results for p-F aniline signal

$$M_{\text{O}}^{\text{A}} = 5.5 \text{ cm (average of 5 scans)}$$

$$M_{\infty}^{\text{A}} = 2.01 \text{ cm (average of 6 scans)}$$

$$T_{1\text{A}} = 3.0 \text{ sec.}$$

$$\therefore \tau_{\text{Aniline}} = 1.73 \text{ sec}$$

and  $\tau_{\text{Anil}} = 0.72 \text{ sec.}$

Comparison of results:

$$\frac{\tau(\text{Me from } ^1\text{H})}{\tau(\text{Anil from } ^{19}\text{F})} = \frac{1.55}{0.72} = 2.1$$

the intensities of the acetone signal and the anil methyl signal beside it. The sample at equilibrium after the addition of the catalyst was 0.66 M in p-F anil, 1.53 M in p-F aniline and  $1.3 \times 10^{-3}$  M in  $\text{ZnTu}_4(\text{ClO}_4)_2$ . The acetone concentration was very small. Acetone h-6 was then added to the sample, so that the solution was 0.22 M in added acetone. This was at least ten times the concentration of acetone already present. However the addition of acetone produced no observable change in the anil methyl signals when added nor did the intensities change with time. This means that the concentration of water in the acetone must be such that the ratio  $[\text{H}_2\text{O}]/[\text{acetone}]$  is equal to the equilibrium constant K defined by:

$$K = \frac{[\text{p-F anil}][\text{H}_2\text{O}]}{[\text{p-F aniline}][\text{acetone}]}$$

The concentration of water in the acetone was measured using the method outlined in Chapter 4 Section (G). The value of  $[\text{H}_2\text{O}]/[\text{acetone}]$  was found to be  $8 \times 10^{-3}$ . This gives an estimate for K of  $\sim 1 \times 10^{-2}$  which is in fact in good agreement with the values obtained in acetone solution and reported in Chapter 4 Section (G).

Addition of water to the other half of the original solution however produced a large shift in the position of the equilibrium. The solution was initially 0.5 M in added  $\text{H}_2\text{O}$ . In Figure 7.2 the intensity of the acetone peak (in arbitrary units) is plotted against the time elapsed in minutes after the addition of the water. By extrapolation a value of the initial rate of formation of acetone from anil and water may be obtained. This

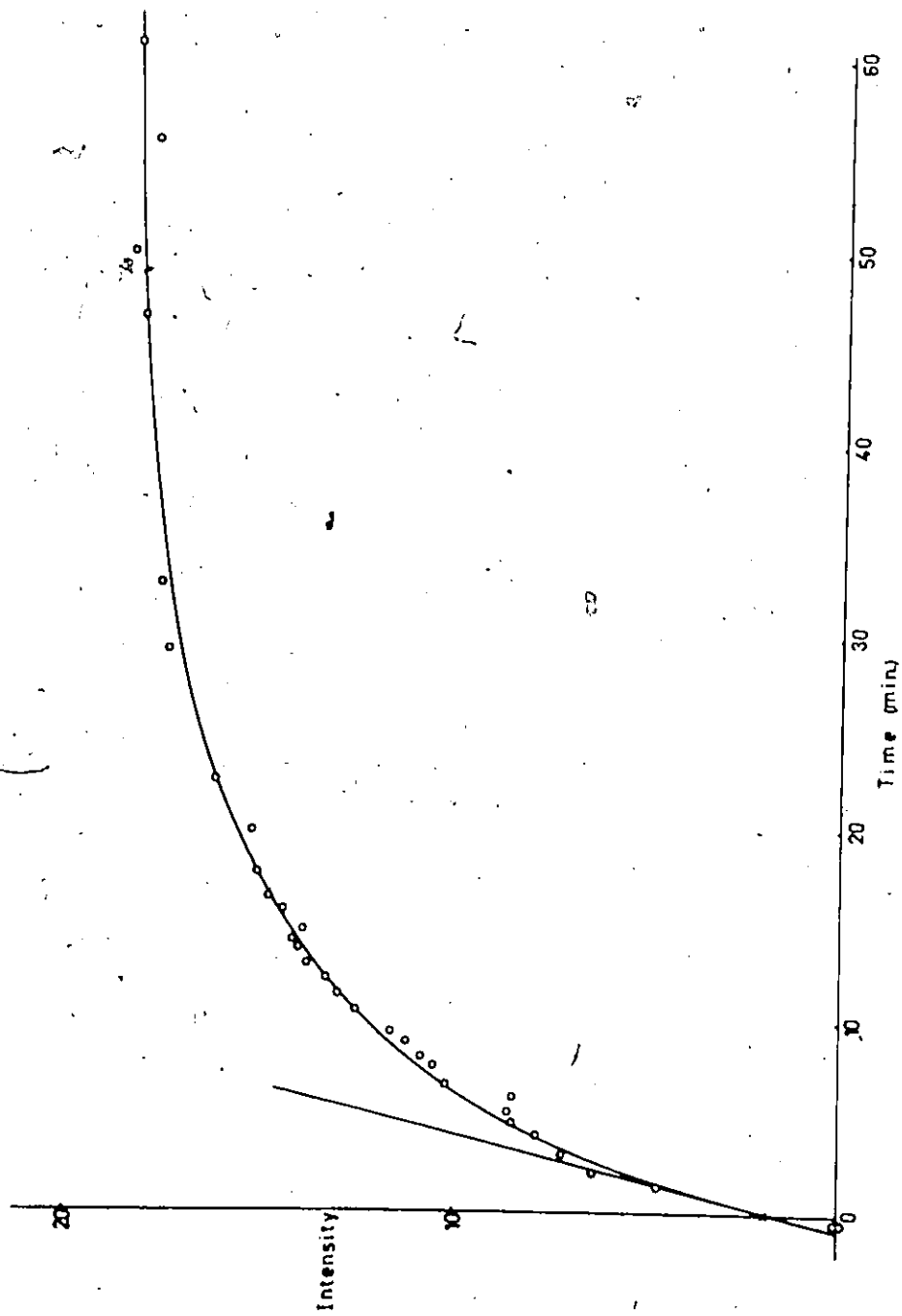
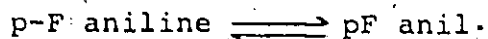


Fig. 7.2 Intensity of acetone peak (arbitrary units) plotted against time elapsed in minutes. The experiment involved addition of water to a catalysed solution of anil in  $\text{CD}_3\text{CN}$ .

is  $3 \times 10^{-3}$  moles/l.sec. It is interesting at this point to compare this rate with the rate obtained from the SST experiment using  $^{19}\text{F}$  NMR. The process observed here is



The lifetime observed for p-F aniline in this experiment was 0.74 sec =  $\tau_{\text{Anil}}$ . The rate of reaction of the anil is then given by

$$\text{Rate} = \frac{[\text{anil}]}{\tau_{\text{Anil}}} = \frac{0.66}{0.74} = 0.9 \text{ moles/l. sec.}$$

Thus expressed in moles/l.sec. the rate measured by SST is roughly  $10^2$  times as large as the rate measured by the initial rate method. There would therefore seem to be two distinct processes involved.

#### (E) FT SST MEASUREMENTS

The experimental conditions which were used for running SST experiments on an FT spectrometer have been described in Chapter 3 Section (E). The main advantages of the FT method are (a) SST experiments can be performed on pairs of peaks that are within 10 Hz or less of each other and (b) the spin relaxation times  $T_1$  may be measured in the presence of exchange thus allowing the effects of the catalyst on  $T_1$  to be determined. In fact the  $T_1$  value measured for the protons of the methyl group in p-toluidine was found to be affected by the metal complex concentration. When the concentration of  $\text{ZnTu}_2\text{Cl}_2$  (C) in a solution containing 0.2 M p-toluidine in acetone d-6 was changed the following

$T_1$  values were obtained by the  $180^\circ$ - $\tau$ - $90^\circ$  method;  $C = 0.15$  M,  $T_1 = 3.0$  sec;  $C = 0.30$  M,  $T_1 = 2.7$  sec; and  $C = 0.45$  M,  $T_1 = 2.4$  sec. This decrease in  $T_1$  as the metal complex concentration is increased could be due to the increase in the concentration of protons in the solution (since they are more effective in promoting dipolar relaxation than deuterons) or it could be due to a very small concentration of a paramagnetic impurity present in the zinc complex.

The SST experiments performed on the FT spectrometer were mainly concerned with determining suitable experimental conditions and exploring the limitations of the technique. However some rate data were obtained for the exchange between p-toluidine and its acetone anil as monitored by their para methyl signals. The samples were catalysed with  $ZnTu_2Cl_2$  and the results are presented in Table 7.4.

The lifetimes for the aniline obtained in this way may be compared with those derived from the initial rate experiments. Measurements of the initial rate of formation of anil from p-toluidine (d-2) catalysed by  $ZnTu_2Cl_2$  are reported in Section (Bii) of Chapter 5. The measured initial rate of formation was  $\sim 1.6 \times 10^{-4}$  moles/l. sec. with an initial p-toluidine concentration of 0.2 moles/l. and a catalyst concentration of 0.02 moles/l. An approximate lifetime for the aniline under these conditions may be derived using the expression

$$\text{Lifetime} = \tau_{\text{Aniline}} = \frac{\text{concentration}}{\text{rate}} = \frac{0.2}{1.6 \times 10^{-4}} = 1200 \text{ sec.}$$

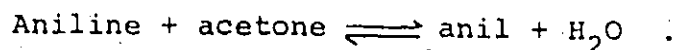
Table 7.4  
Results of FT SST experiments

Conc. of $ZnTu_2Cl_2$ in moles/l.	$\tau_1$ (sec)	$\tau_{Anil}$ (sec)	$\tau_{Aniline}$ (sec)	R
0.14	3.1	7.7	4.6	1.0
0.39	2.4	4.0	2.2	1.16

Both samples were initially 0.2 M in p-toluidine and the temperature was 28°C.

$$R = \frac{M_{\circ} (Anil)}{M_{\circ} (Aniline)} \cdot \frac{\tau_{Anil}}{\tau_{Aniline}} \quad (\text{ideally } R = 1.0)$$

This is the lifetime for an aniline molecule involved in the equilibrium,



It is only an approximate figure since the initial rate and concentration are used instead of the equilibrium rate and concentration. However these factors will compensate for one another and the estimate is certainly good to within an order of magnitude.

To compare the above lifetime from the initial rate studies with that obtained by the FT SST measurements an allowance must be made for the different  $\text{ZnTu}_2\text{Cl}_2$  concentrations. Assuming that the rate is directly proportional to the  $\text{ZnTu}_2\text{Cl}_2$  concentration this would predict that an initial rate experiment with 0.2 M  $\text{ZnTu}_2\text{Cl}_2$  would yield a lifetime for the aniline of  $\sim 120$  sec. The observed value of the lifetime for aniline as measured by FT SST under these conditions is in fact 4 seconds. Other factors involved, if taken into account, would only serve to make the discrepancy even larger. One of these is the fact that the initial rate measurements were performed using p-toluidine (d-2) whereas the FT SST experiments used p-toluidine (h-2). There is also the difference in temperature; the initial rates were measured at 35°C whereas the SST experiments were carried out at 27°C. The third point is that the dependence of the rate on  $\text{ZnTu}_2\text{Cl}_2$  concentration is likely to be less than first order at high  $\text{ZnTu}_2\text{Cl}_2$  concentrations. Thus there is a marked discrepancy between the results of the two experimental techniques which are supposedly measuring the same process. These calculations



are strongly supported by the observation that samples prepared for SST experiments with  $\text{ZnTu}_2\text{Cl}_2$  concentrations of 0.2 moles/l. or less could be observed coming to equilibrium in the NMR spectrometer. With a  $\text{ZnTu}_2\text{Cl}_2$  concentration of 0.14 moles/l. the time to form one half of the equilibrium concentration of the anil was roughly 5 minutes. However the SST lifetime measured for the aniline in this sample was  $\sim 5$  seconds. These results tend to suggest that there is some process which exchanges aniline and anil faster than the reaction of the formation and hydrolysis of the anil.

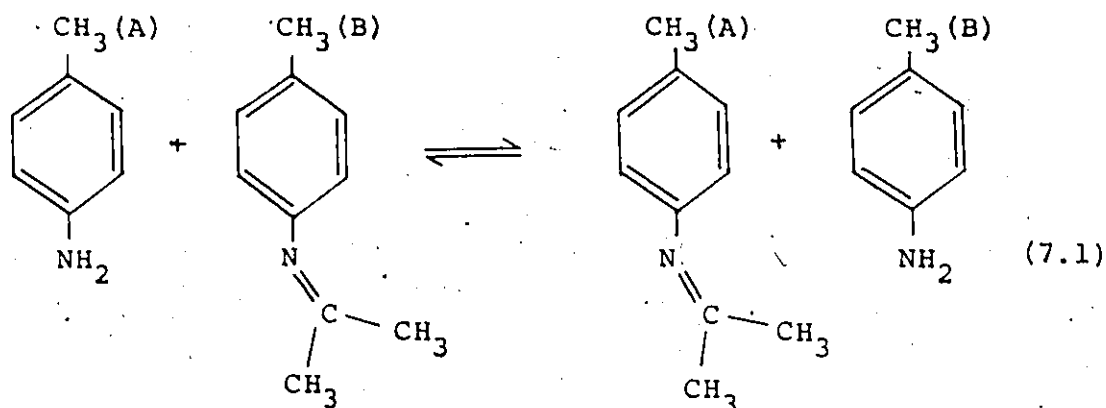
#### (F) DISCUSSION

The results presented so far in this chapter may be summarized as follows:

- (a) Exchange of aniline and anil as observed via their para substituents is metal complex catalysed.
- (b) The observed rate of exchange of aniline and anil as measured by SST experiments ( $^1\text{H}$  and  $^{19}\text{F}$ ) using the para substituents as a probe is much faster than can be explained on the basis of the catalysed formation and hydrolysis of the anil in either acetone or acetonitrile as a solvent.
- (c) The interchange of the methyl groups of the anil is metal complex catalysed but does not proceed via acetone.
- (d) The lifetime of an anil molecule as measured via its para substituent is half that for the interchange of its methyl groups.

Aside from chemically unlikely possibilities involving

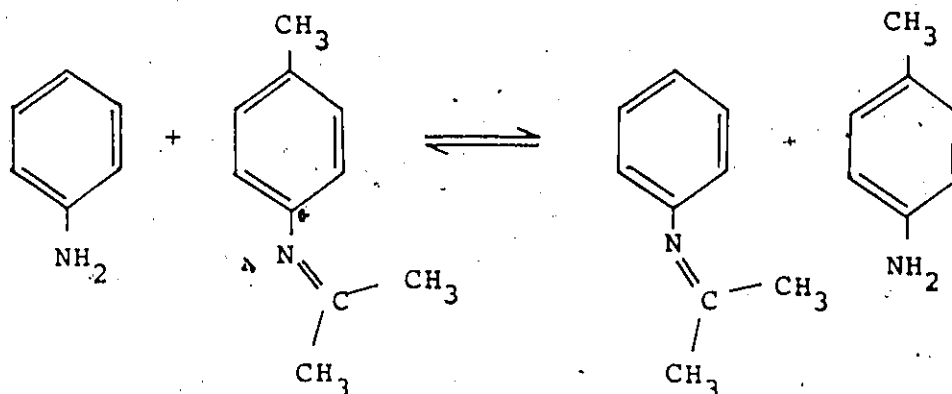
breaking the bond between the para substituent ( $\text{CH}_3$  or  $\text{F}$ ) and the aromatic ring the most reasonable explanation of all the above results is that there is a metal complex catalysed transimination reaction taking place, i.e.



This reaction is analogous to the formation of the anil except that here the aniline attacks the carbon of the imine bond of the anil rather than that of the carbonyl bond of acetone.

To show that there was a transimination process occurring an experiment was carried out using methods for measuring the initial rates. A sample of p-toluidine (0.2 M) in acetone was prepared, a little  $\text{ZnTu}_4(\text{ClO}_4)_2$  was added and the reaction was monitored using the p- $\text{CH}_3$  peaks of p-toluidine and its anil. After thirty minutes the reaction had proceeded roughly 66% to completion. At this point aniline was added to the sample so as to make the aniline concentration  $\sim 0.4$  M. The first sweep through the methyl region after the addition of the aniline showed that the ratio  $\left(\frac{\text{Anil}}{\text{Anil}+\text{Aniline}}\right)$  for the p-toluidine had changed from 0.4 to 0.125. This new "equilibrium" position

was reached in less than one minute. The reaction taking place was



This transimination reaction is at least  $10^2$  times faster than the reaction with acetone forming the anil. The rate of reaction of aniline with acetone is comparable with that of p-toluidine. This means that in the SST experiments the only significant contribution to the measured exchange lifetimes will be from the transimination process.

The role of the metal complex in catalysing the transimination reaction was demonstrated with a sample containing p-toluidine and its acetone anil in acetone d-6. Aniline was added and no transimination was observed. Also, as mentioned in section B of this chapter the transimination reaction is inhibited by Tu.

In a transimination reaction such as that of 7.1, each time that the isopropylidene group is transferred from one ring to another there is a 50/50 chance that the reaction will occur without changing the syn/anti position of the methyl groups. On the other hand the para substituent will be exchanged on every reaction. Thus the predicted lifetime for the anil methyl groups would be twice that of the para substituent of the anil.

The experimental result presented in section D of this chapter is thus in good agreement with this prediction.

The transimination reaction thus explains all the experimental observations and discrepancies presented in this chapter. The catalysed free rotation of the anil methyl groups is not excluded but may well be slower than exchange via a transimination reaction.

## CHAPTER EIGHT

### DISCUSSION AND CONCLUSION

#### (A) INTRODUCTION

A catalysed reaction consists of a number of steps, each with its own rate constant. In general one of these steps will be much slower than any of the others and this is then known as the "rate-determining step". The objective of kinetic studies of catalytic reactions is usually to determine the nature of the rate-determining step, to measure its rate constant, and to infer the mechanism of the step and thus of the reaction.

Since mechanisms are rarely "proved" by kinetic studies, the approach to determining the mechanism used here will be to find the simplest and most chemically reasonable mechanism which will fit the observed facts and measurements.

#### (B) NATURE OF THE CATALYTIC SPECIES

Certain definite conclusions about the metal complex catalysed formation and hydrolysis of anils may be drawn from the results presented in the previous chapters. The first point is that the reaction is homogeneously catalysed by metal complexes, specifically thiourea complexes of Co and Zn. The uncatalysed reaction is very slow and may be ignored at the catalyst concentrations used in these studies. Also, the rate of reaction is directly proportional to the catalyst concen-

tration for the case of  $\text{ZnTu}_4(\text{ClO}_4)_2$  as catalyst. The effectiveness of the various catalysts correlates roughly with the dissociation constant of the complex as measured in acetone solution.

One of the most important questions to be settled is whether one or more of the reagents need to be complexed to the metal for reaction to occur. The need for complexing is strongly suggested by the inhibition studies carried out using thiourea. Furthermore, the observed behaviour of the rate as a function of aniline, anil and water concentrations suggests in the simplest interpretation a fast pre-equilibrium involving association of the substrates with the metal complex.

One possible mechanism not involving any complexed reagents would be a transimination reaction involving complexed Tu. The mechanism would involve the formation of an imine between acetone and the amino group of the thiourea, followed by a transimination reaction between that imine and an aniline molecule. This is unlikely for the following reasons:

- (a) Tu alone is ineffective as a catalyst.
- (b) There is no evidence for catalysed imine formation between acetone and thiourea<sup>(69)</sup>.
- (c) Both  $\text{Zn}(\text{DMTu})_2\text{Br}_2$  and  $\text{Zn}(\text{TMTu})_2\text{Br}_2$  are very effective as catalysts, and here a transimination mechanism could not operate since a nitrogen with two hydrogen atoms is necessary for such a reaction.

At this point it should be noted that any of the individual steps involving complexing of the various substrates cannot be rate determining. This may be seen from a comparison of the measured lifetimes for ligand exchange with the lifetimes for the formation or hydrolysis of the anils. For the case of  $ZnTu_2Cl_2$  as catalyst in acetone which was 0.2 M in p-toluidine, the initial rate of formation was  $1.6 \times 10^{-4}$  moles/l.sec. This can be converted to a lifetime for the forward reaction by

$$\tau = \frac{\text{conc.}}{\text{Rate}} = \frac{0.2 \text{ moles/l.}}{1.6 \times 10^{-4} \text{ moles/l.sec.}} = \sim 10^3 \text{ seconds.}$$

The measured lifetimes for the ligand exchange processes concerned are many orders of magnitude less than this figure. In Chapter 6 Section (E-iii) lifetimes of  $10^{-5}$  and  $10^{-4}$  seconds are reported for exchange of p-toluidine and its anil with  $CoTu_2Cl_2$ . Kinetics for the analogous zinc complex are believed to be very similar<sup>(69)</sup>.

The experiments involving dilution with  $CCl_4$  for both the formation and hydrolysis of the anil have been discussed in Chapter 5. The result for both reactions is that the rate-determining step appears to be first order, that is (the rate is independent of the degree of dilution with  $CCl_4$ ). Since the rate is known to depend on the aniline, anil, water and catalyst concentrations, then this result suggests that the rate-determining step takes place in a ternary complex, i.e. one containing both of the substrates and the catalyst. The simplest ternary complex is one containing both substrates complexed to the metal in the

first coordination sphere of the complex. As was shown in Chapter 5, Section (B-iii), this model will predict the observed behaviour on dilution with an inert solvent. For the forward reaction, i.e. the formation of the anil, the model would predict that the rate of formation of anil would be directly proportional to the concentration of the species containing both acetone and aniline coordinated, or;

$$\text{rate} \propto [\text{MANAcCl}_2]$$

for the case of  $\text{MTu}_2\text{Cl}_2$  as a catalyst.

In order to test this model for the mechanism it is necessary to be able to calculate the concentrations of the various mixed ligand species in a solution with many potential ligands. A method for doing this is presented in Appendix A for the  $\text{MTu}_2\text{X}_2$  and  $\text{MTu}_4^{2+}$  cases. Also derived therein are the appropriate expressions for the rate if it is assumed to depend on the concentration of species containing coordinated acetone and aniline.

The form of equation (A.2) is particularly suitable for iterative computation to find the concentrations of all the species  $[\text{ML}_i\text{L}_j]$ . The program requires values of the equilibrium constants  $K_i$  and the total metal concentration  $m$ . It also requires an initial guess for each of the free ligand concentrations  $[\text{L}_i]$  as well as the total amount of ligand  $i$  in the solution.

The procedure is to use the initial guesses for  $[\text{L}_i]$  in equation (A.2) and to calculate the terms  $[\text{ML}_i\text{L}_j]$ . New values for



$[L_i]$  are then obtained from a series of expressions

$$[L_i]' = [T_i] - \sum_{j=1}^n ML_i L_j$$

where  $[T_i]$  is the total concentration of the ligand  $i$  in the solution.

The new values for  $[L_i]$ , i.e.  $[L_i]'$ , are then substituted into equation (A.2). This process may be repeated until convergence is obtained, i.e. until the value of a particular  $[ML_i L_j]$  changes by less than 1% in two consecutive iterations. The program was found to converge rapidly when  $m$  was small compared to any product  $K_i [L_i]$ . The program is reproduced in Appendix B.

This program was used with the data from the experiment designed to find the dependence of the initial rate on the *p*-toluidine concentration with  $ZnTu_2Cl_2$  as catalyst, as described in Chapter 5, Section (B-ii). The values used for the equilibrium constants were those determined for acetone and *p*-toluidine with  $CoTu_2Cl_2$ , as outlined in Chapter 6, Sections (B) and (E). The input data and the values for the concentrations of some of the species in solution are reported in Table 8.1. The program converged after 12 to 20 iterations.

If the model outlined above (i.e. that involving coordinated aniline and acetone) is the correct one, then the initial rate should be directly proportional to the calculated concentration of the species  $MANAcCl_2$ . A glance at the figures in Table 8.1 shows that in fact the calculated value of  $MANAcCl_2$  actually decreases as the aniline concentration is increased, in direct

Table 8.1

## Calculated Concentrations

Input data: Initial  $ZnTu_2Cl$  concentration 0.0219 M

Acetone concentration 13.65 M

Equilibrium constants:  $K_1(Tu) = 1.0$

$K_2(An) = 0.036$

$K_3(Ac) = 0.000107$

[p-toluidine] moles/l	[MANAcCl <sub>2</sub> ] moles/l	A	B	Initial Rate moles/l sec *
0.064	$1.10 \times 10^{-4}$	$3.74 \times 10^{-5}$	$1.27 \times 10^{-1}$	$7.45 \times 10^{-5}$
0.117	$1.04 \times 10^{-4}$	$4.84 \times 10^{-5}$	$9.31 \times 10^{-2}$	$1.28 \times 10^{-4}$
0.162	$1.00 \times 10^{-4}$	$5.55 \times 10^{-5}$	$7.86 \times 10^{-2}$	$1.44 \times 10^{-4}$
0.213	$9.5 \times 10^{-5}$	$6.17 \times 10^{-5}$	$6.71 \times 10^{-2}$	$1.67 \times 10^{-4}$
0.292	$8.9 \times 10^{-5}$	$6.97 \times 10^{-5}$	$5.59 \times 10^{-2}$	$2.24 \times 10^{-4}$
0.620	$7.3 \times 10^{-5}$	$9.09 \times 10^{-5}$	$3.50 \times 10^{-2}$	$3.31 \times 10^{-4}$

$$A = ([MTuAcCl_2] + [MANAcCl_2])[An]$$

$$B = ([MTuAnCl_2] + 2[MANAnCl_2] + [MANAcCl_2])/[An]$$

\* from Table 5.3

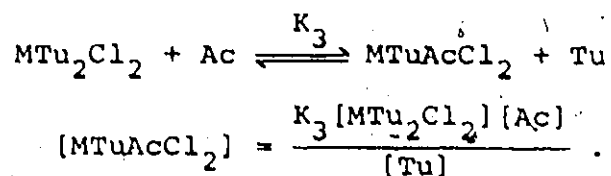
contradiction to the observed result. In fact the value of  $[MAnAcCl_2]$  will not increase as a function of  $[p\text{-tol}]$  unless  $K_3[Ac] \gg K_2[An]$ , (see equation (A.5)). From the experiments described in previous chapters and from the general behaviour of thiourea metal complexes in solution with aniline, it is not reasonable to conceive of  $K_3[Ac]$  being greater than  $K_2[An]$ .

The same conclusion will hold for the case of  $MTu_4^{++}$  as a catalyst since the expression (equation (A.8)) for the concentration of all species containing coordinated acetone and aniline has exactly the same form as for the  $MTu_2Cl_2$  case. The model thus fails to reproduce the experimental behaviour of the initial rate of formation of anil as a function of aniline concentration, both for  $ZnTu_2Cl_2$  and  $ZnTu_4(ClO_4)_2$  as catalysts. 12

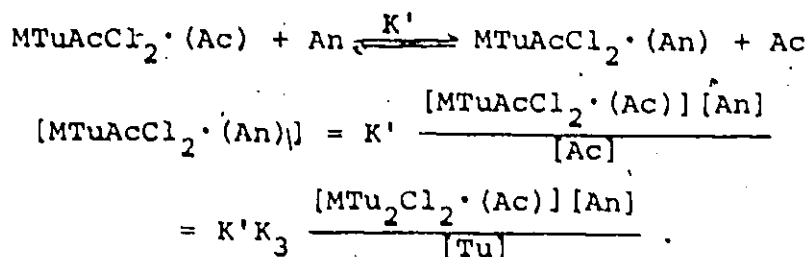
For the above reasons then, it is necessary to abandon the mechanism where both substrates are coordinated prior to reaction. This means returning to a mechanism in which only one substrate is coordinated. However, in order to explain the results of the dilution experiment, the second substrate must be bound to the metal complex in such a fashion that  $CCl_4$  will not dissociate this adduct. Whatever the nature of this binding (be it at weak fifth coordination site, hydrogen bonding, or simply a Van der Waals interaction), the site at which it occurs will be referred to, in the following discussion, as a second coordination sphere site. Thus the condition for the dilution experiment may be expressed by saying that the second substrate is a much better second sphere ligand than  $CCl_4$  and is thus not displaced by  $CCl_4$ . That such

a mechanism will correctly predict the result of the dilution experiment is shown below for the case of  $MTu_2Cl_2$  as catalyst.

Suppose that acetone is to be the first sphere ligand and aniline the second sphere ligand. Then for replacing Tu by acetone



The second coordination sphere will initially contain acetone and may be represented by  $MTu_2Cl_2 \cdot (Ac)$ , or  $MTuAcCl_2 \cdot (Ac)$ . Now for aniline replacing acetone in the second coordination sphere



If the rate is proportional to the concentration of  $MTuAcCl_2 \cdot (An)$  then

$$\text{Rate} \propto K' K_3 \frac{[MTu_2Cl_2 \cdot (Ac)] [An]}{[Tu]}$$

On dilution with an inert solvent to a volume  $V$  times the original volume,

$$\text{Rate} \propto K' K_3 \frac{[MTu_2Cl_2 \cdot (Ac)]}{V} \frac{[An]}{V} \cdot \frac{V}{[Tu]}$$

$$\text{Rate} \propto K' K_3 \frac{[MTu_2Cl_2 \cdot (Ac)] [An]}{[Tu]} \cdot \frac{1}{V}$$

$$\therefore \propto \frac{1}{V} \text{ on dilution.}$$

There is an additional species containing acetone in the first

coordination sphere which will make a significant contribution to the rate, and that is the species  $\text{MANAcCl}_2$ . The other acetone, containing species,  $\text{MACAcCl}_2$ , will only be present in extremely small amounts due to the size of the term  $K_3[\text{Ac}]$  relative to the terms  $K_2[\text{An}]$  and  $[\text{Tu}]$ . The full expression for the rate will then be

$$\text{Rate} \propto [\text{MTuAcCl}_2 \cdot (\text{An})] + [\text{MANAcCl}_2 \cdot (\text{An})] .$$

The second term by a similar analysis will also show  $\frac{1}{V}$  dilution behaviour. This is in fact the observed result.

Although in principle this mechanism could have either aniline or acetone as the first sphere ligand, all chemical experience with reactions of this nature would suggest that acetone in the first sphere is much more likely. As quoted in the first chapter there is much evidence to show that one of the main driving forces in metal catalysis of nucleophilic attack is the polarization of charge which takes place in the carbonyl group, say, on coordination. The relatively larger positive charge on the carbon of the carbonyl group renders it much more susceptible to nucleophilic attack, in this case by the nitrogen of the aniline. On the other hand, the complexing of aniline would reduce its ability to act as a nucleophile towards the carbonyl group since it is doing so already to the metal.

A confirmation of this argument comes from the calculations of the concentrations of the various species in solution. If the rate was proportional to the concentration of complexed

aniline there would be three important species to consider:  $MTuAnCl_2$ ,  $MANAnCl_2$  and  $MANAcCl_2$ . With acetone in the second sphere the rate would then be proportional to the following term:

$$\frac{[MTuAnCl_2 + 2[MANAnCl_2] + [MANAcCl_2]}{[An]}$$

In Table 8.1 the calculated values for this term are listed, and it may be seen that in fact the value decreases as the aniline concentration is increased, in contrast to the observed behaviour.

For the reverse reaction of the hydrolysis of the anil the same arguments apply, with the  $>C=N-$  group replacing the carbonyl group and with  $H_2O$  now being the nucleophile. The mechanism of this reaction would then involve coordinated and polarised anil, and  $H_2O$  in the second coordination sphere.

For the case where  $MTu_2Cl_2$  is the catalyst and the reaction is the formation of the anil, the rate should be directly proportional to  $[MTuAcCl_3 \cdot (An)] + [MANAcCl_2 \cdot (An)]$ . This can be written as

$$\begin{aligned} \text{Rate} &\propto [MTuAcCl_2 \cdot (An)] + [MTuAcCl_2 \cdot (An)] \\ &\propto K' \frac{[MTuAcCl_2 \cdot (Ac)][An]}{[Ac]} + K \frac{[MANAcCl_2 \cdot (Ac)][An]}{[Ac]} \\ \text{Rate} &\propto ([MTuAcCl_2 \cdot (Ac)] + [MANAcCl_2 \cdot (Ac)]) \cdot [An] \quad (8.1) \end{aligned}$$

This last term can be calculated by the computer program previously described and this was done using the conditions of the experiment with  $ZnTu_2Cl_2$  and p-toluidine. The results are contained in Table 8.1. With this model the rate does at least

increase as the concentration of aniline is increased. The observed rate is also directly proportional to the calculated value of the term in equation (8.1), as may be readily seen from figure 8.1 where the initial rate is plotted against the term in question.

With  $\text{MTu}_2\text{Cl}_2$  as the catalyst, it is shown in Appendix A that an approximation, justifiable when the aniline concentration is small, leads to the expectation that  $(\text{Initial Rate})^{-1}$  should be directly proportional to  $(\sqrt{[\text{An}]})^{-1}$ . To check the range of validity of this approximation in Figure 8.2(a), the inverse of the calculated value of  $([\text{MTuAcCl}_2] + [\text{MAnAcCl}_2])[\text{An}]$  is plotted against  $\sqrt{[\text{An}]}$ . The graph shows that, with the data and the values of the equilibrium constant chosen, only the point representing the most concentrated sample does not lie on the straight line. In Figure 8.2(b) the experimental data from Table 5.3 is plotted in the form  $(\text{Initial Rate})^{-1}$  versus  $(\sqrt{[\text{p-tol}]})^{-1}$ , and a linear graph is obtained.

The above model, when applied to the case of  $\text{MTu}_2\text{Cl}_2$  as the catalyst, does not in fact predict that the plot of  $\frac{1}{\text{Rate}} \text{ vs } \frac{1}{[\text{An}]}$  should be linear. In fact, when the data of Table 8.1 are plotted in the form  $([\text{MTuAcCl}_2] + [\text{MAnAcCl}_2])[\text{An}] \text{ vs } [\text{An}]$ , a very shallow curve is obtained. The experimental results for the initial rate of formation of anil from p-toluidine with  $\text{ZnTu}_2\text{Cl}_2$  as catalyst are too scattered for the expected slight curvature of the Lineweaver-Burk plot (figure 5.4) to be detected.

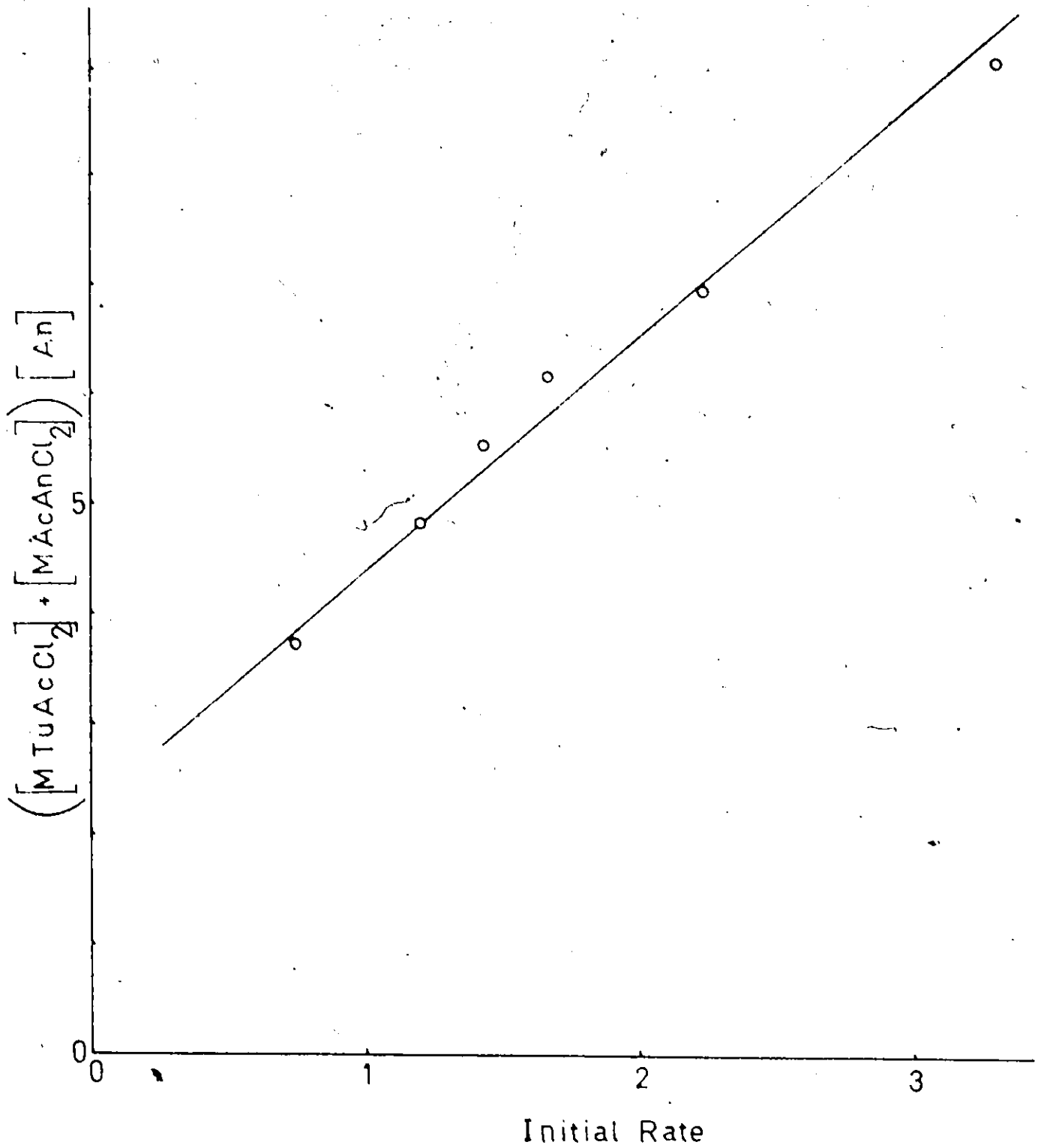
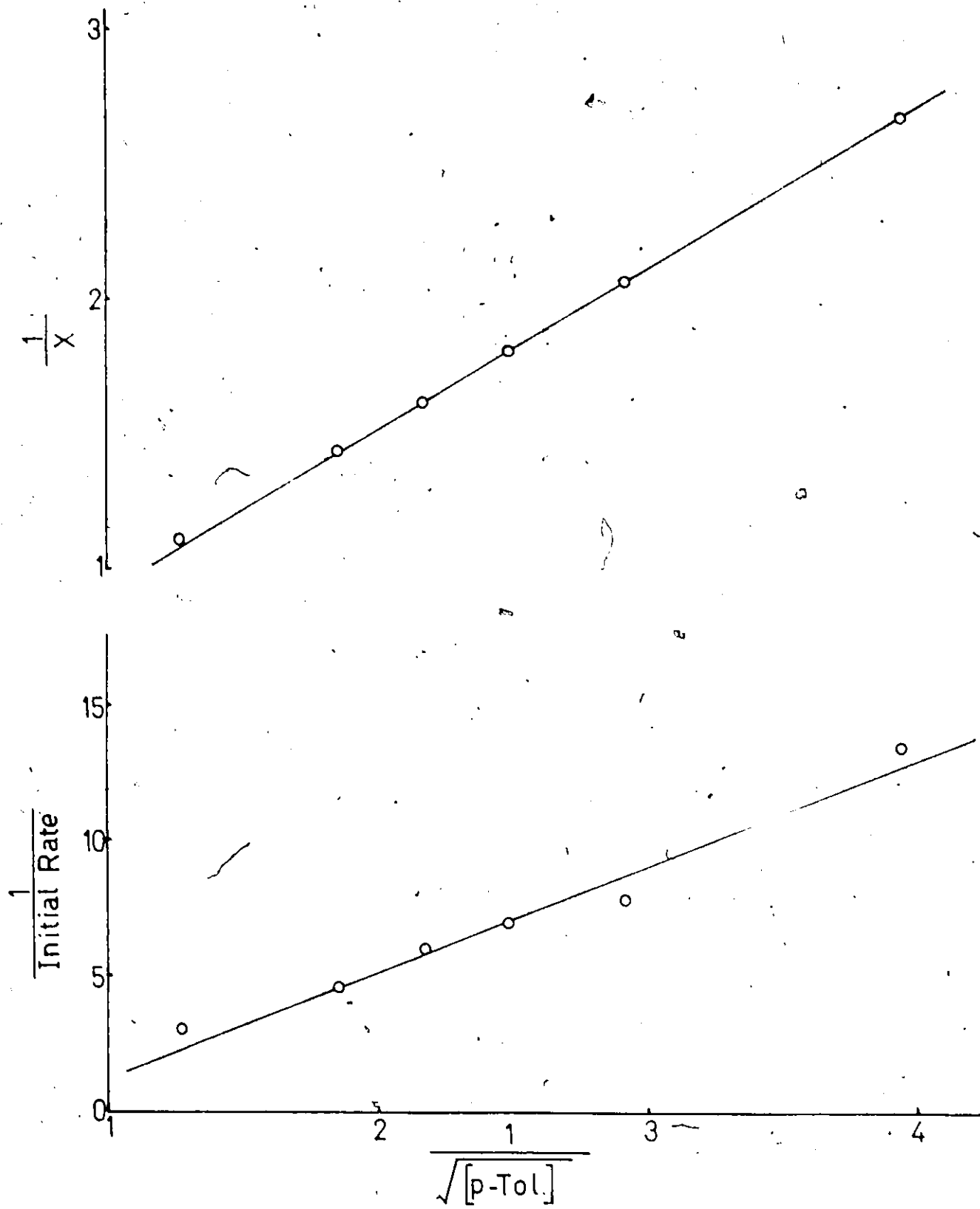


Fig. 8.1 The term  $([MTuAcCl_2] + [MAcAnCl_2])[An]$  (in moles<sup>2</sup>/l<sup>2</sup> $\times 10^5$ ), as calculated from the data in table 8.1, plotted against the initial rate (in moles/l.sec. $\times 10^4$ ), from table 5.3.



- Fig. 8.2 (a) A plot of  $\frac{1}{\bar{X}}$  (where  $\bar{X} = ([\text{MTuAcCl}_2] + [\text{MAnAcCl}_2]) \cdot [\text{An}]$ ) in moles<sup>2</sup>/l<sup>2</sup>  $\cdot 10^{-4}$ , from table 8.1) against  $(\sqrt{[\text{ptol}]})^{-1}$  (in l<sup>1/2</sup>/mole<sup>1/2</sup>).
- (b) A plot of initial rate<sup>-1</sup> (in l.sec/mole  $\cdot 10^{-3}$ ) against  $(\sqrt{[\text{ptol}]})^{-1}$  (in l<sup>1/2</sup>/mole<sup>1/2</sup>) for the data of table 5.3.



When  $MTu_4^{2+}$  is the catalyst, the predicted dependence of the initial rate on aniline concentration is more complex. As discussed in Appendix A, the inverse of the rate should be roughly proportional to  $\frac{1}{[An]}$  and any curvature would probably be experimentally undetectable. Computation of the expected behaviour is precluded in this case by the lack of knowledge about the equilibrium constants. However, using this model where the acetone is coordinated to the metal the results of the Tu inhibition experiment with  $ZnTu_4(ClO_4)_2$  are readily explained. As shown in Appendix A, the model predicts that  $[rate]^{-1}$  should be proportional to the free thiourea concentration  $[Tu]$ . Under the experimental conditions, the free thiourea concentration may be accurately represented by the total concentration of Tu added. As shown in figure 8.3, a reasonable fit to a straight line is obtained. Any slight deviation from linearity may be explained by noting that the model only allows for inhibition by Tu in the first coordination sphere, and ignores effects in the second coordination sphere.

Although not critical to the arguments presented in this section, the equilibrium constants used in the calculations with  $ZnTu_2Cl_2$  are open to some discussion. The analogous tetrahedral complexes of  $Co^{II}$  and  $Zn^{II}$  are known to be similar in properties, and in particular, it was concluded that  $CoTu_2Cl_2$  and  $ZnTu_2Cl_2$  were very similar<sup>(69)</sup>. Shulman<sup>(89)</sup> concluded that the equilibrium constant for the replacement of Tu by water in aqueous acetone

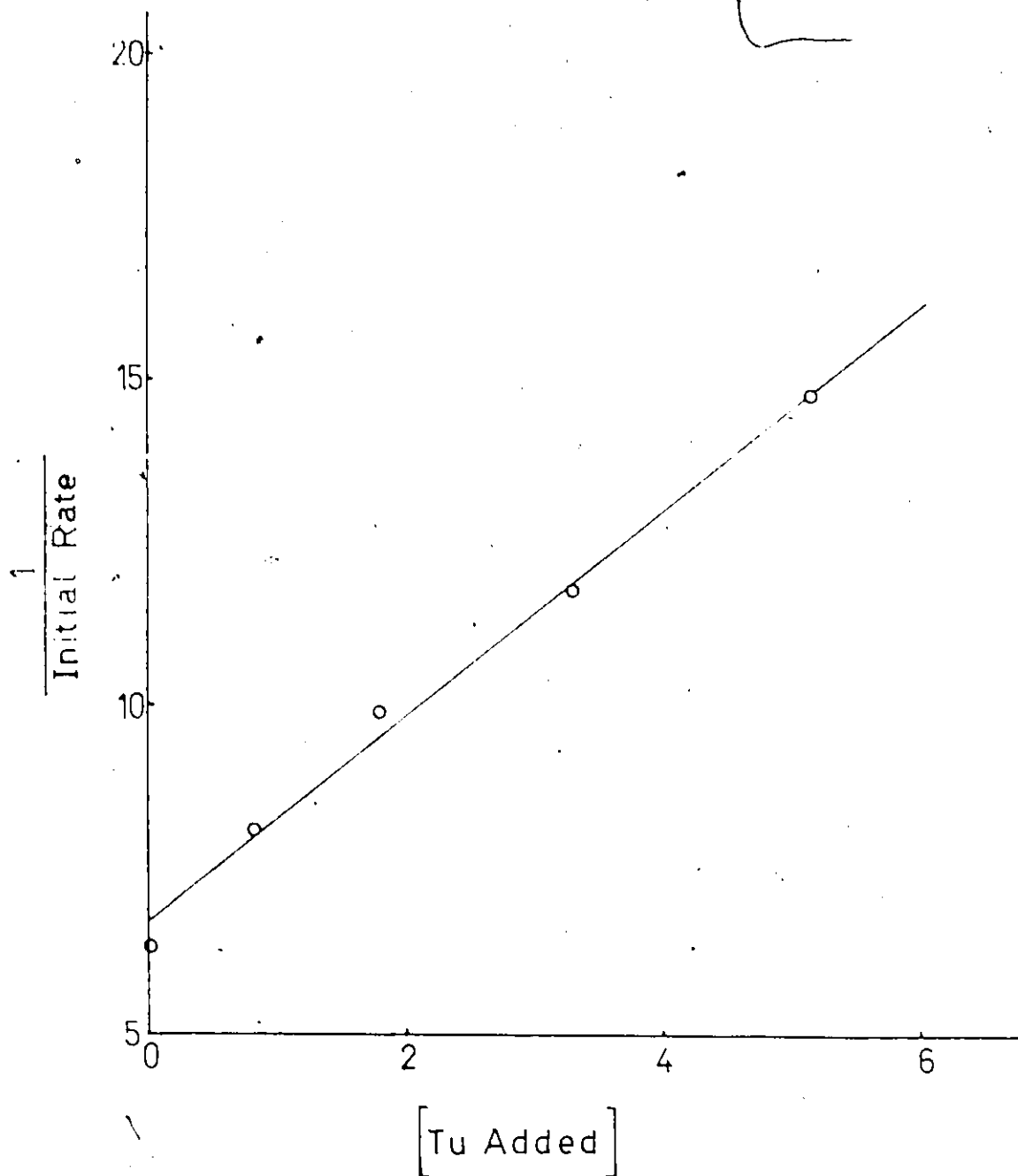


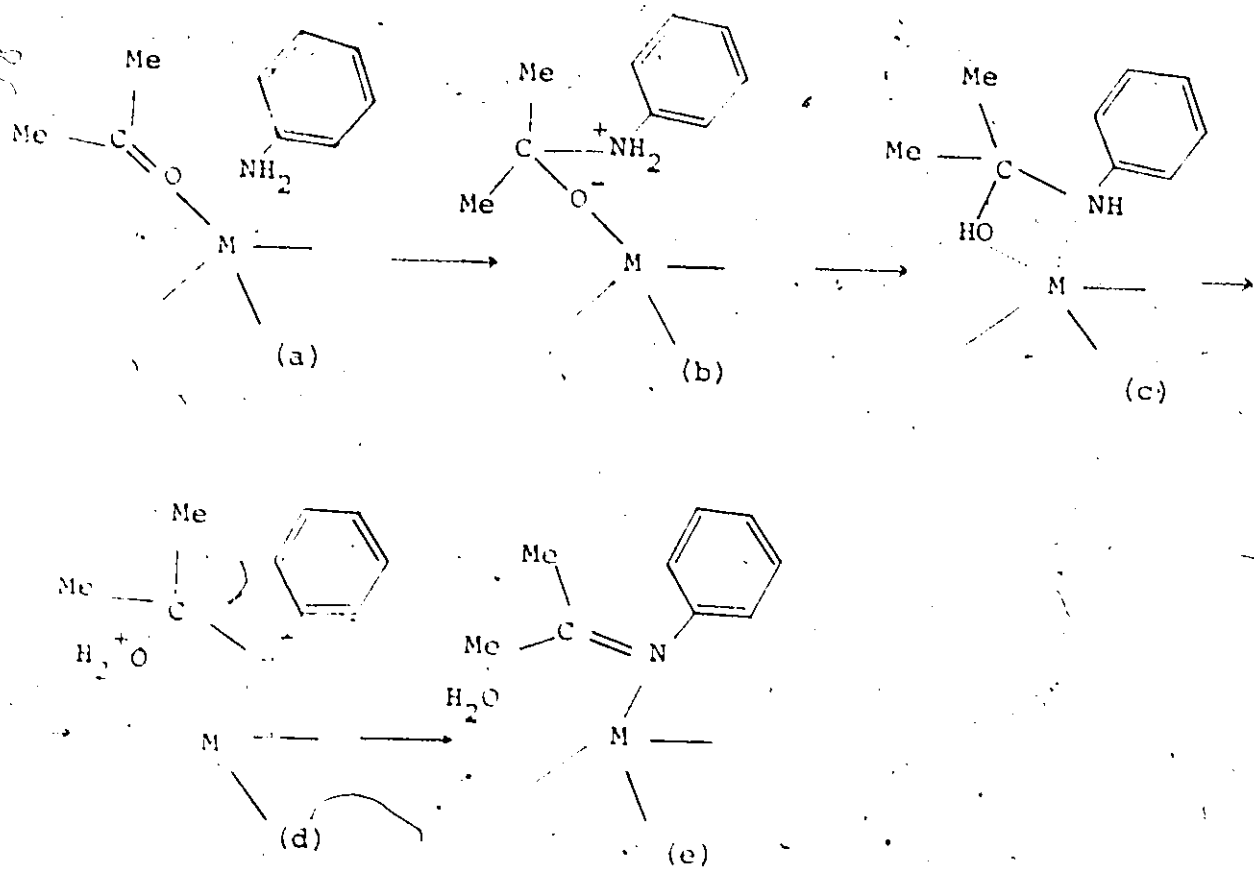
Fig. 8.3 Initial rate<sup>-1</sup> (in l.sec/mole $\times 10^{-1}$ ) plotted against the added Tu concentration (in moles/l $\times 10^2$ ) for the date of table 5.5.

was ~ 10 times larger in the case of  $ZnTu_2Cl_2$  than for  $CoTu_2Cl_2$ . However behaviour of the complexes in aqueous acetone may not be mirrored in dry acetone with anilines. This question can only be resolved by measuring the equilibrium constants with the zinc complex.

### (C) NATURE OF THE RATE DETERMINING STEP

In the previous section it was concluded that for the forward reaction, i.e. the formation of the anil, the species involved in the rate-determining step contained acetone, aniline and the metal complex. The model giving the best agreement with experiment was one having acetone in the first coordination sphere of the complex, and aniline in a second coordination sphere site. The next problem is to determine, as far as possible, which step in the formation of the anil is actually the rate-determining one. As discussed in Chapter 1, Section (C), carbinolamines are generally invoked as intermediates in the formation and hydrolysis of anils in aqueous solution. Either the formation or hydrolysis of the carbinolamine may be rate-determining, and this can be pH dependent. A feasible series of steps for the metal catalysed formation of the anil is the following.

The reaction involves (a) nucleophilic attack of aniline on the carbon of the coordinated carbonyl group, transfer of one proton from N to O to give a coordinated carbinolamine as in (c), transfer of a second proton to give a coordinated anil and water.



The same series of steps in the reverse order would give the mechanism for the hydrolysis of the anil, starting with the anil in the first coordination sphere and water in a second sphere site.

If the step (c) to (d) were to be rate-determining for the forward reaction, then a buildup of the carbinolamine (c) is to be expected. However, experimentally no evidence was ever found for the presence of carbinolamines in the solutions studied, or for the presence of a fast exchange between acetone and aniline on the one hand, and a carbinolamine on the other. This includes studies using acetonitrile as a solvent.

There are two further pieces of evidence which suggest that neither of the steps (b)+(c) or (c)+(d) is likely to be rate-determining. The first of these is the measured value for  $\frac{\text{rate H}}{\text{rate D}}$  for the formation of the anil from p-toluidine and acetone. This was found to have a value of 1.55 (Chapter 5, Section (D)). This value is in the region expected for a secondary isotope effect, but is low for a primary effect (i.e. where proton transfer is important in the rate-determining step).

The second piece of evidence is the observation that the measured lifetime for a catalysed proton exchange between p-toluidine and  $\text{H}_2\text{O}$  is, at most,  $10^{-3}$  sec at  $35^\circ\text{C}$ , with a catalyst concentration less than that used in the initial rate studies. The proton exchanges postulated in the mechanism are unlikely to be  $10^6$  times slower than this.

All these arguments lead to the conclusion that neither of the steps (b)+(c) or (c)+(d) are likely or plausible as rate-determining steps. The zwitterions (b) and (d) are therefore likely to have only a fleeting existence in acetone or acetonitrile solution. The rate-determining step is therefore suggested as being the nucleophilic attack of aniline on coordinated acetone for the forward reaction, and of water on coordinated anil for the reverse reaction.

(D) Transimination

As discussed in Chapter 7, the transimination reaction,



has been studied using SST methods. Since the products are the same as the reactants here, the reaction is difficult to detect by "classical methods", but is very conveniently studied by SST experiments. These are, in a sense, analogous to relaxation methods, such as temperature-jump, which probe the system by small displacements of the equilibrium position. However, SST experiments study the system at chemical equilibrium, but use non-equilibrium states of the spin system as a probe. In the case of the transimination reaction, the SST method proved very useful, giving results which would otherwise have been very difficult to obtain, e.g. from line-broadening studies.

The transimination reaction is formally analogous to the other reactions studied, i.e. the formation and hydrolysis of the anil, which proceed by nucleophilic attack on the  $\delta^+$  end of a polarised double bond. It would therefore be reasonable to invoke the same mechanism, i.e. the anil in the first coordination sphere and the aniline in the second sphere. The fact that the lifetime for the interchange of the anil methyl groups is one half of that of the anil itself would indicate that the process of exchanging the methyl groups is occurring during the transimination reaction. In fact, this process may contribute in a major way to the activation energy of the transimination reaction. The difference between the rate of transimination and that of the formation or hydrolysis of the anil, is probably due to a difference in equilibrium constants, rather than rate constants. The concentration of species with anil as



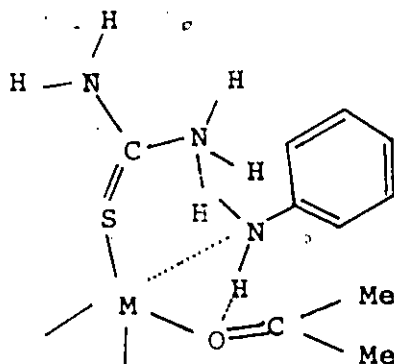
a first sphere ligand, and aniline in a second sphere site, may be much larger than those invoked in the formation and hydrolysis reactions of the anil. In fact, the equilibrium constants known would predict just this result.

#### (E) NATURE OF THE SECOND SPHERE SITE

In the previous section it was shown that in order to explain the observed results, it was necessary to adopt a model in which the rate-determining step involved one ligand in the first coordination sphere, and another in the "second sphere". On the basis of kinetics alone, it is not possible to distinguish between a true second coordination sphere site and a fifth ligand in the first coordination sphere. In fact, five-coordinate intermediates have been invoked to explain ligand exchange reactions in Co(II) and Zn(II) thiourea complexes<sup>(69)</sup>. In those cases, the formation of the five-coordinate intermediate is the rate-determining step. This cannot be true in the present case, and therefore the five-coordinate complex, if it existed, would have to be relatively more stable. There are five-coordinate complexes of Co<sup>II</sup> which are stable, the best known being Co(CN)<sub>5</sub><sup>3-</sup> which has been much studied. However, in these systems, i.e. thiourea complexes of Co(II) and Zn(II), there is no evidence for species of higher coordination number than four in amounts detectable by other than kinetic measurements<sup>(80)</sup>. Therefore the assignment of the nucleophile to a true second coordination sphere site is preferred.

The second coordination sphere of neutral complexes has recently been receiving some attention, and this area has recently been reviewed<sup>(44)</sup>. NMR spectroscopy has been the main tool used, and paramagnetic complexes have proved very fruitful as probes. The interactions are agreed to be predominantly electrostatic, although in some cases hydrogen bonding may be involved. The energies involved in second sphere bonding are usually estimated at 4 to 5 kcal/mole. In this particular case, the only necessary condition is that aniline (or water) be a much better second sphere ligand than carbon tetrachloride, so that on dilution no aniline is replaced by  $\text{CCl}_4$ . This is consistent with quantitative measurements of the ability of various compounds to act as second sphere ligands<sup>(93)</sup>.

The second sphere site for aniline could in theory involve some direct interaction of the lone pair of electrons on the nitrogen with the metal, hydrogen bonding to other ligands (e.g. thiourea or acetone), and electrostatic interactions<sup>(94)</sup>.



One strong argument against a large interaction of the lone pair with the metal (i.e. a fifth coordination site), is that this would reduce the basicity of the aniline and thus make any catalysis much less effective. Evidence exists for such an effect<sup>(95)</sup>.

#### (F) SUGGESTIONS FOR FURTHER WORK

The present metal complex catalysed reactions do show great promise as a system in which to investigate homogeneous catalysis. Many convenient probes are available including SST.

Among suggestions for further work along this line are:

- (a) Investigating in more detail the transamination reaction (i.e. carrying out a dilution experiment with  $\text{CCl}_4$ , determining the dependence on aniline and anil concentration, and studying the inhibition with Tu quantitatively).
- (b) Studying the effect of changing the para substituent on the aromatic ring.
- (c) Determining the activation parameters for both reactions.
- (d) Working with paramagnetic catalysts where the equilibrium constants can be measured.
- (e) Investigating the effectiveness of the present catalysts in other related reactions involving nucleophilic attack on a double bond, and, the transamination reaction.
- (f) Measurement of both processes observed in the transamination reaction with the same sample and spectrometer, i.e. using FT SST with p-toluidine/p-toluidine-anil as the sample.

#### (G) CATALYTIC EFFICIENCY

The experimental data reported in this thesis have demonstrated that metal thiourea complexes are very effective catalysts for anil formation, hydrolysis and transamination. These catalysts are many times more efficient than those usually used in reactions

of Schiff bases (see Chapter 1). It would be very interesting to be able to compare the catalysts used here with enzymes. Unfortunately such a comparison is not possible since the enzymatic data necessary, i.e. limiting rates with very similar substrates, is not available in the literature.

An obvious question is why these metal complexes are so effective at catalysing these reactions of anils. Clearly several criteria need to be satisfied if the catalyst is to be effective. At least one of the reactants must be coordinated to the metal. The extent of coordination will depend on competition with other available ligands. On the other hand the products must not be too tightly bound, otherwise the result is a promoted rather than a catalysed reaction. The equilibrium constants in the systems under discussion are clearly favourable for fulfilling these conditions.

For metal ions in aqueous solution the solvent is too good a ligand for optimum catalysis without the use of chelating substrates. Thiourea is a good enough ligand to induce solubility in non-aqueous solvents but, unlike o-phenanthroline for example, it does not permanently block the reaction site. Another important factor in catalysis may well be the second sphere binding ability of the ancillary ligand. Thiourea has obvious hydrogen bonding possibilities.

In addition to these equilibrium constant considerations, kinetic factors are also pertinent. The rate of ligand exchange must not be a limiting factor. Thus we would predict that Co III or Pt II complexes, which are known to be non-labile, would not

be effective catalysts. Once a reactant is complexed, the metal atom plays a further role in "activating" the substrate. It appears that for this type of reaction this is a simple electron-withdrawing process from the acetone or anil. Thus, both the transition metal Co and the non-transition metal Zn are effective catalysts. This may be compared with the activation of ethylene, for example, in homogeneous hydrogenation, where it would appear that specific interactions between  $d$  orbitals and  $\pi^*$  orbitals are required, and catalysis is limited to transition metals.

Finally, the role of the catalysts in bringing together the reactants should be mentioned. This has been referred to as the "promnastic" effect<sup>(34)</sup>, and is undoubtedly a factor in any reaction which without catalysis would be bimolecular in nature. In the present case the effect of the catalyst is to produce an essentially "unimolecular" rate-determining step. Hydrogen ions in aqueous solution are effective in activating a ketone by charge polarization but lack any promnastic ability. Acid catalysed anil formation proceeds by a different mechanism than the metal complex catalysed reaction, and is slower.

#### (H) CONCLUSIONS

The proposed mechanism of the reactions studied involves rate-determining nucleophilic attack of a second sphere ligand (aniline or water) on the polarised double bond of a first sphere one (anil or acetone). In the original definitions of the "template effect" and "promnastic effect" (Chapter 1), it was implicitly assumed that both of the reactants were, in fact, first sphere ligands. However, it seems reasonable to extend the

definition of a promnastic effect<sup>(34)</sup> to cover the present case of a first sphere ligand and a second sphere one, since the metal is truly fulfilling its role as a "matchmaker".

The present reactions also bear a close analogy to ligand exchange reactions. In the notation of Langford and Gray<sup>(96)</sup>, an  $I_a$  mechanism involves as its rate-determining step the interchange of ligands between first and second sphere sites. For an  $I_a$  process, the essential feature is the nucleophilic attack of a second sphere ligand on the metal ion, displacing a first sphere ligand. In the present case we postulate the nucleophilic attack of the second sphere ligand on a positively charged ligand centre, rather than on the positively charged metal. These two processes have obvious similarities. The direct attack of a "free" aniline molecule (for example) on coordinated acetone, would, in a similar way, be analogous to an associative A mechanism of ligand exchange.

The results of this work may contribute to the understanding of some enzymatic reactions. The protein moieties in metalloenzymes could provide many possibilities for the specific binding of substrates in the equivalent of the "second sphere" of the metal atom. Reactions involving the metal as the active site could then proceed in a manner quite analogous to the reactions studied in the present work. In fact, the association or binding constants determined kinetically may, in some cases, refer to binding at such sites, rather than at the primary, or metal centre.

## APPENDIX A

(i) The  $MTu_2Cl_2$  case

The following is a general solution of the problem of determining the concentration of any particular species in a solution of a metal complex with two available ligand binding sites, with any number of potential ligands in the solution. The ligands are labelled  $L_i$  where  $L_1$  may be Tu and  $L_2$  acetone etc. The equilibrium constants  $K_i$  are defined in terms of the equilibrium



where

$$K_i = \frac{[ML_jL_i][L_1]}{[ML_jL_1][L_i]}$$

That is, the constants  $K_i$  are defined for replacement of ligand  $L_1$  by the ligand  $L_i$ , and the same constant  $K_i$  refers to all replacements of  $L_1$  by  $L_i$ , regardless of the nature of the second ligand  $L_j$ .

The concentration in solution of any species  $ML_iL_j$  will then be proportional to the concentrations of the free ligands, i.e.  $[L_i]$  and  $[L_j]$ , and to the equilibrium constants  $K_i$  and  $K_j$ . Thus, for all the possible species  $ML_iL_j$ ,

$$[ML_iL_j] = \alpha K_i K_j [L_i][L_j]$$

or

$$[ML_iL_j] = \alpha K_i K_j [L_i][L_j] \quad (A.1)$$

However, the sum of the concentrations of all the species  $ML_iL_j$  must be the total amount of metal in solution. Let the total amount of metal in solution be  $m$ . Then

$$\sum_{i,j=1}^n [ML_iL_j] = m$$

where there are  $n$  potential ligands in solution. From equation (A.1)

$$\alpha \sum_{i,j=1}^n K_i K_j [L_i][L_j] = m$$

$$\therefore \alpha = \frac{m}{\sum_{i,j=1}^n K_i K_j [L_i][L_j]}$$

Then the concentration of any species  $ML_iL_j$  is given by

$$[ML_iL_j] = \frac{mK_i K_j [L_i][L_j]}{\sum_{i,j=1}^n K_i K_j [L_i][L_j]} \quad (A.2)$$

The expression  $\sum_{i,j=1}^n K_i K_j [L_i][L_j]$  may always be written in the form

$$[ML_iL_j] = \frac{mK_i K_j [L_i][L_j]}{(K_1[L_1] + K_2[L_2] + K_3[L_3] + \dots + K_n[L_n])^2} \quad (A.3)$$

To take a specific case, suppose that there are three potential ligands in solution. The concentration of the species  $ML_2L_3$  is given by the equation

$$[ML_2L_3] = \frac{2mK_2K_3[L_2][L_3]}{(K_1[L_1] + K_2[L_2] + K_3[L_3])^2} \quad (A.4)$$

The factor of 2 arises because both  $ML_2L_3$  and  $ML_3L_2$  are counted as  $ML_2L_3$ .



Equation (A.4) will then apply to cases where both reactants in a reaction must be first coordination sphere ligands, i.e., where the rate is proportional to the concentration of species containing both reactants complexed. For the case of the formation of the anil then,

$$\text{Rate} \propto [\text{MANAcCl}_2] = \frac{2mK_2K_3 [\text{An}] [\text{Ac}]}{([\text{Tu}] + K_2[\text{An}] + K_3[\text{Ac}])^2} \quad (\text{A.5})$$

The second case which needs to be analysed is that where one substrate is a first coordination sphere ligand and the other is a second coordination sphere ligand. For this analysis the first sphere ligand is acetone and the second is aniline, but the equations are completely general.

The species in solution having acetone in the first coordination sphere will be  $\text{MTuAcCl}_2$ ,  $\text{MANAcCl}_2$  and  $\text{MACAcCl}_2$ . From equation (A.4) the total concentration of species with acetone as a first sphere ligand will be given by

$$\begin{aligned} & \frac{2mK_3 [\text{Ac}] \cdot ([\text{Tu}] + K_2[\text{An}] + K_3[\text{Ac}])}{([\text{Tu}] + K_2[\text{An}] + K_3[\text{Ac}])^2} \\ &= \frac{2mK_3 [\text{Ac}]}{([\text{Tu}] + K_2[\text{An}] + K_3[\text{Ac}])} \end{aligned}$$

The factor of 2 for the  $\text{MACAcCl}_2$  case arose from the fact that either of the two ligands may react.

Now with aniline as a second sphere ligand and using the same analysis as in Chapter 8, Section (B), the concentration of species with Ac as a first sphere ligand and An as a second sphere one is given by

$$\frac{2mK_3[Ac]}{([Tu] + K_2[An] + K_3[Ac])} \cdot \frac{K'[An]}{[Ac]}$$

Therefore, Rate  $\propto \frac{2mK_3K'[An]}{[Tu] + K_2[An] + K_3[Ac]}$

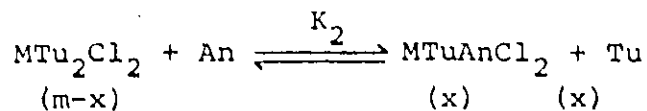
or

$$\text{Rate} = \frac{2kmK'K_3[An]}{[Tu] + K_2[An] + K_3[Ac]}$$

Now the term  $K_3[Ac] \ll [Tu]$  and  $K_2[An]$ , using the equilibrium constants for  $CoTu_2Cl_2$  and the concentrations computed with the data of Table 8.1.

$$\therefore \frac{1}{\text{Rate}} = \frac{1}{2kmK'K_3} \cdot \frac{[Tu]}{[An]} + \frac{1}{2kmK'K_3} \cdot K_2 \quad (\text{A.6})$$

Furthermore, assume the term  $[MTuAnCl_2] \gg [MTuAcCl_2]$ . Using the data of Table 8.1 in the most dilute sample where  $[An] = 0.06 M$ , the ratio  $[MTuAnCl_2]/[MTuAcCl_2]$  is 13.8. This justifies the above assumption. Therefore, all the thiourea free in solution can be considered to come from formation of the species  $MTuAnCl_2$ .



Neglecting the amount of An complexed (which is very small)

then

$$K_2 = \frac{x^2}{(m-x)(An)}$$

$$x^2 + K_2 An x - K_2 mAn = 0$$

$$x = -\frac{K_2[An] \pm \sqrt{K_2^2[An]^2 + 4K_2[An]m}}{2}$$

The term  $K_2^2[An]^2 \ll 4K_2[An]m$

Therefore, 
$$x = \frac{-K_2[An] \pm \sqrt{4K_2[An]m}}{2}$$

or 
$$[Tu] = \frac{-K_2[An]}{2} \pm \sqrt{4K_2[An]m}$$

Substituting into equation (A.6)

$$\frac{1}{\text{Rate}} = \frac{\sqrt{K_2}}{2kK_1K_3\sqrt{m}} \cdot \frac{1}{\sqrt{[An]}} + \frac{K_2}{2kmK_1K_3} \quad (\text{A.7})$$

Thus a plot of  $\frac{1}{\text{Rate}}$  versus  $\frac{1}{\sqrt{[An]}}$  should be linear with a slope of  $\frac{\sqrt{K_2}}{2kK_1K_3\sqrt{m}}$ .

(ii) The  $MTu_4^{2+}$  case

The case of a metal complex with four available first coordination sphere ligand binding sites may be treated in a manner completely analogous to that of two sites. Using the same definitions, then;

$$[ML_iL_jL_kL_\ell] = \beta K_i K_j K_k K_\ell [L_i][L_j][L_k][L_\ell]$$

$$M = \text{total } MTu_4^{2+} \text{ initially added} = \sum_{i=1}^3 \sum_{j=1}^3 \sum_{k=1}^3 \sum_{\ell=1}^3 ML_iL_jL_kL_\ell$$

$$= \beta \sum_{i=1}^3 \sum_{j=1}^3 \sum_{k=1}^3 \sum_{\ell=1}^3 K_i K_j K_k K_\ell [L_i][L_j][L_k][L_\ell]$$

Thus, 
$$\beta = \frac{M}{\sum_{i=1}^3 \sum_{j=1}^3 \sum_{k=1}^3 \sum_{\ell=1}^3 K_i K_j K_k K_\ell [L_i][L_j][L_k][L_\ell]}$$

$$\sum_{i=1}^3 \sum_{j=1}^3 \sum_{k=1}^3 \sum_{\ell=1}^3 K_i K_j K_k K_\ell [L_i][L_j][L_k][L_\ell] = (K_1 L_1 + K_2 L_2 + K_3 L_3)^4$$

Suppose the rate of reaction is proportional to the concentration of species containing complexed  $L_2$  and  $L_3$ .

These are

$$ML_1 L_1 L_2 L_3 + ML_1 L_1 L_3 L_2 + ML_1 L_2 L_1 L_3 + \text{etc.}$$

$$ML_2 L_2 L_3 L_3 + ML_2 L_3 L_2 L_3 + \text{etc.}$$

$$ML_2 L_2 L_2 L_3 + ML_2 L_2 L_3 L_2 + \text{etc.}$$

$$ML_3 L_3 L_3 L_2 + \text{etc.}$$

$$ML_1 L_2 L_3 L_3 + \text{etc.}$$

$$ML_1 L_3 L_2 L_2 + \text{etc.}$$

Now neglecting the order we have

$$M(L_1^2 L_2 L_3) \quad 12 \text{ such terms}$$

$$M(L_2^2 L_3^2) \quad 6 \text{ such terms}$$

$$M(L_2^3 L_3) \quad 4 \text{ such terms}$$

$$M(L_3^3 L_2) \quad 4 \text{ such terms}$$

$$M(L_1 L_2 L_3^2) \quad 12 \text{ such terms}$$

$$M(L_1 L_3 L_2^2) \quad 12 \text{ such terms}$$

Counting the number of  $L_2, L_3$  pair interactions, the appropriate numerical factors are

$M(L_1^2L_2L_3)$	$12 \times 1$	$=$	12
$M(L_2^2L_3^2)$	$6 \times 4$	$=$	24
$M(L_2^3L_3)$	$4 \times 3$	$=$	12
$M(L_3^3L_2)$	$4 \times 3$	$=$	12
$M(L_1L_2L_3^2)$	$12 \times 2$	$=$	24
$M(L_1L_3L_2^2)$	$12 \times 2$	$=$	24

Now,

$$\text{rate} \propto 12[M(L_1^2L_2L_3) + 2M(L_2^2L_3^2) + M(L_2^3L_3) + M(L_3^3L_2) + 2ML_1L_2L_3^2 + 2M(L_1L_3L_2^2)]$$

$$\propto \frac{12MK_2K_3[L_2][L_3]}{(K_1[L_1] + K_2[L_2] + K_3[L_3])^4} [K_1^2[L_1]^2 + 2K_2K_3[L_2][L_3] + K_2^2[L_2]^2 + K_3^2[L_3]^2$$

$$+ 2K_1K_3[L_1][L_3] + 2K_1K_2[L_1][L_2]]$$

$$\propto \frac{12MK_2K_3[L_2][L_3]}{(K_1[L_1] + K_2[L_2] + K_3[L_3])^4} [K_1[L_1] + K_2[L_2] + K_3[L_3]]^2$$

$$\propto \frac{12MK_2K_3[L_2][L_3]}{(K_1[L_1] + K_2[L_2] + K_3[L_3])^2} \quad (\text{A.8})$$

This expression is identical (except for a numerical factor) with equation (A.4) which applies to the  $MTu_2Cl_2$  case.

The second case to be treated with  $MTu_4^{2+}$  as a catalyst, is where one substrate (say acetone) is in the first coordination sphere and the other (aniline) is in the second. This problem is approached as was the analogous one with  $MTu_2Cl_2$  as catalyst, allowing for the appropriate numerical factors for species with more than one coordinated acetone molecule.

The total concentration of all species with Ac complexed (with numerical factors) is given by

$$\frac{4mK_3[Ac]([Tu] + K_2[An] + K_3[Ac])^3}{([Tu] + K_2[An] + K_3[Ac])^4}$$

$$= \frac{4mK_3[Ac]}{[Tu] + K_2[An] + K_3[Ac]}$$

If the rate now depends on those species having acetone as a first sphere and aniline as a second sphere ligand then

$$\text{Rate} \propto \frac{4m_K[Ac]}{[Tu] + K_2[An] + K_3[Ac]} \cdot \frac{K'[An]}{[Ac]}$$

$$\propto \frac{4mK'K_3[An]}{[Tu] + K_2[An] + K_3[Ac]} \quad (\text{A.9})$$

Once again, except for a numerical factor, this expression is identical with that obtained using the same model with  $MTu_2Cl_2$  as a catalyst.

For a double reciprocal plot then

$$\frac{1}{\text{Rate}} \propto \frac{1}{4mK'K_3} \cdot \frac{[Tu]}{[An]} + \frac{1}{4mK'K_3} \cdot K_2 + \frac{1}{4mK'} \cdot \frac{[Ac]}{[An]} \quad (\text{A.10})$$

Unfortunately in this expression both terms containing  $\frac{1}{[An]}$  are of comparable size

$$\therefore \frac{1}{\text{Rate}} \propto A \frac{[Tu]}{[An]} + B \frac{1}{[An]} + C \quad (\text{A.11})$$

Since  $[Tu]$  itself depends on  $[An]$  it is not possible to predict the exact dependence of  $(\text{Rate})^{-1}$  on  $[An]^{-1}$ , but from the form of (A.11) a double reciprocal plot should be fairly close to linear.

For the inhibition of the reaction by Tu, the dependence of  $(\text{Rate})^{-1}$  on  $[\text{Tu}]$  may be obtained as follows:

$$\frac{1}{\text{Rate}} \propto \frac{[\text{Tu}] + K_2[\text{An}] + K_3[\text{Ac}]}{4mK'K_3[\text{An}]}$$

$$\propto \frac{[\text{Tu}]}{4mK'K_3[\text{An}]} + \frac{K_2}{4mK'K_3} + \frac{[\text{Ac}]}{4mK'[\text{An}]}$$

Since the catalyst concentration is very small compared to  $[\text{Ac}]$  or  $[\text{An}]$ , these terms may be treated as constants with respect to changes in  $[\text{Tu}]$ .

$$\therefore \frac{1}{\text{Rate}} \propto [\text{Tu}]. \quad (\text{A.12})$$

It is to be noted that the model with Ac and An coordinated as first sphere ligands gives a different prediction for the inhibition behaviour. It predicts for  $\text{MTu}_4^{2+}$  that  $(\text{Rate})^{-1}$  will depend on  $[\text{Tu}]$  at low values of  $[\text{Tu}]$ , and on  $[\text{Tu}]^2$  at high values of  $[\text{Tu}]$ .

MICROFICHE OF POOR REPRODUCTION  
OF ORIGINAL COPY OF LEAF 210.





## BIBLIOGRAPHY

1. C. A. Tolman Chem. Soc. Rev. 1, 337 (1972).
2. J. A. Osborn, F. H. Jardine, J. F. Young and G. Wilkinson. J.C.S. (A), 1711 (1966).
3. F. A. Cotton and G. Wilkinson. "Advanced Inorganic Chemistry, a Comprehensive Text". 3rd ed. N.Y. Interscience, 1972.
4. F. R. Hartley. "The Chemistry of Platinum and Palladium". N.Y. Wiley, 1973.
5. D. H. Busch. Rec. Chem. Progr. 25, 107 (1964).
6. R. W. Hay. Rev. Pa. Chem. 13, 157 (1963).
7. M. M. Jones and W. A. Connor. Ind. Eng. Chem. 55, 15 (1963).
8. R. W. Hay. J. Chem. Ed. 42, 413 (1965).
9. M. L. Bender, "Mechanisms of Homogeneous Catalysis from Protons to Proteins". N.Y., Wiley-Intersciences, 1971.
10. M. M. Jones. "Ligand Reactivity and Catalysis", N.Y., Academic Press, 1968.
11. D. H. Busch. Science. 171, 241 (1971).
12. F. Basolo and R. G. Pearson. "Mechanisms of Inorganic Reactions, a Study of Metal Complexes in Solution". N.Y. Wiley 1967.
13. L. F. Lindoy. Quart. Rev. 25, 379 (1971).
14. W. Gibbs and F. A. Geneth. Amer. J. Sci. 2, 241 (1857).
15. H. Kroll. J.A.C.S. 74, 2036 (1952).
16. H. L. Conley and R. B. Martin. J. Phys. Chem. 69, 2914, 2923 (1965).
17. M. L. Bender and B. W. Turnquest, J.A.C.S. 79, 1889 (1957).

18. R. W. Hay and P. J. Morris. Chem. Comm. 23 (1967).
19. M. D. Alexander and D. H. Busch. J.A.C.S. 88, 1130 (1966).
20. D. A. Buckingham, D. M. Foster and A. M. Sargeson, J.A.C.S. 91, 3451 (1969).
21. W. P. Jencks. "Catalysis in Chemistry and Enzymology", N.Y., McGraw-Hill, 1969.
22. G. L. Eichhorn and J. C. Bailar. J.A.C.S. 75, 2905 (1953).
23. G. L. Eichhorn and I. M. Trachtenberg. J.A.C.S. 76, 5183 (1954).
24. G. L. Eichhorn and N. D. Marchand. J.A.C.S. 78, 2688 (1956).
25. L. J. Nunez and G. L. Eichhorn. J.A.C.S. 84, 901 (1962).
26. M. C. Thompson and D. H. Busch. J.A.C.S. 86, 213 (1964).
27. R. K. Y. Ho and S. E. Livingstone. Austral. J. Chem. 18, 659 (1965).
28. M. E. Farago and T. Matthews. J.C.S. (A) 609, 1969.
29. C. V. McDonnell, M. S. Michailidis and R. B. Martin. J. Phys. Chem. 74, 26 (1970).
30. D. L. Leussing and C. K. Stanfield. J.A.C.S. 88, 5726 (1966).
31. K. S. Bai and D. L. Leussing. J.A.C.S. 89, 6126 (1967).
32. D. Hopgood and D. L. Leussing. J.A.C.S. 91, 3740 (1969).
33. D. L. Leussing and L. Anderson. J.A.C.S. 91, 4698 (1969).
34. B. E. Leach and D. L. Leussing. J.A.C.S. 93, 3377 (1971).
35. A. Carrington and A. D. McLachlan, "Introduction to Magnetic Resonance". Harper, New York, 1967.
36. J. W. Emsley, J. Feeney and L. H. Sutcliffe, "High Resolution Nuclear Magnetic Resonance Spectroscopy". Pergamon, Oxford, 1965.

37. J. A. Pople, W. G. Schneider, and H. J. Bernstein, "High Resolution Nuclear Magnetic Resonance". McGraw-Hill, New York 1959.
38. T. C. Farrar and E. D. Becker. "Pulse and Fourier Transform NMR. Introduction to Theory and Methods". Academic Press N.Y. 1971.
39. D. G. Gillies and D. Shaw. Ann. Ref. NMR Spectroscopy, 5A, 580 (1972).
40. D. R. Eaton and W. D. Phillips. Adv. Magn. Resonance. 1, 119 (1965).
41. E. R. Dier and H. van Willigen. Prog. NMR Spectrosc. 2, 111 (1967).
42. G. A. Webb. Ann. Ref. NMR Spectroscopy, 3, 211 (1970).
43. D. R. Eaton and K. Zaw. Coord. Chem. Rev. 7, 197 (1972).
44. G. N. La Mar, W. DeW. Hoorocks and R. H. Holm. "NMR of Paramagnetic Molecules". Academic Press, N.Y. 1973.
45. R. J. Kurland and B. R. McGarvey. J. Magn. Res. 2, 286 (1970).
46. G. N. La Mar and G. R. Van Hecke. J.A.C.S. 92, 3021 (1970).
47. W. D. Perry and R. S. Drago. J.A.C.S. 93, 2183 (1971).
48. C. S. Johnson. Advan. Mag. Resonance 1, 33 (1965).
49. H. S. Gutowsky, D. W. McCall and C. P. Slichter. J. Chem. Phys. 21, 279 (1953).
50. H. M. McConnell, J. Chem. Phys. 28, 430 (1958).
51. H. M. McConnell and D. D. Thompson. J. Chem. Phys. 26, 958 (1957).
52. H. M. McConnell and D. D. Thompson. J. Chem. Phys. 31, 85 (1959).

53. S. Forsen and R. A. Hoffman. J. Chem. Phys. 39, 2892 (1963).
54. F.A.L. Anet and A.J.R. Bourn. J.A.C.S. 89, 760 (1967).
55. M. F. Johnson and J. H. Forsberg. Inorg. Chem. 11, 2683 (1972).
56. J. W. Faller, in "Determination of Organic Structures by Physical Methods". Ed. F.C. Narhod and J. J. Zuckerman. Academic Press, N.Y. 1973. Volume 5, p. 75.
57. S. Forsen and R. A. Hoffman. J. Chem. Phys. 40, 1189 (1964).
58. J. H. Noggle and R. E. Schirmer. "The Nuclear Overhauser Effect: Chemical Applications". Academic Press, N.Y. 1971.
59. W. von Philipsborn. Ang. Chem. Int. Ed. 10, 472 (1971).
60. B. M. Fung and P.L. Olympia. Mol. Phys. 19, 685 (1970).
61. P. P. Yang and S. L. Gordon. J. Chem. Phys. 54, 1779 (1971).
62. E. S. Gore and H. S. Gutowsky. J. Chem. Phys. 48, 3260 (1968).
63. S. A. Sherrod, R. L. da Costa, R. A. Barnes and V. Boekelheide. J.A.C.S. 96, 1565 (1974).
64. D. S. Kabakoff and E. Namanworth, J.A.C.S. 92, 3234 (1970).
65. P.W.N.M. van Leeuwen and A. P. Praat. J. Orgmet. Chem. 22, 483 (1970).
66. R. W. Creekmore and C. N. Reilley. Anal. Chem. 42, 725 (1970).
67. R.K. Gupta, S.H. Koenig and A. G. Redfield, J. Mag. Res. 7, 66 (1972).
68. R. K. Gupta and A. G. Redfield. Science 169, 1204 (1970).
69. K. Zaw. Ph.D. Thesis, McMaster University, 1974.
70. L. A. McLachlan, D.F.S. Natusch and R.H. Newman. J. Mag. Res. 3, 489 (1970).

71. Operating Manual for Varian HA 100 NMR spectrometer.
72. Operating Manual for Brucker WH 90 NMR spectrometer 1974.
73. C. Weygand and G. Hilgetag "Preparative Organic Chemistry". Wiley 1972.
74. I. W. Elliott and P. Yages, J. Org. Chem. 26, 1287 (1961).
75. G. Reddelien and A. Thurm. Ber. 65, 1511 (1932).
75. (a) G. Reddelien. Ber. 42, 4759 (1909).
75. (b) G. Reddelien. Ber. 43, 2471 (1910).
75. (c) G. Reddelien. Ber. 46, 2718 (1913).
76. J. Hoch. Compt. Rendus. 199, 1430 (1934).
77. D. Y. Curtin, E. J. Grubbs and C. G. McCarty. J.A.C.S. 88, 2772 (1966).
78. R. Suhn and H. Schretzmann. Ber. 90, 557 (1957).
79. H. A. Staab. Ann. Chem. 708, 36 (1967).
80. D. R. Eaton and K. Zaw. Can. J. Chem. 49, 3315 (1971).
81. J. L. Dye and V. A. Nicely. J. Chem. Ed. 48, 443 (1971).
82. K. J. Laidler. "The Chemical Kinetics of Enzyme Action". Oxford 1958.
83. E. F. Caldin, "Fast Reactions in Solution". Blackwell, Oxford, 1964.
84. O. A. Gansow and R. Holm. J.A.C.S. 91, 573 (1969).
85. V. S. Sharma and D. L. Leussing. Chem. Comm. 1278 (1970).
86. D. R. Eaton and K. Zaw. Submitted to Inorg. Chim. Acta.
87. D. F. Evans, J.C.S. 2003 (1959).
88. V. Gold and C. Tomlinson. Chem. Comm. 472 (1970).
89. V. M. Shul'man, S.V. Larinov, T. V. Kramareva, E. I. Arykova and V. V. Yadima, Russ. J. Inorg. Chem. 11, 580 (1966).

90. P. R. Wells, S. Ehrenson and R. W. Taft. Prog. Phys. Org. Chem. 6, 147 (1968).
91. J. W. Rakshys. Inorg. Chem. 9, 1521 (1970).
92. M. Eigen in "Technique of Organic Chemistry" (Ed. A. Weissberger) Vol. 8, Pt. 2, Interscience, New York, 1963.
93. D. R. Eaton and K. L. Chua. Can. J. Chem. 51, 4137 (1973).
94. D. R. Eaton. Can. J. Chem. 47, 2645 (1969).
95. A. C. Dash and R. K. Nanda. J.A.C.S. 91, 6944 (1969).
96. C. H. Langford and H. B. Gray. "Ligand Substitution Processes". Benhamin, N.Y. 1965.